Design and Performance analysis of High speed optical communication links

THESIS

Submitted in partial fulfillment of the requirements for the degree of

DOCTOR OF PHILOSOPHY

by

VINITA TIWARI

2009PHXF026P

Under the Supervision of

Prof. V. K. Chaubey

BITS Pilani
Pilani | Dubai | Goa | Hyderabad

BIRLA INSTITUTE OF TECHNOLOGY & SCIENCE PILANI (RAJASTHAN) INDIA

2016

BIRLA INSTITUTE OF TECHNOLOGY & SCIENCE
PILANI (RAJASTHAN) INDIA

CERTIFICATE

This is to certify that the thesis entitled **"Design and Performance analysis of High speed optical communication links"** submitted by **Ms. Vinita Tiwari** bearing **ID No. 2009PHXF026P** for the award of the Ph.D. degree of the institute embodies original work done by her under my supervision.

Signature of the Supervisor:

Name: V.K.CHAUBEY

Professor

Department of Electrical and Electronics Engineering

BITS-Pilani

Date:

Dedicated to

My Mother

ACKNOWLEDGEMENTS

During the course of this work, I have been fortunate to have the support of many people without which this work would not have been possible. I would like to take this opportunity to convey my thanks and gratitude to them in my humble acknowledgment.

Firstly, I would like to thank Prof. Souvik Bhattacharyya, Vice-Chancellor and Prof. A.K. Sarkar, Director, BITS Pilani for their constant support. I would like to greatly acknowledge Prof. S.K.Verma, Dean and Prof. Hemant Jadhav, Associate Dean, Academic Research Division (Ph.D. Program) for their valuable suggestions and support.

I am indebted to my supervisor, Prof V.K.Chaubey, for accepting me as a student, for his faith in me during the term of my candidature, and for providing valuable guidance and inspiration. He is also an excellent teacher, and attending his classes was really an enjoyment. Also, I would like to express my gratitude to two of my Doctoral Advisory Committee (DAC) members, Prof Navneet Gupta, Head of the Department and Dr. Rahul Singhal for reviewing my thesis and providing valuable advice.

I would like to thank the Departmental Research Committee (DRC) convener Dr. Abhijit R. Asati and all members of the DRC for their support. I would like to thank all senior professors Prof. G. Raghurama, Prof. S.Gurunarayanan, Prof. Surekha Bhanot, Prof. Anu Gupta, Prof. Hari Om Bansal, Prof. H.D. Mathur, Prof. S.K.Sahoo and Prof. K.K.Gupta for their guidance, constructive criticism, and continuous motivation. I am also grateful to Dr. Pawan Kamalkishor Ajmera and Dr. Praveen Kumar for their constructive comments. I want to thank them for their willingness to share their knowledge with me, which remains very useful in shaping my ideas and research. Collective and individual acknowledgments are due to all my colleagues who have directly or indirectly helped me in my work. I must acknowledge my friends Dr. Debabrata Sikdar, Dr. Sanghamitra Kundu and all my students for many great suggestions.

My hearty gratitude goes to my parents, family and my cute nephew Siddhant for their inseparable support and prayers during the toughest time of my life. I owe to my mother Sushma Tiwari without her continuous encouragements, care and love this thesis would not have come in this shape. Finally, I would like to thank the almighty God for gifting me with the best family, teachers, and friends that one can have.

Vinita Tiwari

ABSTRACT

In recent years, research in the field of lightwave communication has emerged to a completely next level. The optical communication has evolved as a viable solution to a high speed transmission systems owing to its higher bandwidth encompassing higher data rates. Use of advanced modulation formats which can support higher data rates with easier transmitter and receiver designs is one of the attractive solution to design the spectrally efficient high speed optical transmission links. This strategy also motivates the researchers and design engineers to further explore the capabilities of different modulation formats.

In the recent past optical communication networks have been specifically engineered and optimized to support various communication standards exploiting the capabilities of fiber, integrated waveguides and related optical hardware, and signal conditioning circuits. The present thesis attempts to study, model, simulate and analyze the optical channel performance under various transmission conditions encountered in a practical high speed design.

To improve the overall performance of the optical transmission links operating at 1550nm wavelength, this thesis focuses on mainly four approaches 1) channel capacity enhancement by reducing the fiber impairments through spectral management techniques, 2) improving the spectral efficiency by adopting robust pulse shaping and multilevel modulation techniques, 3) increasing the transmission capabilities with the use of multichannel WDM systems and 4) implementation of dispersion managed maps to maintain the nearly Gaussian shape of the propagating pulse for the long haul optical transmission links. Each of these methods has been implemented by addressing design challenges with an appropriate tradeoff. To start with the first approach, analysis of linear and nonlinear impairments in 40Gbps RZ-modulated Gaussian pulse propagation has been done. For this analysis, Gaussian pulses of different duty cycles are considered and the spectrum of these pulses is altered with the help of initial chirp. From the obtained results, it has been observed that the higher duty cycle pulses with negative chirp conditions show more tolerance towards the self phase modulation (SPM) and amplified spontaneous emission (ASE) induced impairments. Although, RZ modulation format requires simple transmitter and receiver designs but lacks in spectral efficiency. Therefore, to improve the spectral efficiency, duobinary technique which shows more resilient towards dispersion has

been considered for the optical link design. Optical transmission link at 40Gbps is designed for RZ-duobinary (DB-RZ) and NRZ-duobinary (DB-NRZ) pulse shapes. Optical signal to noise ratio (OSNR) influences the transmission characteristics at higher data rate in the presence of fiber impairments. The proposed link is optimized for electrical and optical parameters at fixed OSNR value and subjected to dispersion and self phase modulation induced impairments. The analysis shows the superiority of DB-NRZ pulses over the DB-RZ case at the higher OSNR values.

Multilevel modulation formats are emerging as a popular approach to increase the information carrying capacity of the optical transmission links. Therefore, differential quadrature phase shift keying (DQPSK) is utilized to further increase the spectral efficiency of the optical links. For the same, RZ-DQPSK modulated transmission link has been designed and analyzed. In this link, for the comparative analysis of different single mode fibers, three commercially available fiber types namely Standard Single Mode Fiber (SSMF), True Wave-Reduced Slope Fiber (TW-RS) and the Large Effective Area Fiber (LEAF) has been considered. Performance analysis of the link has been carried out for the varied duty cycles of the input pulse in ASE noise limited channel conditions. The analysis reveals the critical duty cycle for a superior performance. The performance analysis also validates the expected good performance of a LEAF out of the three attempted fiber types for long haul optical communication applications but definitely this comes at the higher cost of installation. Findings of the simulations also shows that the performance of SSMF fiber is also satisfactory and appears to be an economical solution compared to the LEAF when used for the short and metro links.

To fulfill the demand of future 100Gbps systems, data carrying capacity of the optical channel need to be further increased. One of the techniques to achieve this is by transmitting the data in both the polarization state of transmitting carrier. This thesis is focusing on exploring the spectrally efficient and cost effective schemes, therefore, to design the optical multichannel transmission system, with capacity of 112Gbps per channel here, dual polarization differential quadrature phase shift keying (DP-DQPSK) modulation format with direct detection is considered. The DP-DQPSK transmission model is designed for symbol aligned and symbol interleaved data formats and analyzed for various intrachannel and interchannel fiber impairments. The analysis reveals that DP-DQPSK modulated pulses in symbol interleaved formats shows better tolerance towards various fiber impairments, thus their transmission distance is higher than their symbol aligned counterparts

In long haul WDM systems, periodic dispersion management is required to maintain the shape of the transmitting optical pulse, thus, implementation of dispersion maps along the length of the transmission channel is a widely used and a popular scheme. In this thesis, numerical analysis has been performed to find the suitable dispersion map profile for the dispersion managed pulse propagation. Stability analysis for the pulse propagating in these maps has been done with residual dispersion and initial chirp. From the analysis, it was observed that dispersion maps having a certain amount of residual dispersion and negative chirp support the dispersion managed pulse for the longer fiber length. It is also observed that undercompensated dispersion managed profiles shows improved spectral efficiency in the analysis of collision dynamics of initially chirped dispersion managed pulses.

Table of Contents

LIST OF ABBREVIATIONS

WDM	Wavelength Division Multiplexing
EDFA	Erbium-Doped Fiber Amplifier
DWDM	Dense Wavelength Division Multiplexing
DM	Dispesrion Managed
CD	Chromatic Dispersion
SSMF	Standard Single Mode Fiber
LEAF	Large Effective Area fiber
TW-RS	True Wave –Reduced Slope
PMD	Polarization Mode Dispersion
DGD	Differential Group Delay
SPM	Self Phase Modulation
XPM	Cross Phase Modulation
GVD	Group Velocity Dispersion
SRS	Stimulated Raman Scattering
SBS	Stimulated Brillouin Scattering
FWM	Four Wave Mixing
OSNR	Optical Signal to Noise Ratio
BER	Bit-Error-Rate
ER	Extinction Ratio
DCF	Dispersion Compensating Fiber
FBG	Fiber Bragg Grating
MZM	Mach-Zehnder Modulator

List of Tables

List of Figures

CHAPTER 1

Introduction

1.1 Background

Use of light for the information transmission is nothing new as light or flash have been used to communicate Morse code from the ages [1]. However, if we just concentrate on the lightwave communication then the same can be traced back to the middle of the 20th century, with multiple independent researchers working on the ways to harness the wide bandwidth capacity of the lightwave in the data transmission [2]. In 1956, Abraham van Heel, Harolad H. Hopkins, and N.S. Kapany separately announces the optical imaging bundles mainly for medical image transfer and published in Nature [3] but by that time it had not been used for communication purpose. Theodore Maiman of the Hughes aircraft industry then developed the first ruby laser in the year 1960 [4], in a move that spread the serious research and speculation among network engineers about the possibility of communication over the optical medium. Consequently in the year 1965, Charles Kao and Charles Hockham suggested that the fibers available that time cannot be used for optical communication due to their extremely high losses i.e. approximately 1000 dB/km [5]. However, these fibers would emerge as a transmission solution if the attenuation is appreciably reduced.

It was in the 1970s, that Maurer, Keck, and Schultz of the Corning Glass Corporation developed a glass fiber that succeeded in producing an attenuation of less than 20dB/Km [6].This then ensures that optical fiber communication stayed relevant. Also, further research being focused on the various aspects, including optoelectronics devices, materials for fiber construction, refractive index profiles, etc. Side by side communication engineers was observing the explosion of internet traffic in the 1980s which even surpasses the volume of voice traffic [7-9]. The large bandwidth of the optical fibers encourages the adoption of wavelength division multiplexing (WDM) based transmission models which was first proposed by Delange in the 1970s [10]. Although research in WDM area is carried out since the 1980s, but WDM systems are more actively developed during 1990s when there was a huge demand for cost-effective solutions to provide large data capacity [11-14].

Developments in fiber optic communication can be divided into various generations based on their operating wavelength and data transmission capacity. Starting with the first generation in 1975 operated at a wavelength of 0.8μm based on GaAs semiconductor lasers, and was able to provide around 45Mbps data rate with a repeater spacing of 10km. To further increase the data rate in the year 1980's second generation comes into picture which operates at a wavelength of 1.3 μm and uses InGaAsP semiconductor laser as a source. Second generation systems were capable of providing a data rate of around 1.7Gbps with the repeater spacing of 50km. Repeater spacing is mainly decided by the losses provided by the fibers, and further reduction in the losses up to ~0.2dB/km increases the repeater spacing ~100km leading to the third generation of lightwave systems, which comes into existence in the 1990s [15-18].

The third generation of lightwave systems operates at the wavelength of 1.55 μm was actually developed by Nippon Telegraph and Telephony (NTT) and were able to provide 2.5Gbps data rate when operating with silica-based single mode fibers. Research in the area of optical communication is going from last thirty years. One has observed the various technological advancements and the same was also evident from the fourth generation of lightwave systems which uses optical amplifiers in place of repeaters after the development of erbium-doped fiber amplifier (EDFA) in the 1980s [19]. This generation makes use of the large bandwidth of optical fibers and encourages the adoption of wavelength division multiplexing (WDM) based transmission models. Transmission of up to 11,300km at 5Gbps has been demonstrated using submarine cables [20]. Same was the period of development of coherent optical communication, which had lagged behind in that time, but now once again attracting researchers due to its higher receiver sensitivity and various other features [21,22].

Presently fifth generation of optical communication utilizes dense wavelength division multiplexing (DWDM) schemes to meet the ever growing demand of data and supporting various types of optical networking capabilities [23]. These developments in the area of optical transmission parameters for different generations are shown in Figure 1.1

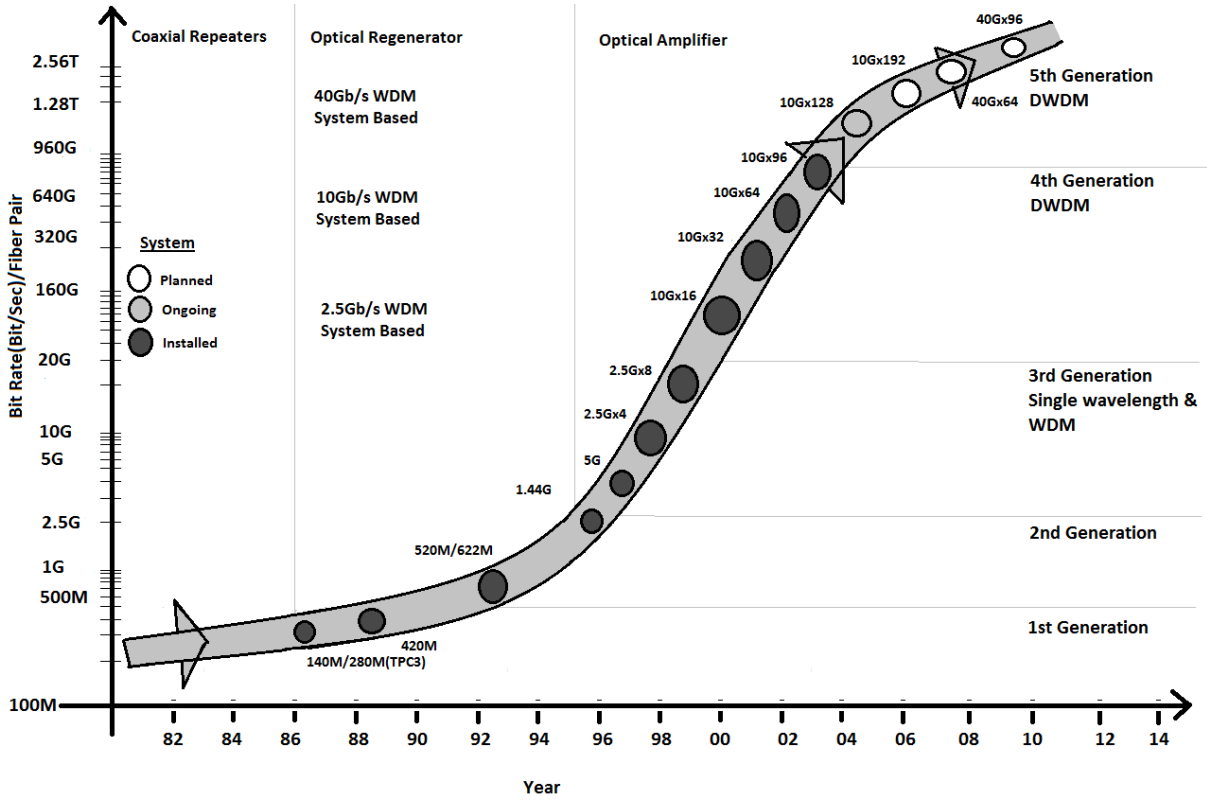

Figure 1.1: Generations of fiber transmission capacity [24]

From these discussions, it is observed that optical communication field is quite an established field but at the same time has a huge potential to explore the new capabilities. In the present generation of optical transmission systems, 10Gbps and 40Gbps is quite attractive in WDM or DWDM configuration with channel spacing of 200 GHz to 50GHz or even smaller [25]. The main problem with the sucessful implementation of these high-speed links lies in the management of various linear and nonlinear effects to achieve the required bitrate distance (BL) product. Some of the techniques used to improve the transmission capacity of the lightwave systems include the use of advanced modulation formats, various dispersion management schemes, use of more robust pulse shapes i.e. solitons or dispersion managed solitons, design of broadband optical components, different types of fibers etc [26-30].

Selection of optimal modulation format and dispersion management scheme which helps to increase the BL product along with the overall spectral efficiency of the system is one of the prime area of interest in the optical link designs. Apparently, dispersion management technology has evolved over past few decades and has proved to be very effective in various lightwave applications [31-35]. Periodic dispersion management is popular in modern WDM designs which comprises of sections of normal and anomalous

dispersion fibers connected in a periodic manner. This periodic combination of fiber sections is known as dispersion maps. Variation of fiber dispersion in these maps leads towards quasi-periodic breathing effect in time domain pulse propagation. Advantage of using these dispersion maps for the dispersion management in WDM systems are less modulation instability, less timing jitter caused by the collision between different pulses [36-38], and also less Gordon-Haus effects [39-41]. Another important feature of dispersion managed links is that the propagating pulse remains "Gaussian" known as dispersion managed soliton as compared to the "sech" pulse shape as in the case of normal soliton communication [42,43].

Fiber cables with large bandwidth are the core of optical transmission systems but they have a low tolerance for nonlinearities, and this will limit the maximum transmission power [44-47]. Thus, linear and nonlinear impairments of the fiber medium influence the overall optical link performance and thus need a careful study and analysis of various design aspects. Moreover, these effects become more difficult to handle in case of WDM and DWDM systems due to higher launched power and channel interaction. Therefore, it's important to discuss and investigate some of the dominating fiber impairments and their influence on the pulse transmission. Section 1.2 and 1.3 provides the brief discussion of linear and nonlinear effects respectively in optical fiber.

1.2 Linear effects in optical fiber

Fiber loss and dispersion are the important linear effects which mainly influence the data transmission through optical fibers.

1.2.1 Fiber loss

Fiber attenuation is although very low ~0.2dB/km in modern fibers but still it is an important linear effect which gradually reduces the signal power and signal needs to be amplified after certain distances to compensate these losses. Fiber losses are wavelength dependent and mainly occurs due to material absorption and Rayleigh scattering. Mathematically the fiber losses can be expressed as [48]:

$$P_o = P_i \exp(-\alpha L) \tag{1.1}$$

where, P_i is the lunched power at the input of the fiber of length L, P_o is output power at the other end of the fiber, α is attenuation coefficient.

Thus the attenuation coefficient (α) can be related with the input and out power as:

$$\alpha(dB/km) = -\frac{10}{L}\log_{10}(\frac{P_o}{P_{in}}) \approx 4.343\alpha \quad (1.2)$$

In this thesis, proper attenuation is considered in all fiber channels and amplifiers are used to compensate these fiber losses.

1.2.2 Amplified spontaneous emission

To compensate the fiber losses in optical links amplifiers are required at certain distances. Erbium doped fiber amplifier (EDFA) are the most popular type of amplifiers in long distance optical link designs. Ideally, to amplify the incoming optical signal in these amplifiers Erbium ions generated through stimulated emission transfer their energy to the optical signal field in the form of additional photons of the same phase, frequency, and polarization. But in real practice, some of the Erbium ions generated through the spontaneous emission also transfer their energy to the optical field in the form of photon with random phase, frequency, and polarization. This spontaneously emitted signal known as amplified spontaneous noise (ASE) is amplified in the same manner as the desired signal and degrades the signal to noise ratio at the receiver [26]. ASE noise is one of the important limiting factors in the amplifier based optical link design. In the present thesis, appropriate ASE noise is considered in the design of optical links and included in the models as an amplifier noise figure F_n which is related with the gain of the amplifier (G) and the spontaneous noise factor (n_{sp}) as:

$$F_n = \frac{2n_{sp}(G-1)}{G} \approx 2n_{sp} \quad (1.3)$$

1.2.3 Chromatic dispersion

Chromatic dispersion is basically due to the dependency of the refractive index on the frequency. Thus, different frequency component of the pulse travels with different velocity and causes pulse broadening at the receiving end [49,50]. This pulse broadening effect is more significant at higher data rate transmissions. Transmitted signal power gets attenuated due to this broadening of the propagating pulse. In fibers, group velocity dispersion parameter β_2 is the main parameter that causes pulse broadening. The effect of dispersion in the design and modeling of the optical links is accounted with the use of dispersion parameter D(ps/km-nm). In optical fiber, dispersion parameter D and the group velocity parameter β_2(ps^2/km) at a given operating wavelength (λ) are related as:

$$D = -\frac{2\pi c}{\lambda^2}\beta_2 \tag{1.4}$$

1.2.4 Polarization mode dispersion

Polarization mode dispersion (PMD) is the inherent property of the single mode fibers in the presence of birefringence. This variation of the fiber birefringence along the length of the fiber changes randomly both in direction and magnitude [51-53]. Birefringence causes one polarization mode to travel faster than the other and create the delay between the propagation times of two modes. RMS pulse broadening for the link of length L is related with the PMD parameter D_p. ΔT is the relative delay along the two principle states of polarizations.

$$\sigma_T^2 = \left\langle (\Delta T)^2 \right\rangle \approx D_p^2 . L \tag{1.5}$$

PMD induced differential group delay estimation is a complex analytical problem because it is a time-dependent effect in fibers, unlike the chromatic dispersion which is constant effect. Basically, PMD is a limiting factor in high data rate optical links. In the present work PMD effect is taken in to consideration for the dual polarized data transmission link design by considering $D_p = 0.1 ps/\sqrt{km}$ in the fiber.

1.3 Nonlinear effects

Fiber loss, ASE noise, dispersion are the linear effects and comparatively easier to manage whereas nonlinear effects, which depend on the intensity of the propagating pulse are more difficult to manage. Some of the important nonlinear effects are discussed in this section.

1.3.1 Self phase modulation and Cross phase modulation

Ideally, it is assumed that the refractive index of the fiber remains constant during the transmission of the signal but in practice, when the high-intensity signal travels through the optical fiber it modifies the effective refractive index of the fiber and this is known as Kerr effect [54]. Change in the intensity profile of the pulse with time leads to the time dependent changes in the refractive index and the pulse will observe different velocity at the different locations of the fiber. This velocity variation induces time dependent frequency chirp and thus time dependent phase variations. In single channel, optical links since this phase changes are introduced by the intensity of the pulse itself this is the reason it is known as

self phase modulation (SPM). SPM introduces the pulse broadening and it will increases with increase in the launched power of the pulse and severely degrades the link performance especially at the higher data rate. In multichannel systems this refractive index variations, so as the phase variations not only depend upon the intensity of the pulse itself but also on the intensities of the neighboring pulses propagating in the adjacent channels. Thus the total phase shift in a given channel is due to the cumulative effect of intensities of all transmitted channels and results in a coupling effect among different optical fields [55-57]. Spectral broadening in XPM is much higher compared to SPM [58-61]. Therefore, the proper selection of power is essential for the transmission of high speed optical transmission links and this becomes more crucial in multichannel optical systems. As the present thesis deals with single channel as well as multichannel link designs therefore, SPM and XPM both are considered and their related nonlinearities are properly modeled to evaluate their role in high speed optical link designs.

1.3.2 Stimulated Raman scattering and Stimulated Brillouin scattering

Stimulated Raman scattering (SRS) is another important nonlinear effect specifically in WDM systems. Due to SRS, the power of small magnitude will transfer from one optical field to another field whose frequency is downshifted by an amount governed by the optical vibration phonons of the medium. This effect was discovered by Raman in 1922 and was first observed in optical fibers in the 1970s [62]. Unlike SRS, simulated Brillouin scattering (SBS) is the scattering of light from acoustic phonons when the input power exceeds a threshold level (~5mW) for long fiber. SBS is similar to SRS but here the scattered light is downshifted by the frequency of an acoustic phonon (~10GHz) and with a narrower bandwidth. One major difference between SRS and SBS is, former is a bi -directional phenomenon whereas the latter occurs only in the backward direction [63,64]. Understanding of these effects is crucial, especially for multichannel systems as they add more scattered noise and thereby limit the performance of high-speed links. In the present thesis initially the single channel and thereafter multichannel optical links are analyzed at appropriate power levels.

1.3.3 Four wave mixing

Four wave mixing (FWM) is another important limiting factor for multichannel or WDM optical transmission. FWM is a parametric effect, results from the interaction of two or more photons from one or more waves annihilated, and leads to the generation of a new

photon at the different frequency. The net energy and momentum are conserved during this interaction [65,66]. FWM is a coherent process and occurs when the two optical pulses are phase matched along with the sufficient high power. In four wave mixing, there is interaction not just between intensities and powers but also between the fields. FWM is independent of the bit rate of the channel and can be minimized by changing the channels spacing in WDM lightwave transmission systems and choosing appropriate residual dispersion [67,68]. In the present work, FWM effect is properly explored in the multichannel link designs. To evaluate and understand the performance of the optical communication link under the given operating conditions certain performance criterion are required. Section 1.4 discusses some of these parameters which have been used in this thesis as a performance measures.

1.4 Performance Measures

One of the key issues for an effective design of optical communication links is to make the right choice of the performance evaluation criteria. The performance evaluation parameters should provide a platform to carry out comparative study and analysis. Some of the important measures, and used during this research work to evaluate the performance of a transmission links are optical signal to noise ratio (OSNR), Bit-error- rate (BER), *Q*-factor, jitter and extinction ratio.

1.4.1 Optical signal to noise ratio

Optical signal to noise ratio is popular and benchmark indicator for the analysis of the optical transmission systems [1,2]. It is the ratio of optical signal power to the optical noise power. When using an OSNR for the measurement it is important to define the optical measurement bandwidth as it actually provides the assessment of the received signals that are distorted by ASE noise [69].

$$OSNR = \frac{P_{out}}{N_{ASE}} = \frac{P_{out}}{(NF.G-1)hf\Delta f} \tag{1.6}$$

where, NF is the noise figure, G is Amplifier gain, hf is photon energy and Δf is the optical measurement bandwidth and typically ~12.5GHz ($\Delta\lambda$ =0.1nm) is considered.

1.4.2 Bit error rate and Q-factor

Bit error rate (BER) is another widely used measurement criteria for the optical amplifier based transmission systems and is decided by the electrical signal to noise ratio

(SNR) at the decision circuit of the receiver. Basically, BER define the probability of incorrect identification of the bit [4,5]. For optical transmission systems error, free transmission is often referred to as having BER less than 10^{-9}, although modern systems often require BER to be less than 10^{-12} [70].

Q-factor which is again used frequently in the literature approximates the BER to quantify the optical link performance [70]. Usually, for the reliable optical communication operating at a BER of 10^{-9}, the Q-factor comes out to be nearly 6. BER-equivalent Q-factor or simply Q-factor is mostly used during the designs of links in this thesis work, which is related to the BER as:

$$Q(dB) = 20(2^{1/2} erfc^{-1}(2BER)) \tag{1.7}$$

1.4.3 Timing jitter

Timing jitter is a fluctuation in the sampling time of the transmitting bits. Ideally, it is assumed that the signal is sampled at the peak of the voltage level of the pulse, but in practice, sampling time fluctuates from bit to bit. If the bit is not sampled at the center or the peak value then the sampled value is reduced and that causes the timing jitter (Δt). Timing jitter is a random process so as the reduction in the SNR at the receiver [71].

In optical transmission GVD and ASE also contribute to jitter due to time and phase shifts respectively and limits the transmission data rate [72]. Basically, in long haul optical communication, fiber dispersion contributes to phase shifts which are converted as amplitude fluctuations and cause jitter also known as Gordon-Hauss jitter as was first observed by American physicist James Power Gordon together with H.A. Hauss in the year 1986 specifically for solitons. Also, the jitter caused collectively due to the presence of SPM and ASE noise is known as Gordon-Mollenauer jitter due to Gordon work along with L.F. Mollenauer [73]. During the link designs in the present research work jitter effect is properly taken care of especially in the design and analysis of dispersion managed maps for long haul optical links.

1.4.4 Extinction ratio

The extinction ratio is the ratio between the output optical power corresponding to the maximum transmission value and the one corresponding to the minimum transmission value. In the transmission of 1's and 0's ideally there should be maximum power difference but this may cause a sharp power gradient at the edge of 1's results in a frequency chirp and

thus leads to a power penalty. However lesser power difference may causes more confusion at the receiver end due to extinction ratio induced power penalty [69]. Therefore, appropriate selection of extinction ratio is an important aspect and properly considered during optical link designs. Extinction ratio (r_{ex}) in terms of zero state power P_0 and the power corresponding to one state P_1 is expressed as:

$$r_{ex} = \frac{P_0}{P_1} \tag{1.8}$$

1.5 Motivation and Objectives

Due to the higher demand of data in a metro and long haul optical communication links, pursuit of high spectral efficiency has been increasing [74]. In high speed optical communication links interaction of fiber dispersion with the spectral components of the propagating pulse makes the evolving pulse at the receiver end more complex especially in the case of realistic fibers with nonlinearities. A good signaling scheme plays a crucial role in achieving the higher spectral efficiency by optimum utilization of bandwidth. Thus, one of the main concerns of design engineers is to get the best utilization of bandwidth with optimum signal to noise ratio at the receiver end [75, 76]. As the demand of data is keep on increasing therefore, various strategies are required to further enhance the capacity. Few of such techniques are increasing the data rate per channel, employing more number of channels in a multichannel configuration, use of different fiber types, and efficient dispersion management schemes for long haul links [77].

Advanced and multilevel modulation formats provide a cost effective approach to increase the data rate per channel thus to obtain a better spectral efficiency and the quality research is being carried out to use appropriate modulation schemes in the design of high speed optical links [75-77]. To increase the transmission capacity of the link various dispersion management schemes are cited in the literature [15,78] such as pre-chirping at the transmitter level, dispersion compensating fibers at the fiber link level and the optimum filters at the receivers to mitigate the linear dispersion effects. Basically, all these dispersion management schemes are useful for improving the performance of metro and short distance optical transmission links, however, for a long haul transmission, presence of nonlinearities induces phase and frequency shift influences the overall system performance severely. Thus for the long haul links merely GVD compensation at the receiver end is not sufficient to get the original signal back but the periodic dispersion management schemes are required

[15,79]. The aim of the present work is to widen and deepen the understanding of optical channel behavior for various pulse spectrums under sufficient signal strength to visualize the effects of expected linear and nonlinear impairments in the optical transmission. The main focus of this thesis work is to design the cost effective solutions for the optical data transmission, using different advanced modulation formats exposed to different fiber types and terminate with different demodulator or receiver types. During this dissertation, single channel as well as closely packed multichannel optical links are designed and optimized for various fiber impairments. The present thesis also discusses the mathematical modeling for the analysis of various dispersion management profiles for the propoagtion of dispesrion managed pulse. Basically, the shape of the pulse propagating in these maps remains gaussian.

Optical transmission links in the present thesis are designed using commercially available simulation platform OptSim^{TM} and MATLAB with optimum operating conditions.

The objective of the thesis can be summarized as follows:

1. Channel capacity enhancement by reducing the fiber impairments through spectral management techniques.
2. Data rate improvement of the optical communication channel using robust pulse shaping technique.
3. Transmission distance and data rate enhancement using multilevel modulation formats.
4. Long haul optical transmission through pulse shape management.

1.6 Organization of Thesis

This thesis consists of seven chapters. The organization of this thesis is as follows:

Chapter 1 presents an introduction and a brief review of the background of the optical communication along with the issues and challenges encountered in the designing of a high speed optical transmission link. The motivation and objectives are also discussed in this chapter. In the rest of thesis, we discuss different strategies and techniques to overcome the various optical link design challenges and propose some simulation testbed experiments to mitigate the linear and nonlinear impairments present in the practical optical links. The findings of the study show an enhanced capacity of the optical transmission system to meet the future demand of such links.

Chapter 2 provides the literature review of various aspects of optical link design, issues and challenges of the high speed optical link design and strategies adopted in the existing literature to resolve them.

Chapters 3 describe the pulse propagation model through the optical fiber and highlight the effects of spectral management on various linear and nonlinear distortions of the Gaussian pulse propagation. This chapter proposes a model to analyze the SPM and ASE-induced limitations at 40Gbps Gaussian pulses transmission and the effect of chirping. For this analysis RZ pulse of different duty cycle has been considered.

Chapter 4 provides the data rate improvement through the pulse shaping technique. For the same, duobinary technique is used. This chapter provides the duobinary pulse optimization with the optimum selection of electrical filter bandwidth at the transmitter side and optical filter bandwidth at the receiver side. After obtaining the proper duobinary pulse shape optical transmission link for the transmission of duobinary modulated data at 40 Gbps data rate is designed and analyzed for various fiber impairments with fixed OSNR conditions.

Chapter 5 discusses the transmission distance and data rate improvement using multilevel modulation format. This chapter starts with the single channel optical link design using RZ-DQPSK modulation format. The designed single channel transmission link has been tested for three different commercially available fiber types i.e. SSMF, TW-RS and LEAF to evaluate the performance under various fiber conditions. The system simulation has been carried for 10Gbps and 40Gbps data rate to observe the effect of increase in data rate on the performance of fiber. The 10Gbps design is used especially, to compare the performance with the commercially used data rate in optical transmission. To further enhance the capacity, this chapter provides the input data is transmission using both polarization states of the optical carrier in a dual polarized scheme of DQPSK format i.e. DP-DQPSK. This designed DP-DQPSK transmission is subjected to various fiber impairments in symbol aligned and symbol interleaved format of transmitted data.

Chapter 6 discusses the pulse shape management using dispersion management technique for long haul optical communication. This chapter reports an optimum dispersion map profile for the propagation of dispersion managed pulse propagation. The numerical analysis done in this chapter mainly concentrates on comparing various dispersion map profiles and eventually investigates the critical fraction i.e. the ratio of L_{Map} to L_{NL} for each

of these profiles for zero residual condition. The analysis has been further extended for dispersion managed links with negative residual dispersion and initial chirp to ensure stable dispersion managed pulse propagation over a long distance. Finally, the study of collision dynamics between the propagating dispersion managed pulses has been explored to find out the optimum dispersion map profile in this chapter.

Chapter 7 summarizes the outcome and conclusions of the thesis and presents the scope of the thesis for further research.

CHAPTER 2

Optical Link Design Challenges : A Literature Review

2.1 Introduction

Higher demand of data in intense internet applications for metro and long haul networks are the challenges to the researchers and technology developers to explore and exploit the potential of fiber optic communication systems [77]. As discussed in the previous chapter, advancements in optical data transmission and its telecommunication usage is grouped in different generations as per the capability achieved therein. Starting from the first generation in 1980 when the data rate was around 45 Mbps to the present status where the fifth generation is meeting the specification of 100G. However, still the demand of higher capacity motivates the researchers to innovate new technologies or methodologies to further improve the data transmission rate in existing network links [80]. As per Cisco global IP traffic forecast and methodology, by 2019 there will be around 3.9 billion internet users globally, that is more than 51% of global population in 2014 [81]. Large amount of video sharing, Facebook, Youtube and many other multimedia applications based global IP videos will capture 80% of all the projected traffic by 2019 [82].

Thus, the optical communication systems with high data carrying capacity emerged as a hope for these data hungry applications. To meet all these requirements focus is on, first, increasing the data rate per channel, second, increasing the number of information carrying channels in multichannel optical systems. To increase the data carrying capacity of a channel, various techniques are proposed in the literature [85,86] such as the use of complex and spectrally efficient modulation formats e.g. duobinary, DPSK,QPSK, DP-QPSK, M-ary QAM, use of different fiber types e.g. SSMF, LEAF etc , use of various dispersion management schemes etc. Whereas for increasing the number of channel, compact packing of channels in WDM systems, also, focusing towards extending the operating wavelength range from existing C-band (1530nm-1565nm) to L-band (1570nm-1610nm) or S-band (1485nm-1520nm). These approaches again provide different challenges in terms of achieving a flat gain across these three different bands.

Basically, increasing the data rate of a channel birefringence induced PMD appears as one of the challenging factor and since it is a time dependent parameter thus, it will vary

from fiber to fiber and working wavelength of the channel [54]. Basically, significant lengths of fibers were installed before this problem was surfaced, thus the issues of PMD have been carefully addressed in the link designs to increase the data rate [26]. From the initial work of Poole and Wagner in the year 1986 extensive research has been done and proposed useful solutions [87, 88]. Also, because of the improved fabrication facilities, today's commercial fibers have minimum PMD effect.

Another limiting factor in optical links is a chromatic dispersion (CD). In optical link designs it can be compensated using various techniques such as, using fiber Bragg gratings (FBG), using dispersion compensating fibers (DCF) of appropriate length and higher order fiber mode etc. Each of these methods have their own pros and cons, FBG's have lesser insertion loss, small size and less costly but at the same time they have limited operation bandwidth and need circulators to separate out the input and output signals because of the retro-reflected signals. Use of DCF is one of the popular dispersion compensation technique used by the system designers. Although, DCF can provide polarization independent broadband dispersion compensation but at the same time require a significant amount of fiber length (1/4 or 1/6 of SMF). These compensating fibers also suffer from the wavelength dependent losses in case of WDM systems and thus incur additional losses [89, 90]. Higher order mode fibers provides vary high value of negative dispersion thus require vary less fiber length for the compensation but the back and forth transformation of the mode will induce losses and also these fibers induce polarization sensitivity. Although, these linear effects limits the data transmission capacity but still they are easier to manage.

More challenging situation in the design of high data rate optical links comes from the kerr nonlinear effects. For single channel systems SPM is one of such effect. SPM induced pulse broadening was actually observed in CS_2 by R.G. Brewer in 1967 in his experiment for Q-switched ruby laser and later by F. Shimizu in the same year [91]. Also the pulse compression through SPM was first observed by R.A. Fisher and P.L. Kelley in the year 1969 and spectral broadening in fibers was observed by R.H.Stolen together with C. Lin in 1978 respectively [92]. Intensity depended nonlinear effects become more injurious in multichannel systems as optical beam modifies not only its own phase but also the phase of co-propagating pulses due the XPM effect [93]. SPM and XPM are some of the major limiting factor in the design of high speed optical links and can be maintained to a limiting range by properly selecting the transmitting pulse power.

Although, in many practical link designs some time it is not possible, also not beneficial, to completely eliminate linear and nonlinear effects and thus the system designers utilize them to produce a more robust ultrashort pulses which are useful for very long distance optical transmission [94,95].

Advanced and multilevel modulation formats are very effective to achieve the higher spectral efficiency when used in optical transmission channels in the presence of linear and nonlinear impairments. Apart from various other advantages, there are two main advantages of using optimal modulation formats, first, they are more tolerant to linear and nonlinear impairments and, second, their implementation appears to be more economical as they can be suitably fit with the already existing optical network without upgrading the overall systems [75, 77, 96]. Therefore, this chapter provides the basic principle behind the optical modulation and demodulation techniques and the cost-effective modulation formats which can provide good spectral efficiency. Also, how the controlled amount of linear and nonlinear effects is utilized to get the robust pulse shapes for the long haul multichannel optical transmission has also been discussed in this chapter. Organization of this chapter is as follows: section 2.2 provides the various modulation and demodulation techniques employed in optical communication systems. Section 2.3 discusses various data modulation formats used in this thesis for the optical link design. Section 2.4 provides the significance and need of this research work.

2.2 Modulation and Demodulation

Modulation and demodulation are the important functions of any communication systems including optical communication. Section 2.2.1 and 2.2.2 provides the modulation and demodulation techniques used to impress the electrical data on an optical carrier and retrieving back the original data signal respectively.

2.2.1 Modulation in optical transmission

In optical communication, the carrier signal can either be directly modulated by the information data bits or can be externally modulated. In former technique, the optical signal from the laser is directly modulated by transmitting data by switching “on” and “off” the light signal. This is the easiest way to superimpose the data on the optical carrier. Direct modulation of the laser was the main technique till the 1980s and the early 1990s. However, direct modulations have several inherent limitations and one of them is a pulse chirp which results in a spectral broadening of the signal causing several dispersion penalties. Directly-

modulated optical signals experience fluctuations in intensity due to Relative Intensity Noise (RIN) of the semiconductor laser [97]. The non-zero linewidth of laser sources introduces laser phase noise thus for high-speed transmission link designs direct modulation is usually not preferred. Therefore, external modulators become an essential choice for high-speed long-haul optical communication systems. External modulators remove a large amount of wavelength chirping. In optical transmission mainly two types of semiconductor external modulators are used i.e. electro-absorption modulators (EAM) and electro-optic modulator (EOM). Working operation of EAM modulator is based on the Franz-keldysh effects i.e. change in optical absorption with the applied electric voltage [98]. In EAM modulators, the intensity of the light is controlled by an electric voltage. These modulators with less driving voltage requirement and economical in large production, are available for the modulation rate of up to 40 Gbps to 80 Gbps. However EAM modulators have some limitations such as their absorption characteristic is depend on the wavelength, residual chirp, limiting power handling capability and limited extinction ratio (not more than 10 dB) [99].

Electro-optical modulators (EOM) are preferred over EAM due to various advantages of electro-optic materials such as linear response characteristic, high extinction ratio, and capability to control phase, frequency or amplitude of the optical carrier signal [100]. Basically, $LiNbO_3$ EOM has been developed since the 1980s but become popular only with the advent of EDFAs in the late 1980s and mainly employed for coherent optical communication to overcome the problem of laser line width and RIN noise [101]. The operation of EOM is based on the principle of Pockels electro-optic effects of solid-states, polymeric or semiconductor materials which are the change in refractive index of a medium with applied electric field [102]. From many years waveguides of EOMs are mostly integrated on lithium niobate ($LiNbO_3$) materials which have inherent properties such as high electro-optic coefficient, low attenuation and are able to generate chirp-free signals [69].

One of the popular EOM modulators is Mach-Zehnder Modulator (MZM). MZM is preferred with advanced modulation scheme due to their good modulation performance and capability of independently modulating the phase and intensity of optical carrier [103-105]. In this thesis, MZM modulators are used as external modulators.

Proper extraction of information from the transmitted optical signal is an important aspect of the transmission link design. Basically, demodulator design is largely influenced by the type of modulation scheme used at the transmitter.

2.2.2 Demodulation in optical transmission

Major challenges for the design of higher data rate optical transmission systems lay in the design of a suitable receiver for a given transmitted data in the presence of various fiber impairments of the optical fiber. Demodulator or receiver design is an important building block of optical communication systems and needs to perform satisfactorily at the minimum received SNR.

2.2.2.1 Direct detection

Choice of optical receiver depends on the modulation technique or the pulse shape used at the transmitter to encode the input signal. Therefore, detection method will be different for the modulation technique which uses only two levels to encode the signal (on-off schemes) from that which utilizes the multilevel encoding schemes (or Multilevel modulation techniques) [69]. In year 1970s when the research in the area of optical fiber communication started, systems use intensity modulation of the semiconductor laser, this intensity modulated signal transmitted through optical channels and detected by optical receiver consists of photodiode (PIN or APD). This type of optical transmission systems are commonly known as intensity modulated direct detection (IMDD) systems and they are simple to implement. IMDD systems are commonly employed in optical transmissions and due to their simplicity in design they are in use till the present date [106-108]. In Photodiode detection of the optical signal, the electrons generated in the photodetector are electronically amplified through front-end electronic amplifiers which amplify them and then this signal is decoded to get the original information. Electronic amplifiers are the key components of these types of optical receivers. Along with the amplification, their low noise contribution and compact size is an essential attribute for the design of good optical receivers. Some of the main features of IMDD systems are their less complex circuitry, easy detection, low electric power consumption and latency [109]. Chapter 3 of this thesis uses IMDD scheme for the optical link design and analysis.

Although, IMDD schemes are less complex and easy to implement, but to increase the spectral efficiency of the optical transmission various advanced modulation formats like

QPSK, DQPSK, QAM, etc. are required and to retrieve the original information signal from these encoded schemes coherent as well as balance detectors are required.

2.2.2.2 Coherent and Balanced detection

Coherent detection techniques for optical transmission systems were studied extensively in the early to mid-1980s, even the first proposal of coherent detection was done by DeLange in 1970 [110], but this does not attract any attention from optical service providers, as by that time IMDD techniques were the main detection technique. Also, at that time it was difficult to get the stable frequency laser sources. It was in year 1980s when Okoshi, Kikuchi, Fabre and LeGuen independently presents precise frequency stabilization methods for laser sources [111,112]. The important feature of the coherent transmission system is their ability to store the complete information in its carrier in the form of in-phase and quadrature components and state of polarization. They are also able to provide longer repeaterless transmission distances [113]. But definitely, all these advantages of coherent systems will not come free of cost and there are some problems associated with them, such as coherent receivers are more complex and sensitive towards change in phase of the input signal or state of polarization. The phase noise of a semiconductor laser is a major limiting factor for coherent systems. Therefore, even if one can control the frequency drift, carrier phase can fluctuate because of the phase noise, thus small linewidth laser sources are the important requirement for the coherent system designs. These are some of the reasons why coherent detection requires more complex design compare to their IMDD counterparts.

In the year 1990s, many systems were proposed for coherent detection [114], also invention of EDFA at the same time make the short noise receiver sensitivity of coherent receivers less significant, as for the EDFA based transmission systems carrier to noise ratio is mainly determined from the accumulated amplified emission (ASE) rather than by short noise [115]. Many technical difficulties such as stability, stable locking of laser etc. were not properly addressed by that time thus further research and development in coherent detection systems were almost interrupted for years but restarted due to the high demand of data capacity [116]. As the demand for capacity and bandwidth is increasing exponentially thus the multilevel modulation formats with coherent detection attract system designers and engineers. H.Sun K.-T.Wu et al. in the year 2008 presented the use of advanced ADC and DSP and proposed an application specific integrated circuit (ASIC) for 11.5-Gsymbols/s PM-QPSK signal transmission [117]. Later on various advancements in the ASIC and DSP based transceivers has been reported in the literature [118-120].

As discussed earlier in coherent receivers, sensitivity is higher compared with direct detection but they are more sensitive towards the phase and frequency variations and the optimum choice of the local oscillator is a serious task in these types of receivers. Therefore, to avoid complications of coherent receivers but to improve the receiver sensitivity, another scheme popularly used for the constant-envelope modulation formats is balanced detection [121,122]. One of the advantages of balanced detector receiver is their ability to cancel relative intensity noise (RIN) and provides higher reliability. Balanced detector is reported to perform approximately 3dB better when used with sufficiently narrowband filtering in front of MZI compared to their single-ended PIN counterparts [123]. Since the aim of this research work is to provide the easily implementable and cost effective techniques for the capacity enhancement, therefore, coherent receivers are not specifically used here, whereas balanced detectors are used in chapter 5 for the demodulation of transmitted data.

Section 2.3 discusses some of the popular modulation formats based on direct and balanced detection technique. These modulation formats are utilized for the link design in the subsequent chapters of this thesis.

2.3 Data modulation formats

An optical channel provides the vast bandwidth between transmitter and receiver and the good modulation scheme plays a vital role in making the efficient use of this channel bandwidth. The conventional non return to zero (NRZ) and return to zero (RZ) also known as on- off –keying (OOK) is one of the simplest and preferred modulation techniques when the huge bandwidth is available. In fact, in the year 1844 Samuel Morse sent the first telegraph message using the first version of OOK modulation known as Morse code [124]. Therefore, this discussion starts with NRZ and RZ modulation formats as they are the oldest but still in use and also provide a good reference to compare the other modulation formats.

2.3.1 Nonreturn to zero / Return to zero

NRZ is widely used binary intensity or amplitude shift keying type of modulation format it requires minimum bandwidth and minimum optical peak power per bit interval, and less sensitive to laser phase noise [125]. For long distance optical systems NRZ modulation is found to be less susceptible to SPM and GVD effects because of its narrower spectral width. However, in higher bit rate optical transmission systems RZ modulation formats proved themselves better than NRZ in terms of robustness towards distortions and

time synchronization. Although, the performance of RZ format is betters than NRZ but at the same time their transmitter design is more complex than NRZ [126]. Basic block diagram to generate NRZ pulse shape is shown in Figure 2.1. NRZ modulated signal can be generated using MZM modulator where input electrical signal is modulated by external MZM modulator and convert the electrical signal to optical signal at the same data rate. MZM modulator is biased at its quadrature point and is driven from minimum to maximum transmission with switching voltage V_{π}. A simple photodetector is sufficient at the receiver to detect the NRZ coded signal. For coherent detection NRZ modulation has an inherent problem, such as there is no error correction and self-clocking features. Therefore, for the long strings of ones and zeros, there is a problem of timing information also ISI is more dominated in NRZ format [75].

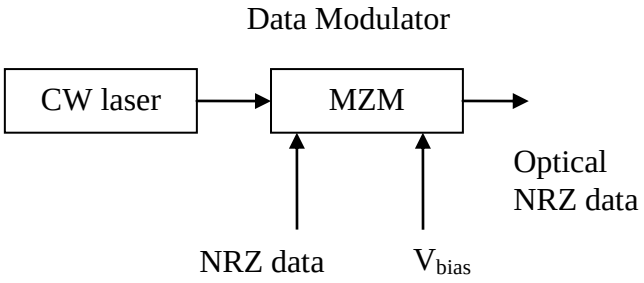

Figure 2.1: Generation of optical NRZ signal

Figure 2.2 shows the generation of RZ modulated pulse in optical domain. Unlike NRZ, for RZ pulse the width is smaller than its bit period. Basically, to generate RZ pulse two modulators are required, the first modulator known as pulse carver consists of dual drive MZMs driven by two opposite sinusoidal signals.

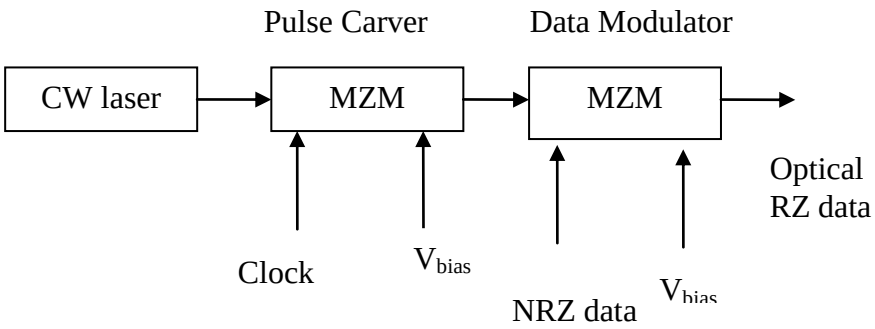

Figure 2.2: Generation of optical RZ signal

To generate the RZ pulses this carver is biased at $\pm V_{\pi/2}$ with the Vp-p of $V_{\pi/2}$ and the generated pulses have a π phase difference for the state "1" and state "0" of the input pulse sequence. Different types of RZ pulses can be generated by varying the amplitude of the driving voltage. Out of various other RZ pulse shapes, 67% duty cycles RZ or CSRZ is more popular in high-speed optical transmission [127]. Basically, in the year 1999 Sano, Miyamoto et al. proposed the CSRZ transmission over a periodically dispersion compensated optical link [128,129].CSRZ perform better in the presence of chromatic dispersion and fiber nonlinearities. An early study of the impact of nonlinearities on modulation formats conducted for per channel data rate of 40Gbps has used CSRZ [130]. Initially, CSRZ was preferred choice for short distance high power WDM systems as it is able to suppress IFWM and later it was used for long distance communication as well [131]. In chapter 3 different duty cycle RZ pulses are used for the 40 Gbps data transmission.

2.3.2 Duobinary

Another modulation format or pulse shaping technique which is very popular for transmission link designs due to its various inherent features is duobinary. Duobinary technique was first proposed by A. Lender in 1960s for electrical signals and later it was used for optical transmission [132]. In the year 1980, an optical three amplitude level duobinary experiment was reported at the data rate of 280Mbps in which the improvement in the receiver sensitivity was confirmed by utilizing the matched filters at the receiver side [133]. Price, Mercier et al analyzed a reduced bandwidth optical intensity modulation with improved CD tolerance [134]. Yonenaga and Shibata et al experimentally analyzed an optical duobinary transmission system with no receiver degradation [135]. Now a day's duobinary modulation has been used for high-speed optical transmission systems. Duobinary is a type of modulation with data capacity comparable to quaternary modulation schemes but at the same time implementation complexity is almost comparable to the normal binary system. Also, there is no need of ideal low pass rectangular baseband filters. Duobinary is also a cost effective approach compared with other advanced modulation formats as it requires less dispersion compensation [136]. Block diagram to generate the duobinary signal is shown in Figure 2.3. Duobinary transmitters use differential pre-coders at the input to avoid the error propagation. Low pass electrical filter converts this pre-coded signal into three-level electrical signals.

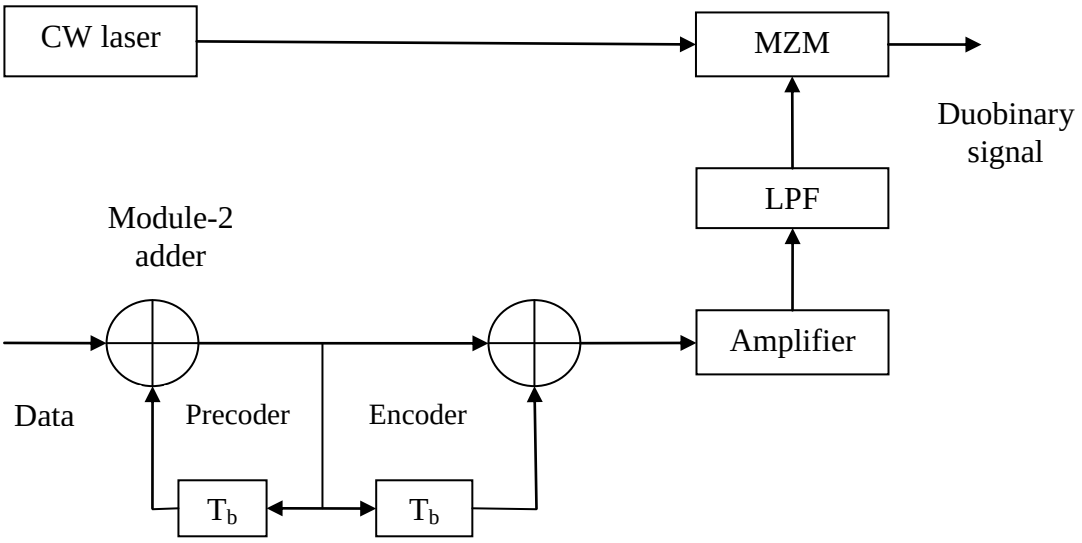

Figure 2.3: Generation of duobinary signal

The selection of this low pass filter is very crucial as it will improve the chromatic dispersion tolerance. Normally the bandwidth of this electrical LPF is equaled to the quarter of bit rate [137]. Optical link design using duobinary technique has been proposed in chapter 4 of this thesis.

2.3.3 Differential phase shift keying

Differential phase shift keying (DPSK) is a phase modulation format. Advantages of phase modulation formats in optical transmission have been known since mid-1980's and phase shift keying (PSK) modulation was used as early as 1962, when the Bell 201modem was introduced [138]. In the beginning of the year 1980, the DPSK protocol for air traffic control radio communication was implemented. In early days of these communication link implementations, designers use low-cost FSK or PSK modulation schemes to minimize the cost. Compared to the performance of these schemes to the DPSK format there is an added performance improvement but the main challenge was the availability of low-cost DPSK demodulators [138]. From recent years a good amount of research is going to use the PSK schemes for optical data transmission [139]. DPSK is a fast and stable modulation format and the modulated signal is not the binary code itself, but a code that record change in the phase of the binary stream and this make receiver design simple as it has to detect only the changes in phase not the absolute phase of the incoming signal [140,141]. Several studies have compared the performances of OOK modulation with DPSK and reveal the improvement in the transmission distance (improving the range by 3-6 dB) using DPSK modulation as compared to OOK modulation [123]. DPSK have some added advantages

compared to PSK as well, as the information is stored in the phase change, not in the absolute phase so it is good for the specific systems where exact phase is not known or if the system is affected by the phase noise and still detection is possible using DPSK modulation [142]. Experimental demonstration using DPSK at 10Gbps for submarine transmission shows improvement in BER compared to amplitude modulated or OOK modulation schemes and justify that the DPSK modulated data is more tolerant towards nonlinear effects in ultra long haul systems [143,144]. Also, the lower OSNR requirements of DPSK modulation technique make it suitable for long haul transmission.

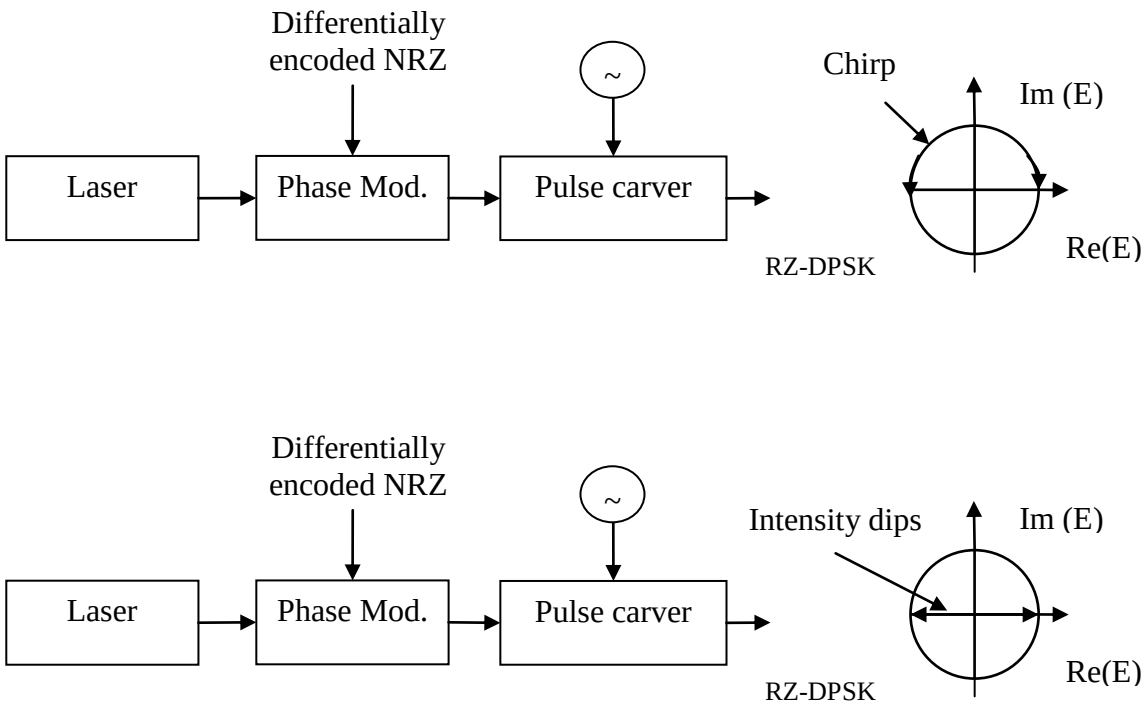

Figure 2.4: Generation of RZ-DPSK signal

DPSK signal can be generated by using either phase modulator or using MZM as shown in Figure 2.4. The optical power appears in each bit slot, with the binary input data is encoded as either 0 or π phase difference between the two symbols. The power in each bit can occupy by either full bit slot (NRZ-DPSK) or can appear as an optical pulse (RZ-DPSK).

Since the phase modulation cannot occur instantaneously and the phase modulation technique of DPSK introduces chirp across the bit transmissions. Here as well, to generate RZ pulses pulse carver is required which is performed by the second MZM modulator it

carve the pulses coming from phase modulator and generating the RZ-DPSK modulated signal. MZM needs to be biased at the null to generate the phase modulated signal and switching voltage should be double of that is required for OOK modulation [75].

2.3.4 Differential quadrature phase shift keying

There are many applications of phase modulated schemes in optical communications and to further increase the spectral efficiency, researchers are moving towards multilevel schemes. Differential quadrature phase shift keying **(**DQPSK) is the only true multilevel modulation scheme [145]. In DQPSK modulation the input data sequence is converted into four phase states of optical carrier i.e. 0, +π/2, -π/2, π and at the receiver side transmitted signal will be demodulated through the phase difference between two successive bits. Spectral efficiency of DQPSK is higher than the DPSK encoded signal although the spectrum of both are comparable. This is due to that fact that in case of DQPSK the symbol rate is half of the bit rate thus the spectrum is compressed in frequency by a factor of two [146-148]. Narrow spectrum makes DQPSK modulated signal performs better in the presence of CD and other fiber nonlinearities.

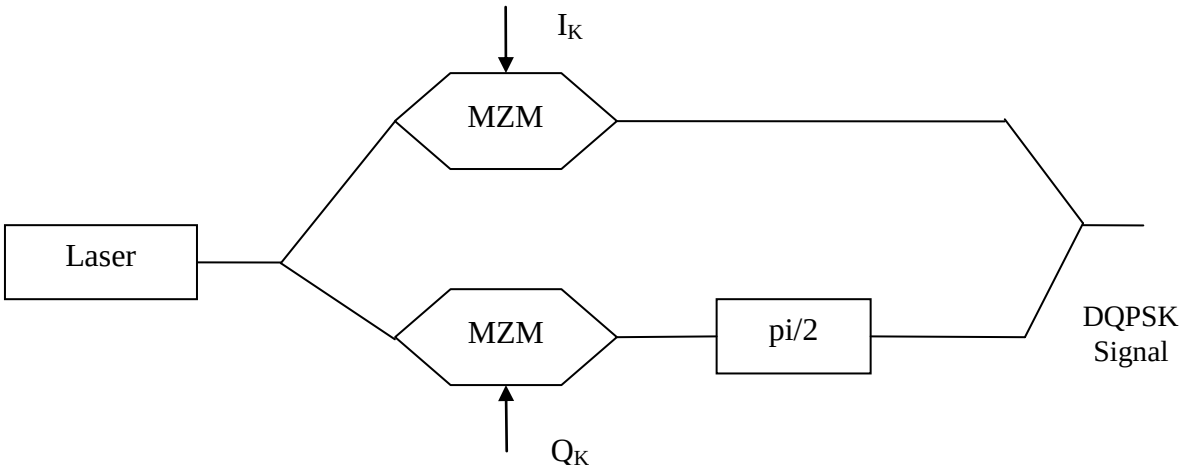

Figure 2.5: Generation of DQPSK signal

Generation of DQPSK modulated signal is shown in Figure 2.5. The input optical signal is divided into two paths with a phase shift of π/2 and applied to two different MZMs which are driven by the in-phase and quadrature-phase electrical signals and in this way both branches of optical carriers are converted into two DPSK signals. The upper branch will be mapped into 0 and π in the real axis and the lower branch will be shifted by π/2 phase shift and mapped as +j and –j [75]. Chapter 5 of the thesis provides an optical link design using RZ-DQPSK modulated signal.

2.3.5 Dual polarization-differential quadrature phase shift keying

Over the time, system designers have already utilized the amplitude, frequency, and phase of optical carrier to transmit the input information bits, but to meet the everyday increasing demand of data, there is a need to keep on upgrading the existing information carrying capacity of the channels. Multilevel modulation formats came to further improve the information carrying capacity of existing optical transmission systems. Data capacity can be further improved by encoding data in both the polarization state of the carrier. As the current transmission rate is moving toward the 100Gbps per channel and the modulation formats used for 10 and 40Gbps cannot be directly applied to them [149,150]. Therefore, one of the major challenges with 100Gbps transmission link designs is to choose the best modulation formats. The modulation format should satisfy lower bandwidth specifications of existing optoelectronic components and also will be able minimize the limitations of chromatic and polarization mode dispersion. Thus, low symbol rate multilevel modulation formats are popular choices in 100Gbps transmission systems. Some of the popularly used 100Gbps modulation formats are: differential phase shift keying-three level amplitude shift keying (DPSK-3ASK), Dual polarization- DQPSK (DP-DQPSK), four carrier-optical duobinary (FC-ODB), Dual carrier-DQPSK (DC-DQPSK), Dual polarization-QPSK (DP-QPSK) etc. The basic attributes of these formats are summarized in Table 2.1.

Table 2.1: 100Gbps Modulation formats [149]

Format	**DPSK-3ASK**	**DP-DQPSK**	**FC-ODB**	**DC-DQPSK**	**DP-QPSK**
Detection	Direct	Direct	Direct	Direct	Coherent
Application	Metro	Metro	Metro	Metro/Core	Core
Symbol Rate(GBd)	43	28	28	28	28
WDM Grid (GHz)	100	50	100	50x2/100	50

From the table 2.1, it can be observed that DPSK-3ASK, DP-DQPSK, FC-ODB, DC-DQPSK and DP-DQPSK are direct detection modulation formats whereas DP-QPSK is coherent detection technique. Although the performance of coherent demodulation formats is better than the direct detection formats but this comes at the cost of more complex electronic circuitry and more electric power consumption [151,152]. Direct detection is

more economical approach compared to the coherent systems for short distance optical communication. The simplicity of the systems is one of the attributes of direct detection systems and this is the reason that various advanced modulation formats are optimized for direct detection. Direct detection schemes are very popular and a good amount of literature is available with the comparison of direct detection based modulation schemes for metro area networks [153-154]. For the transmission of data, spectral planning plays a crucial role and as per ITU channel grid standard, 50GHz is used for the core network and 100 GHz is used for the metro networks. Basically, filter technology mainly affects this standardization [155]. This thesis aims to provide the good spectral efficiency with the easy and cost effective implementation, thus, the dual polarized modulation format with direct detection DP-DQPSK is selected for the optical transmission link design.

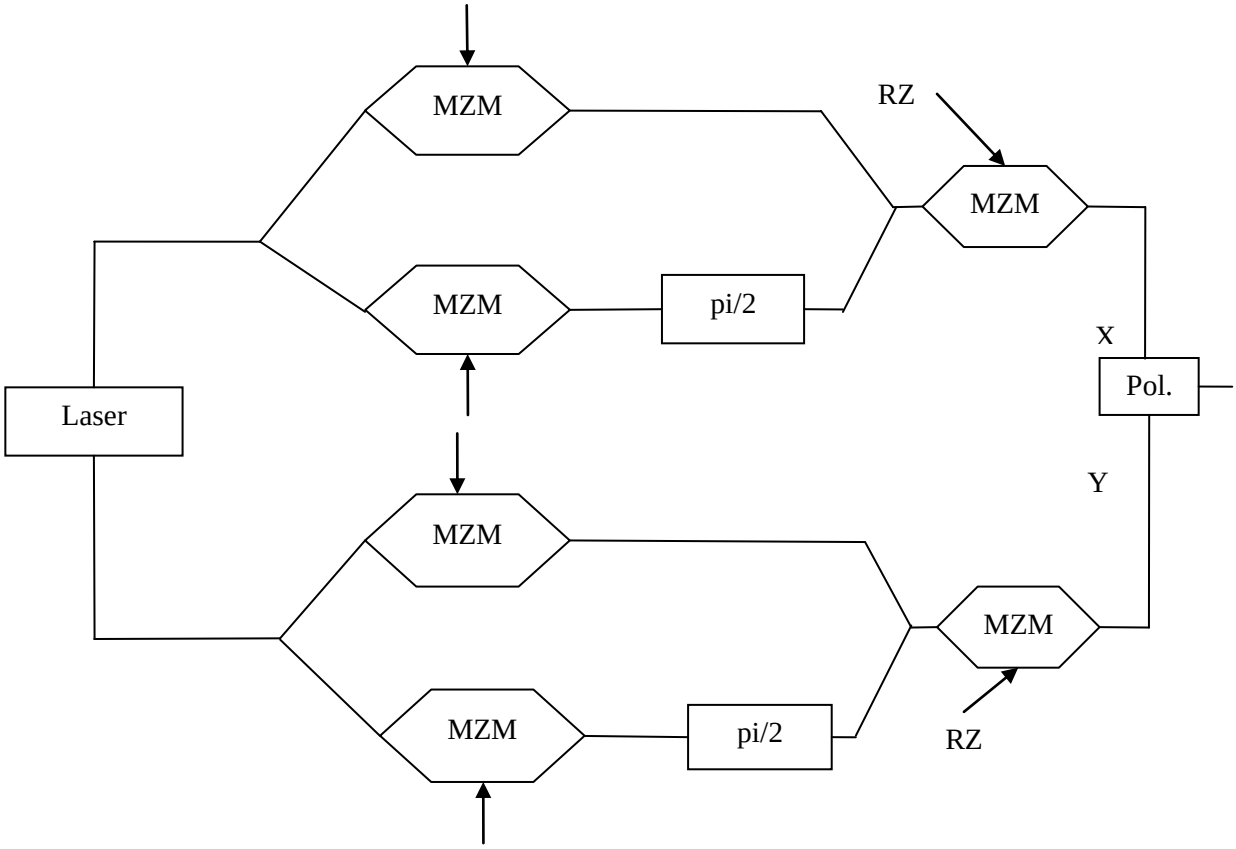

Figure 2.6: Generation of DP-DQPSK signal

Figure 2.6 shows the generation of DP-DQPSK modulated signal where X and Y-polarized components are combined at the transmitter and at the receiver polarization de-multiplexer separate out them to retrieve the original information signal [156,75]. Chapter 5 of the thesis provides the link design using DP-DQPSK modulation format for 9 channel

DWDM configuration with 50GHz ITU grid. The designed DP-DQPSK link has been optimized for various linear and nonlinear effects.

All the above discussion justified the fact that the use of spectrally efficient modulation formats is a good approach to upgrade the transmission capacity of the channels. Similarly, it is also observed that if one will keep on upgrading the modulation formats then their circuit complexity also increases. Also, in long haul optical transmission links, nonlinearities become so dominant that it becomes really difficult to accommodate more number of bits per symbol and retrieve them properly at the receiver. Therefore, along with the use of advanced modulation formats, implementation of different types of dispersion management schemes along the length of the transmission links is a another technique and widely adapted in multichannel long distance optical links [157,158].

Choice of proper pulse shape for these dispersion management maps is an important design requirement to get the optimum advantage from them. Popular pulse shapes used in dispersion managed systems are NRZ, chirped RZ, DPSK and dispersion managed (DM) soliton [159-163]. Out of these shapes, DM soliton is the most appropriate, as it balances out the dispersion and nonlinear effects thus overcome one or the other shortcomings of other pulse shapes [164,165]. Although, the existence of solitons in lossless fibers was theoretically explained by Hasegawa and Tappert in 1973 and study of soliton transmission in optical fibers was first done by James P. Gordon along with R.H. Stolen and L.F. Mollenauer in 1986 [166,167]. But it was in the year 1987 when the concept of the existence of dispersion managed soliton was first proposed [168]. Basically, soliton opens the scope of much awaited all-optical transmission and after the proposal of use of Raman gain of the fiber itself for the transmission. The concept was first used for long distance experiment in 1988 by Mollenauer and Smith [169], later these Raman amplifiers were replaced by EDFAs in year the 1990 [170]. Also all optical communication was challenged by many researchers, Gordon and Hauss predicted that amplifier noise induces timing jitter as it introduces frequency fluctuations and influences the SNR of the transmission link [170]. Dispersion managed solitons have been a topic of extensive research from last few decades owing to their capability in meeting the demand of higher data rate while providing improved quality of information transmission in nonlinear optical fiber [171-173].

In linear systems, amplifier noise deteriorates the signal to noise ratio but this will not be the case with solitons as one can easily increase the amplitude of the signal with appropriate selection of dispersion in a fiber. However due to amplifier noise, frequency

modulation introduces a velocity modulation, results in a jitter in the arrival time of soliton pulses and contributes to the overall jitter [173].Therefore, through the rigorous literature review it is evident that in modern optical transmission systems various techniques have been implemented to improve transmission distance and capacity. Some of the popularly used methods are the use of advanced modulation formats, dispersion compensation techniques, different types of fibers, parallel transmission at different windows, and implementation of dispersion managed maps etc. Although lot more research has already been done in optical link design and optimization but still there is a scope of further research. Based on the extensive literature review we have identified some of the areas for the further work.

2.4 Scope of the thesis

1. Literature is available showing various spectral management techniques to improve the performance of the optical transmission link but limited literature shows the analysis at 40Gbps of different duty cycles pre-chirped Gaussian pulses. The present thesis investigate and explore this scope.

2. Use of spectrally efficient modulation technique is another approach to improve the data carrying capacity of the optical transmission links. Duobinary is an efficient data transmission scheme but less data is available for the mitigation of the fiber impairments through electrical and optical filter optimization at different OSNR conditions. This thesis shows propagation of RZ/NRZ duobinary pulses at 40Gbps at different OSNR values. Optimized electrical and optical filter are used which can shape the spectrum of the pulses and make it robust towards various fiber impairments.

3. Multilevel modulation formats are popularly used for the design of high speed optical links. Limited literature is available showing the comparison of SSMF, LEAF, TW-RS types of single mode fibers in the DQPSK modulated transmission channel, Present thesis provides the comparison among LEAF, TW-RS and SSMF fibers for the RZ-DQPSK modulated data transmission at different data rates. Also, for the future high speed optical links dual polarization format of DQPSK i.e. DP-DQPSK is utilized in the multichannel transmission system with the data rate of 112Gbps per channel and designed link is subject to various linear and nonlinear effects.

4. In long haul WDM systems pulse shaping technique to maintain the shape of the propagating pulse is a useful approach. Dispersion managed maps are used for the stable pulse propagation. For the same dispersion managed soliton is a popular choice and a good amount of literature is available which demonstrated the pulse propagation, but still there is a limited literature which can provide the comparison among the various dispersion map profiles. This thesis provides a numerical analysis to find the optimum dispersion map profile for dispersion managed soliton propagation and methods for the further intensification of the transmission distance

CHAPTER 3

Optical Link Performance Enhancement: RZ-Modulated Gaussian Pulse

3.1 Introduction

Ever increasing demand for high speed metro and long haul communication links has triggered a growing interest in deploying optical communication systems and networks. The lower chromatic dispersion at 1300nm has extensively been explored, however, the advent of EDFA as a line amplifier has shifted that preferred wavelength choice to 1550nm. In general, the speed of optical data pulse is mainly limited by pulse spread due to dispersion and therefore pulse spectrum manipulation at the launching point at the fiber plays a crucial role during propagation. Various modulation schemes provide different spectrum and thus gives a choice to use them appropriately to counter the deterministic caused in the pulse shape during propagation through dispersion and nonlinear limitations. Modulation schemes such as Return to Zero (RZ) and Non-Return to Zero (NRZ) are the oldest yet preferred modulation formats for data transmission in optical transmission links. The performance of RZ modulation formats proves better than NRZ in terms of robustness against distortion and time synchronization. Moreover, RZ modulated signal stream consisting of a sequence of similar pulse shapes is more tolerant to non-optimized dispersion maps. In the literature, dependency on the pulse shape to achieve an optimum balance between fiber nonlinearities and dispersion using RZ formats has been well appreciated for high data rate optical links [174].

The core of optical communication systems is a fiber. When data is transmitted through the fiber, it gets influenced by the various impairments of the fiber. Therefore, before starting the analysis on transmission pulse, here, the mathematical model to understand the pulse propagation through single mode fiber under appropriate fiber conditions has been discussed. So this chapter starts with the discussion of the Gaussian pulse propagation in section 3.2, Section 3.3 provides the analysis of SPM induced limitation on the chirped RZ modulated Gaussian pulse. In the section 3.3 influences of chirp parameters, under different duty cycles of the RZ format has been simulated to evaluate the link performance in terms

BER-equivalent Q-factor in the graphs written as Q-factor. Section 3.4 presents the influence of ASE noise on the propagation of these chirped Gaussian pulses. The important result of the chapter is summarized in section 3.5.

3.2 Pulse propagation in optical fiber

An optical signal power attenuates while propagating through the fiber which is usually compensated by placing all optical amplifiers at certain distances. This signal amplification is required to maintain the desired SNR. Sometimes higher input peak power is considered a choice to increase the separation distance between line amplifiers to reduce the number of repeaters in the link. However, in such cases increased input peak power forces the fiber to operate in the nonlinear regime. Therefore, it becomes important to study and investigate various linear and nonlinear effects for proper optical communication link design [15]. Fiber acts as a nonlinear medium for the propagating signal where the refractive index depends on the intensity of pulse which makes the medium characteristics a time dependent and can be characterized by pulse intensity profile $I(t)$. This nonlinear refractive index (n_{nl}) can be expressed as:

$$n_{nl} = n_0 + n_2 I(t) \tag{3.1}$$

$$n_{nl} = n_0 + n_2 \frac{P}{A_{eff}} \tag{3.2}$$

where n_0 is a linear refractive index, n_2 is Kerr coefficient or nonlinear coefficient of the guided medium, $I(t)$ is the intensity of the pulse train, P is the average optical power of the pulse corresponds to $I(t)$ and A_{eff} is the effective area of the fiber.

A Nonlinear Schrodinger Equation (NLSE) is used to analyze the behavior of signal propagating in an optical fiber including the amplitude, dispersion and nonlinear effects of the propagating signal. The basic form of NLSE is [26]:

$$\frac{\partial A}{\partial z} + \frac{i\beta_2}{2}\frac{\partial^2 A}{\partial t^2} = i\gamma |A|^2 A - \frac{\alpha}{2} A \tag{3.3}$$

where $A = A(z, t)$ is an amplitude of a Gaussian input pulse and is associated with the electric field E of an optical signal in a fiber. Propagation of Gaussian pulse in fiber is considered by taking initial amplitude of that pulse, which can be expressed as [26].

$$A(0,t) = A_0 \exp\left[-\frac{1+iC}{2}\left(\frac{t}{T_0} \right)^2 \right] \tag{3.4}$$

here, A_0 is peak amplitude, C is chirp factor, T_0 and t are the input pulse width and time period of the wave travelled respectively. β_2 is Group velocity dispersion coefficient, α is fiber loss and γ is the nonlinear coefficient.

Dispersion, as discussed in chapter 1, is a linear effect and the major limiting factor in high speed data transmission and must be addressed properly for the reliable communication link design. Equation (3.3) has to be solved to analyze the group velocity dispersion (GVD) effects on the pulse propagation. Moreover, the dispersion is a cumulative effect and gets accumulated with the fiber length. Usually owing to GVD effects, pulse width broadens to $\sqrt{2}$ times beyond each of the dispersion length L_D defined as $\frac{T_0^2}{|\beta_2|}$. Thus dispersion length is an important scale over which dispersion effect becomes important for pulse evolution and plays a crucial role in determining the related limitation in the optical link design. Along with the dispersion, Chirp (C) is another important factor which affects the pulse shape during the propagation. This chirp parameter is the change in carrier frequency with time as mentioned in equation (3.4). A pulse is said to be chirped when there is a sudden change in carrier frequency, and this can be either in-phase or out of phase. The frequency change as a function of chirp parameter is expressed as [26]:

$$\Delta f(t) = \frac{1}{2\pi}\frac{C}{T_0^2}t \tag{3.5}$$

Basically, the product of β_2 and C decides the pulse shape during propagation. Thus, the pulse will either broaden or compressed during transmission and this is decided by the product of $\beta_2 C$ and the same can be observed from Figure 3.2 and 3.3 for the positive and negative value of $\beta_2 C$ factor respectively. Figure 3.1 shows the unchirped Gaussian pulse shape at the launching stage of the fiber. Thus, for a system working at 1.55μm the GVD (β_2) is a negative quantity, therefore, for a negatively chirped pulse $\beta_2 C$ factor becomes positive and this leads to a quicker broadening of the pulse as depicted in Figure 3.2 whereas when $\beta_2 C$ is a negative quantity in case of positive chirp value, the pulse will observe compression as can be observed from Figure 3.3. These results validate the

influence of pulse and channel parameter on the propagating pulse shape and thereby on the spectrum of the launched pulse.

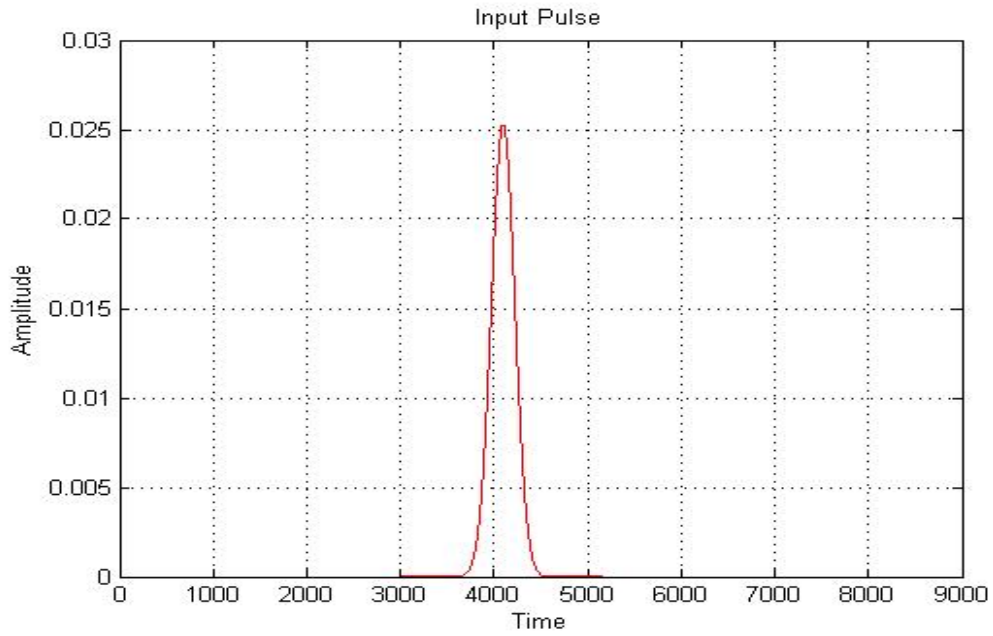

Figure 3.1: Initial input Gaussian pulse shape.

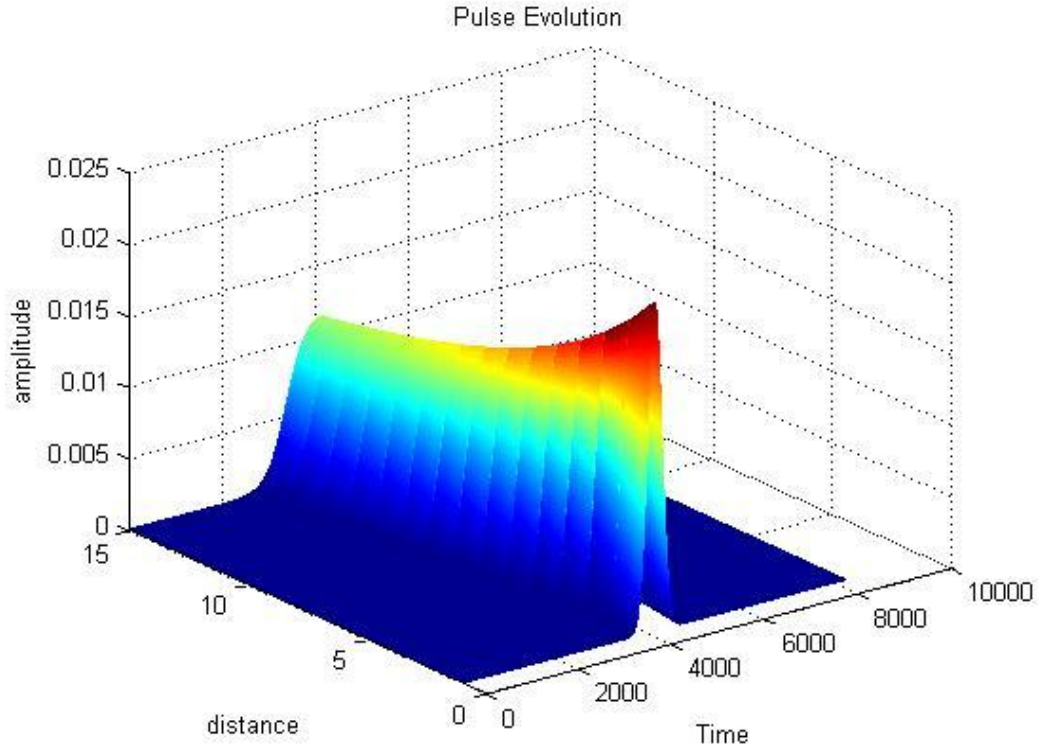

Figure 3.2: Propagation of Gaussian pulse with $\beta_2 C$ factor positive

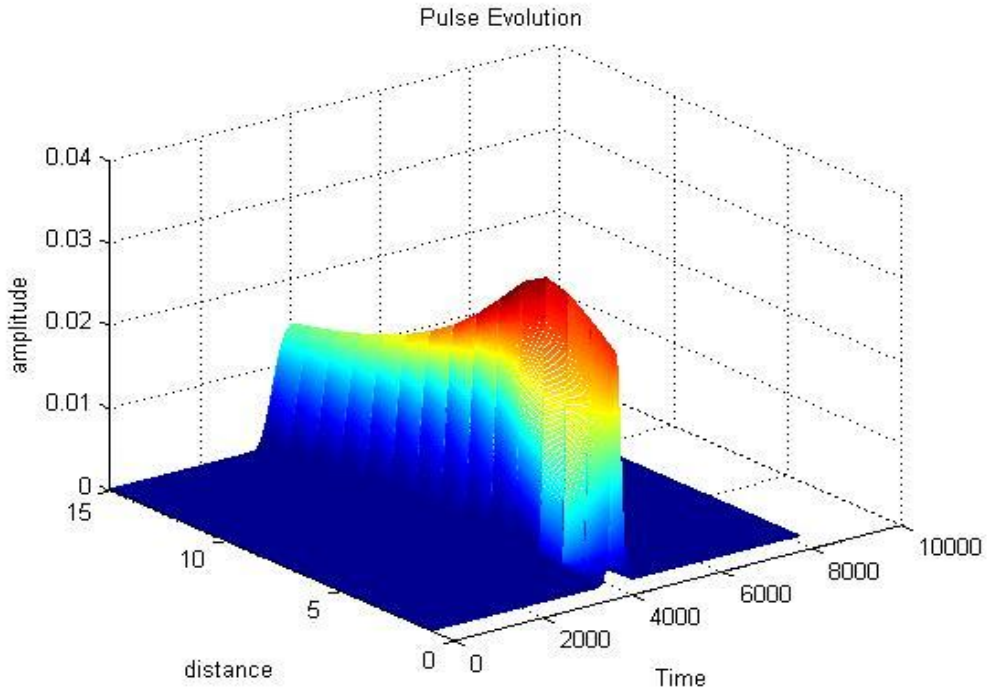

Figure 3.3: Propagation of Gaussian pulse with β_2C factor negative

Although, dispersion and chirp affect the shape of transmitting pulse but they only introduce a linear distortion which is comparatively easier to compensate, however, the nonlinear phenomenon occurring in optical fibers due to Kerr effect as expressed with the coefficient γ in equation (3.3) introduce a rather complex spectral distortion. For single channel transmission systems this dominates in terms of self phase modulation (SPM) as discussed in chapter 1 and causes a time dependent nonlinear phase variation which leads to frequency chirp.

Also, the effect of nonlinearity grows with the intensity of the fiber, for a given power, the intensity is inversely proportional to the area of the core, As the power is not uniformly distributed within the cross section of the fiber thus it is important to define an effective area of the fiber which is related to the actual area as [26]:

$$A_{eff} = \frac{(\int_{-\infty}^{\infty}\int |F(x,y)|dxdy)^2}{\int_{-\infty}^{\infty}\int |F(x,y)|^4 dxdy} \tag{3.6}$$

A_{eff} is an important parameter as the nonlinear effects are defined in terms of it for the fundamental mode propagating in the given type of fiber.

Similar to the dispersion length it's important to understand a nonlinear length after which nonlinear effects start dominating the pulse propagation in the fiber and this is expressed as below where P_0 is the peak power of the pulse

$$L_{NL} = \frac{1}{\gamma P_0} \tag{3.7}$$

The increase in P_0 reduces the nonlinear length, thus, deteriorate the performance of the communicating link. As nonlinear interaction depends on the transmission length and the cross-sectional area of the fiber, thus careful management of pulse energy and shape management is required for a high speed optical fiber communication link design.

Similarly, the third parameter present in the equation (3.3) is the fiber attenuation coefficient (α) associated with the internal fiber losses. As the signal propagates along the transmission link its power decrease because of the fiber attenuation, and this is the reason most of the nonlinear effects occur early in the fiber span and corrupt the pulses for the rest of their journey. Basically, material absorption and Rayleigh scattering are the two main mechanics of losses in optical fibers. In today's fibers material absorption loss is reduced to almost negligible level for the wavelength of interest (0.8-1.6μm), left with the loss due to Rayleigh scattering [1]. Since the complete modeling of these effects throughout the propagating path is fairly complex so for simplicity it is possible to assume that for a certain length, power remains constant and this is known as effective length (L_{eff}) of the fiber. In the absence of fiber losses ($\alpha = 0$), L_{eff} becomes equal to L i.e. the actual length of the fiber. The maximum phase shift $\phi_{\max}$ related to the effective length and the actual length of the fiber and occurs at the pulse center located at $T = 0$.

After understanding the basic mechanism of Gaussian pulse propagation through optical fibers, simulation test bed is prepared using commercially available optical communication tool OptSim^{TM} to analysis the effect of SPM on the behavior of chirped Gaussian pulse. The transmission link is designed at 40 Gbps data rate as discussed in section 3.3.

3.3 SPM induced limitations for chirped Gaussian pulse propagation at 40Gbps

As discussed earlier to maintain the SNR in optical transmission links, amplifiers are important and need to be placed at certain distances to boost up the signal power. Higher input peak power than would have been a choice to increase the separation distance between amplifiers. But as the input peak power increases SPM starts dominating the pulse transmission in the single channel fiber systems, thus it is important to analyze SPM effect for high-speed links. For the present analysis, the bit rate of 40Gbps has been considered for the transmission of pre-chirped RZ modulated pulse at different duty cycles. Figure 3.4 shows the simulation setup of 40Gbps optical transmission link to study SPM induced nonlinear effects. Transmitter section consists of PRBS generator, NRZ pulse generator, and an external modulator. Here, to generate RZ coded pulses electrical NRZ modulator and optical pulse carver are used which provides input to MZM. Here for the SPM analysis dispersion is completely neglected with proper design parameters.

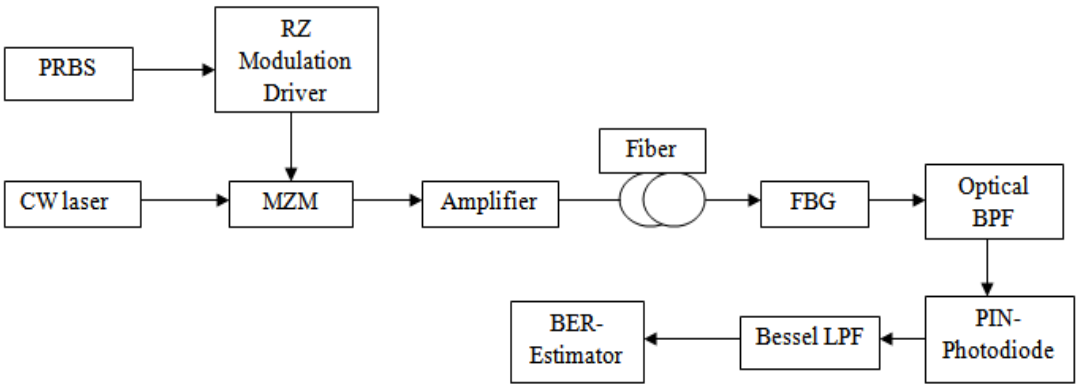

Figure 3.4: Layout for 40Gbps link to study SPM effect

For the simulation dispersion shifted fiber (DSF) of 50 Km length is considered. The other parameters of DSF are: attenuation α = 0.2dB/km, dispersion (D) = 0.2ps/km-nm and dispersion slope S is 0.07ps/nm^2/Km at 1550nm. Similarly, other simulation parameters are nonlinear refractive index n_{nl} is 3 x 10^{-20}m^2/W and core effective area (A_{eff}) as 60.805μm^2. Input peak power of the pulse is varied from 10mW to 80mW, higher power is considered for the extreme case analysis. MZM with an offset voltage of 0.5V, the extinction ratio of 20dB and the 3 dB average power reductions due to modulation is considered. The Optical

splitter is considered as ideal and thus its attenuation is considered to be 0dB. PIN diode with a quantum efficiency of 0.7, the responsivity of 0.8751 A/W, the dark current of 0.1nA and 3dB bandwidth of 20 GHz is used. The simulation has been carried out for chirped Gaussian pulse with the duty cycle of 33.3%, 50%, and 66.67%.Value of the chirp parameter considered for the present work is = -1.0, -0.5, 0, 0.5 and 1.0. As source chirping plays a significant role in deciding whether pulse broadening or compression will take place during pulse propagation through a fiber. Thus, in the present case as β_2 is negative, a negative value of C makes $\beta_2 C > 0$ to broaden the pulse monotonically and for $\beta_2 C < 0$ i.e. for a positive value of C, the pulse width decreases initially and becomes minimum at a distance z_{min} [5]. Thus, $\beta_2 C < 0$ leads to pulse compression for $z < z_{min}$ and pulse broadening for $z > z_{min}$. Table 3.1 discusses all such cases considered for the analysis.

Table 3.1: Variation of pulse shape while propagation for different chirp for duty cycle of 33.33%, 50% and 66.67 % [175].

Duty Cycle	T_0(ps)	L_D(Km)	Chirp (C)	Z_{min} (Km)	Pulse Shape
33.33%	8.33	272.02	-1.0	NA	M.B
			-0.5	NA	M.B
			0	NA	M.B
			0.5	108.81	C.B
			1.0	136.01	C.B
50%	12.5	612.53	-1.0	NA	M.B
			-0.5	NA	M.B
			0	NA	M.B
			0.5	245.01	C.B
			1.0	306.26	C.B
66.67%	16.67	1089.38	-1.0	NA	M.B
			-0.5	NA	M.B
			0	NA	M.B
			0.5	435.75	C.B
			1.0	544.69	C.B

NA: Not Applicable, M.B: Monotonically broadening, C.B: Compressed till Zmin & then broaden

From Table 3.1 it can be observed that for chirp value of -1.0, -0.5 and 0 the pulse will broaden monotonically whereas chirp values of 0.5 and 1.0 will make the pulses undergo compression throughout the length of fiber L (i.e. z = 50 Km) as $z < z_{min}$. The 40 Gbps link shown in Figure 3.4 is simulated for 33.33 % duty cycle to evaluate the BER-equivalent Q factor value of the link with the increase in input peak power for chirped sources and the results are shown in Figure 3.5.

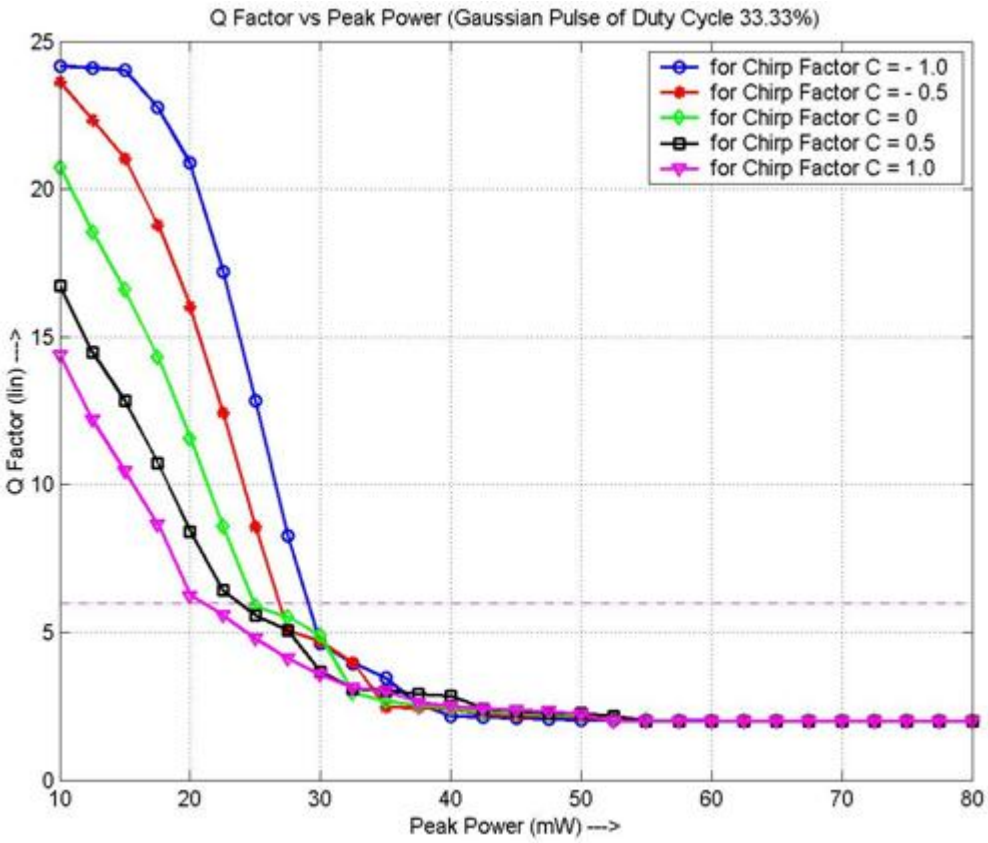

Figure 3.5: Q-Factor vs. Peak Power for duty cycle of 33.33%

From the Figure 3.5 for the 33% duty cycle pulse for different source chirping, it is observed that SPM induced nonlinearity is seen maximum for C = 1.0 and minimum for C = -1.0. Since for the case of C = 1.0, maximum pulse compression i.e. minimum pulse width leads to maximum intensity variation. Hence, intensity dependent nonlinear effect causes the highest reduction in Q factor. Whereas for C = -1.0, pulse broadens monotonically which leads to minimum intensity variation and thus minimum SPM induced effect is observed in this case. Thus, source chirping of -1.0 makes the pulse more resistant to SPM effect as it achieves minimum required Q factor (6) at maximum input power as compared to other chirping values of the source. Maximum allowed input peak power providing a

reliable communication implies a reduction in the number of amplifiers to be used in link design.

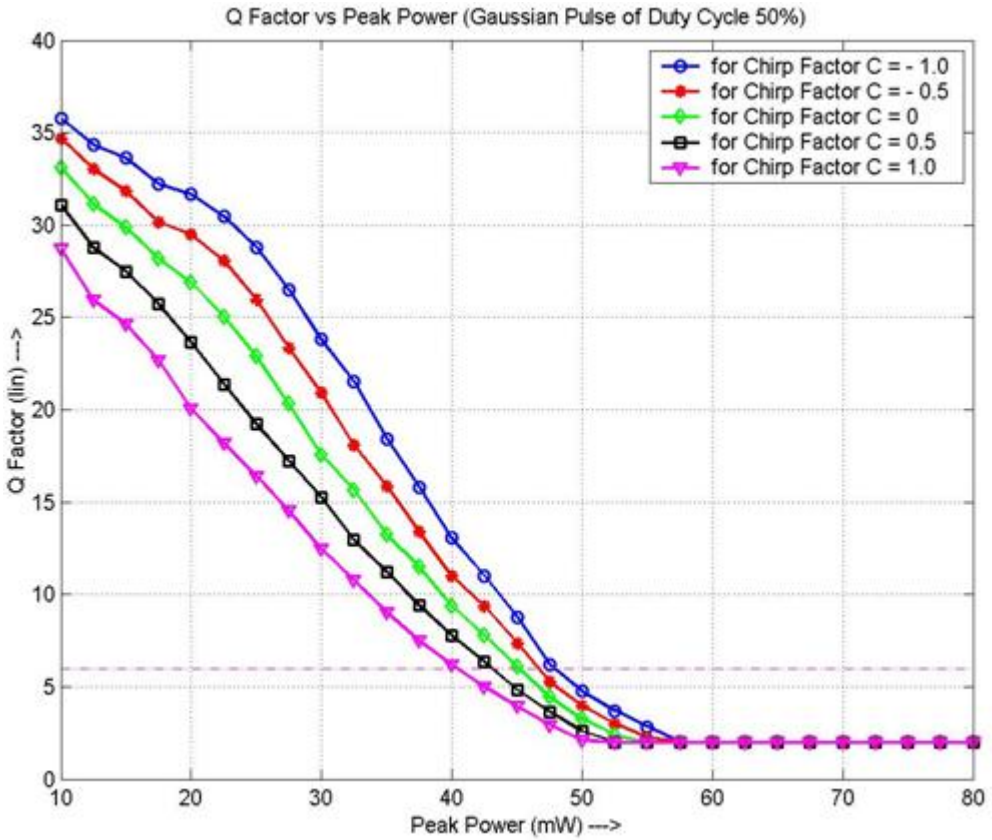

Figure 3.6: Q-Factor vs. Peak Power for duty cycle of 50%

The similar pattern has been observed for 50% and 66.67% duty cycle with a quantitative difference owing to differential SPM influence on pulses of different initial width as is evident from Figure 3.6 and 3.7. It can be concluded from Figure 3.5-3.7 that the pulse having higher initial width is less prone to SPM induced impairment while propagating through the optical channel and when the impairment induced by the GVD is completely neglected.

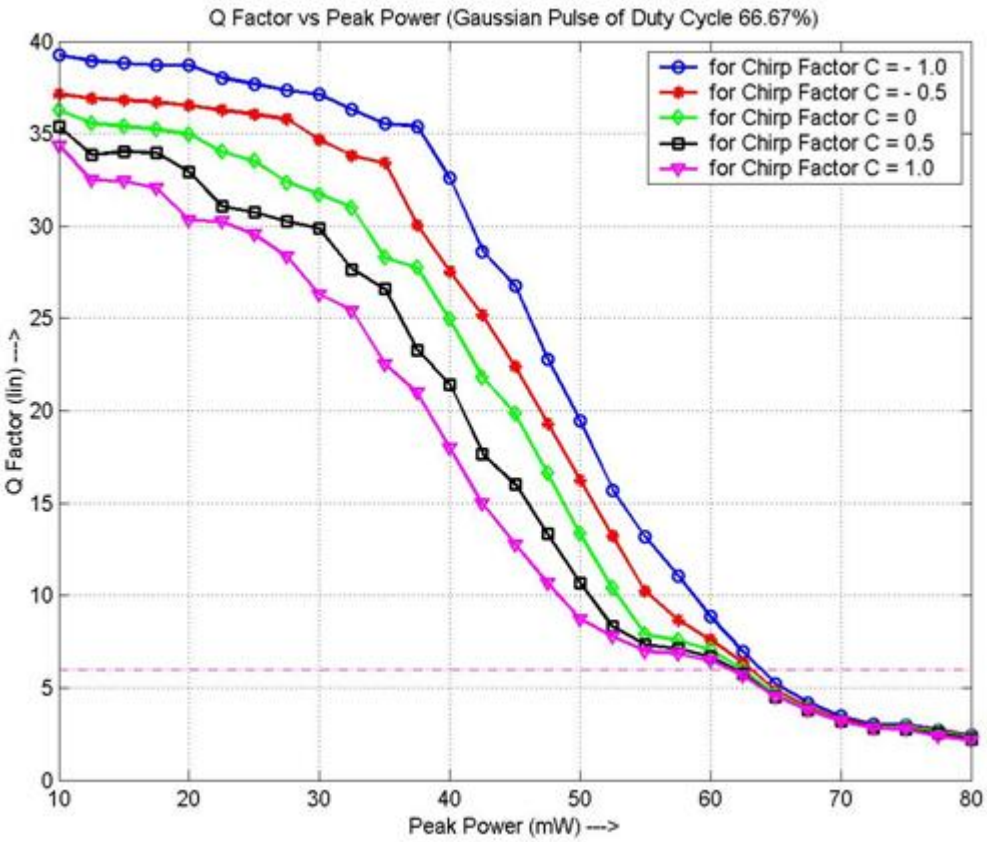

Figure 3.7: Q-Factor vs. Peak Power for duty cycle of 66.67%

After this, to investigate the influence of varying duty cycle on a given chirped source the behavior of different duty cycle pulses is comparatively analyzed in Figure 3.8, 3.9 and 3.10. Figure 3.8 shows the effect of chirp parameter C = -1.0 on 33.33%, 50% and 66.67%. different duty cycle pulses. It is clear from the Figure 3.8 that a pulse with 66.67% duty cycle pulse shows maximum Q factor and maintains the better performance even for the higher values of the input peak power as compared to other two cases. However, for very high input power i.e. 70mw and more the SPM degrades the system performance and the Q factor becomes independent of the initial pulse width.

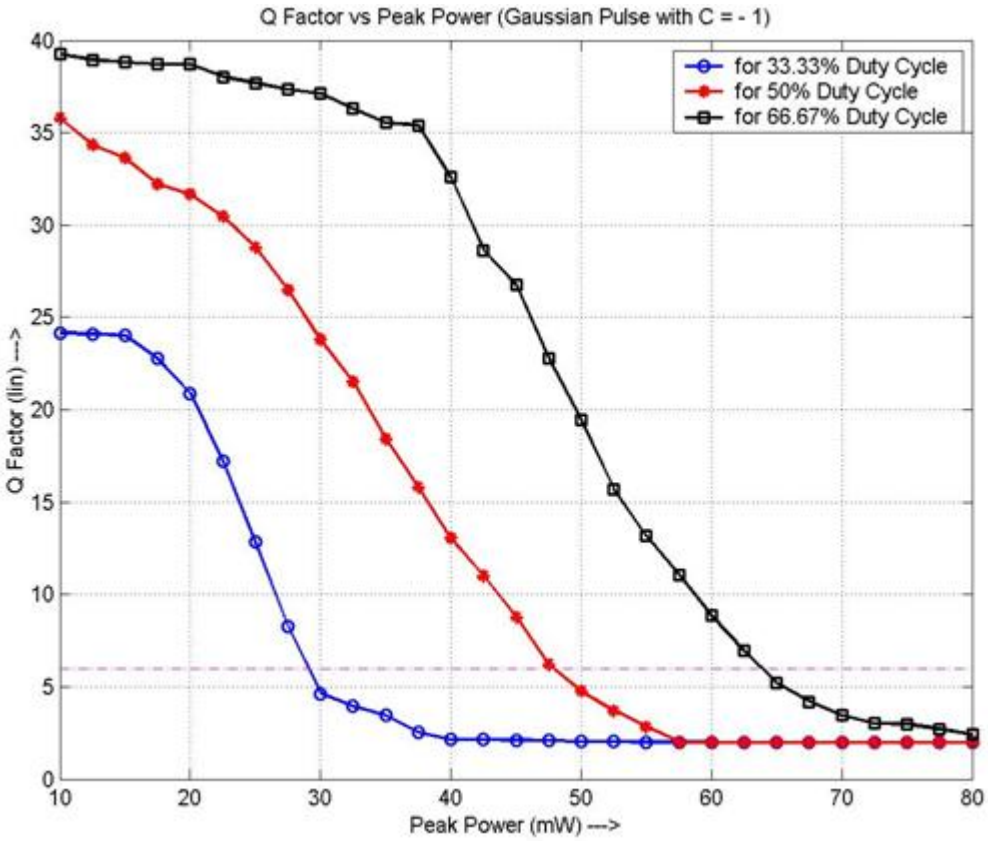

Figure 3.8: Q-Factor vs. Peak Power for Chirp C = -1.0

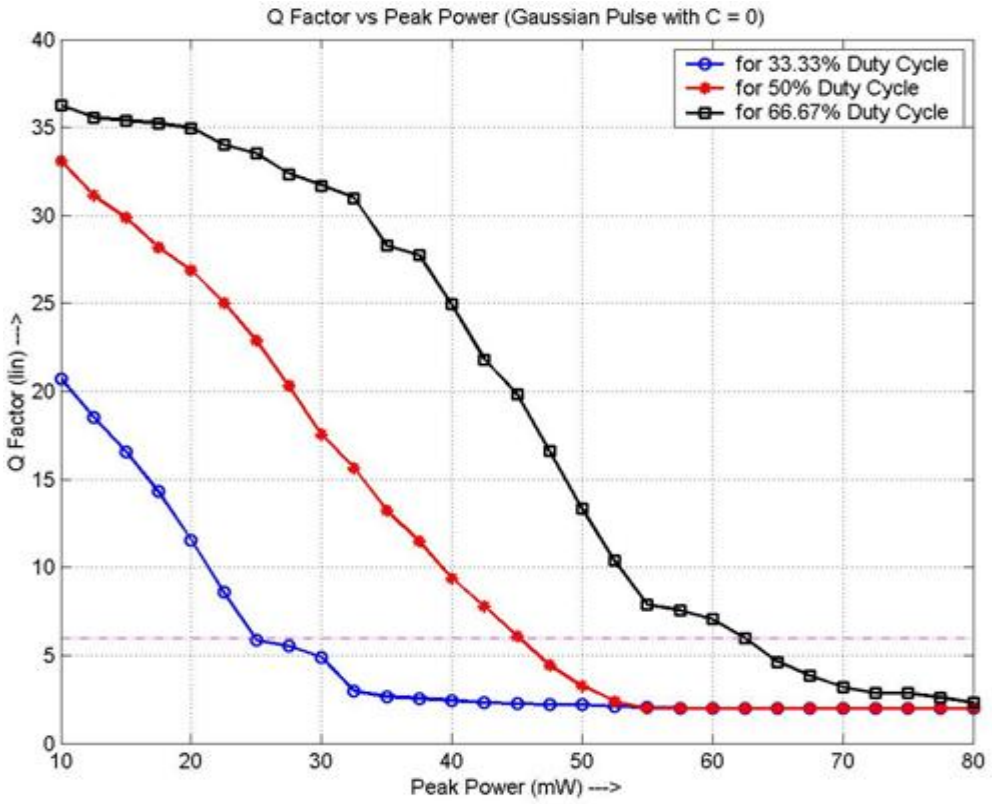

Figure 3.9: Q-Factor vs. Peak Power for Chirp C = 0

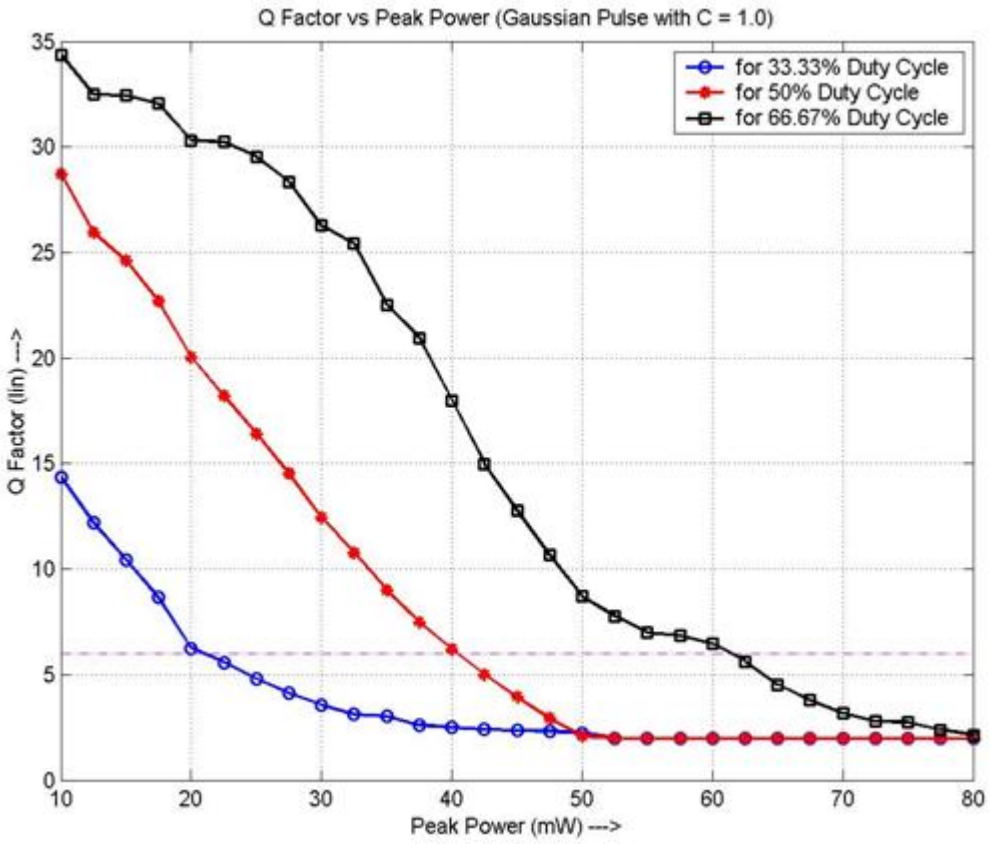

Figure 3.10: Q-Factor vs. Peak Power for Chirp C = 1.0

It is also observed from this curve that positively chirped pulses below 50% duty cycle degrade rapidly as compared to the unchirped case. However, this performance improves further for the negatively chirped cases making the system less vulnerable to SPM impairments. Figure 3.9 shows the performance of different duty cycles pulse with varying peak power this measurement is performed without initial chirp conditions. From the results it is observed that 66.67% duty cycle pulse shows more tolerance towards SPM effects because of its wider spectrum compared to 33% and 50% duty cycle pulse shapes. Similarly, Figure 3.10 shows the effect of positive chirp and the performance of all the three duty cycle pulses.

From this analysis it is observed that 66.67% duty cycle pulse is the best performing duty cycle among the all three compared duty cycles therefore for the further analysis only 66.67% duty pulse has been considered. As known to us for the EDFA based optical link designs, ASE is an important parameter and needs to be addressed properly. Therefore, section 3.4 discusses the performance of existing optical link for ASE noise limited channel conditions along with the SPM effect.

3.4 Combined effect of SPM and ASE induced degradation at 40Gbps

As discussed in chapter 1, in EDFA's stimulated emission occurs at high power levels and amplifier treats the spontaneous emission radiation as another electromagnetic field and the spontaneous emission gets amplified described as amplified spontaneous emission noise. This ASE noise can saturate the amplifier. The ASE noise power spectrum (P_{ASE}) over a bandwidth of Δf is given by equation [69].

$$P_{ASE} = n_{sp}(G-1)hf_s\Delta f \tag{3.8}$$

Where n_{sp} is the population inversion factor which indicates the ion conversion from one state to another G is gain, f_s is the centre frequency of the noise spectrum.

$$\hat{N} = j\gamma|A|^2 A \tag{3.9}$$

From the results obtained in section 3.3, it is observed that the 67% duty cycle pulse with a negative value of chirp performs better in the presence of SPM therefore, only 67% has to be utilized further to observe the performance of link in the presence of ASE noise while propagating through the optical fiber. For this analysis, noise figure (NF) of 4.5dB is included in the link along with the increase in power while maintaining all other parameters same. The performance of the 67% duty cycle pulse in the presence of SPM and ASE noise are presented in Figure 3.11 for different chirp parameters. From the results, it is observed that the negative value of chirp makes pulse more robust even in the present of amplifier noise.

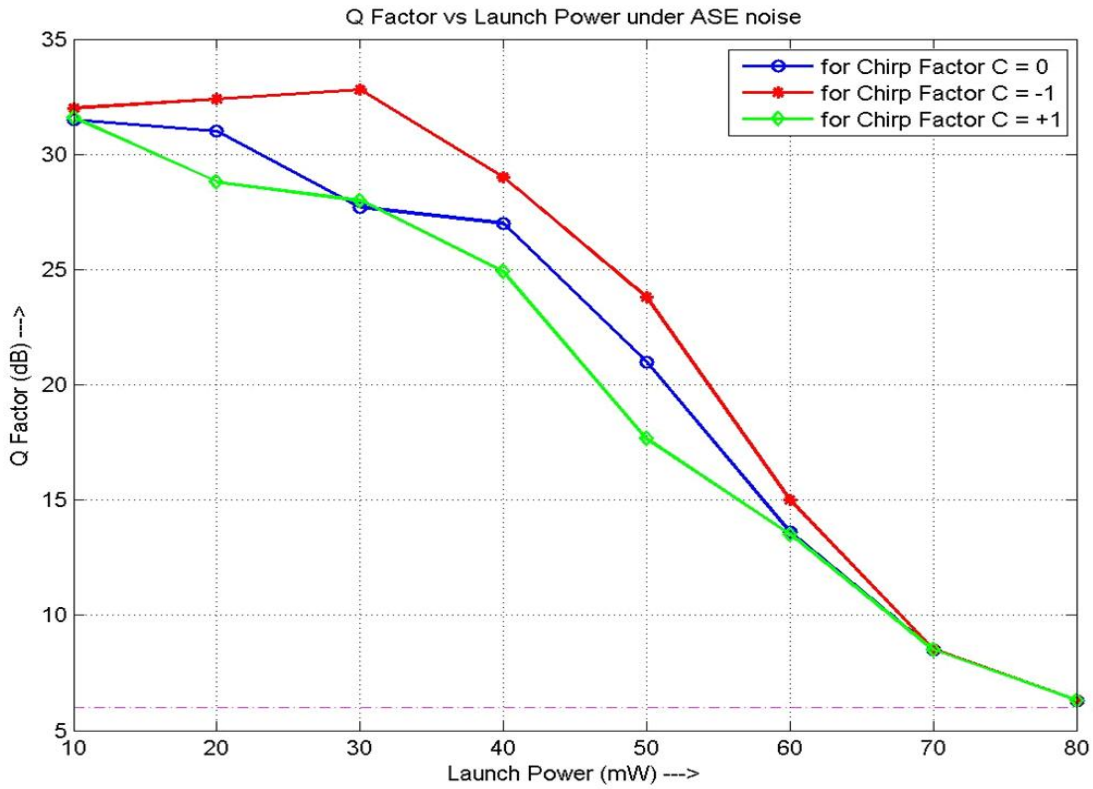

Figure 3.11: Q vs. Launched Power for different types of chirp factor under SPM and ASE noise

From the results, it can also be observed that the performance of the negatively chirped pulse is much better than without chirped and positively chirped pulses at lower values of input power. But as the power starts increasing further this difference starts decreasing but still remains maintained.

3.5 Conclusion

In this chapter, firstly, the basic Gaussian pulse propagation mechanism inside an optical fiber cable has been discussed. Thereafter, 40Gbps data link has been designed and optimized for SPM and ASE effects. For the analysis, high speed chirped Gaussian RZ-modulated pulse with different duty cycles have been considered. Performance measurement is carried for positive, negative and no chirp conditions of the input pulse. The carried analysis shows that wider pulse with the large negative chirp can withstand the SPM and ASE effects for higher range of input peak power. From the obtained results it is rightly to say that the negative chirp and the higher duty cycle pulse has a higher capability to propagate to the longer distance in the presence of SPM and amplifier noise in the single channel transmission link design.

CHAPTER 4

Optical Link Performance Enhancement: Duobinary Modulation Scheme

4.1 Introduction

Nonlinear impairments in conventional RZ modulation formats has been studied in chapter 3. Although RZ modulation formats are easy to implement but have low spectral efficiency. Researchers are continuously exploring more advanced and bandwidth efficient modulation formats to design the data rate transmission links. Duobinary modulation is one of such format and is based on the partial response signaling. In Duobinary modulation scheme, ISI is intentionally introduced during encoding the data and this is removed during the decoding process. This approach gives a better tolerance to various linear and nonlinear effects due to the narrow spectrum offered in duobinary encoding [135-137].

Although duobinary was first proposed by A. Lender in 1960s, but has not been used effectively by that time and later it was overcome by the multilevel modulation schemes, as they could provide better spectral efficiency [176,177]. However, duobinary modulation was used for optical transmission in the 90s when X. Gu. et al [178,179] proposed the three level amplitude modulation but this strategy could not become popular solution due to the poor sensitivity of the used receiver. Literature review reveals that out of various possible implementations of duobinary transmitters, Mach-Zehnder Modulator (MZM) in a push-pull configuration based transmitter design with a suitable electrical filter is a superior choice in the presence of non-linear impairments of the channel [180,181].

In this chapter, duobinary transmitter design for a 40Gbps data rate is presented in section 4.2. This section also provides the bandwidth optimization of the electrical low-pass filter (LPF) and optical band-pass filter suitable for the duobinary pulse shape in an ASE noise limited system. Section 4.3 presents the complete duobinary optical link model design using OptSim^{TM} platform and its performance analysis for various channel impairments at 40Gbps data rate. Section 4.4 summarizes the important findings of the chapter.

4.2 Duobinary transmitter design

As discussed in chapter 2, data modulation in optical is achieved using two types of modulators i.e. optical phase modulators and optical intensity modulators. An EOPM uses one electrode. When a driving voltage is applied to the electrode, the refractive index of the electro-optic waveguide changes accordingly, thus slowing down the light wave and hence inducing a delay on the optical signal. The induced delay corresponds to the phase change. Thus an EOPM is able to manipulate the phase of the light carrier. The induced phase change by an EOPM in lightwave carrier for an applied bias voltage V_{bias} is expressed as:

$$\Phi(t) = \frac{\pi(V(t) + V_{bias})}{V_{\pi}} \tag{4.1}$$

where, V_{π} is the driving voltage required to create a π phase shift, $V(t)$ is a time-varying driving signal voltage. Optical field $E_0(t)$ at the output of the EOPM is given as:

$$E_o(t) = E_i(t)e^{j\varphi(t)} \tag{4.2}$$

Equation (4.2) shows that the output electrical field is the contribution of the input electrical field with the additional phase term. Optical intensity modulator uses two EOPMs in a parallel structure to form a Mach-Zehnder interferometer, commonly known as Mach-Zehnder intensity modulator (MZIM) [69]. Input optical signal splits equally in the two arms of the MZIM which are actually EOPMs for modulating the phase of the optical carrier. At the output, the two arms are coupled either constructively or destructively to provide intensity modulated optical pulses.

MZM are of two types: single-arm MZM and dual-arm MZM. Figure 4.1 shows the block diagram of single-arm MZM. As shown in the figure, only one single driving voltage is applied to the either arm of MZM to obtain the phase modulation of the input optical pulse. The main problem with single-arm MZM configuration is the chirped output signal. This makes them not suitable for long distance optical transmission systems [69].

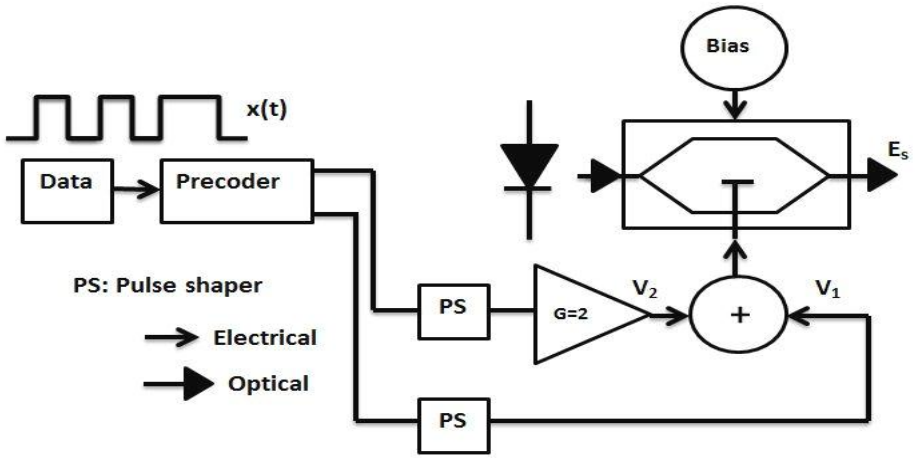

Figure 4.1: Single-arm MZM

Figure 4.2 shows the dual-arm MZM in a push-pull arrangement where the dual drive voltages V_1 and V_2 are inverse to each other and thus, able to completely eliminate the chirping effect in the modulation.

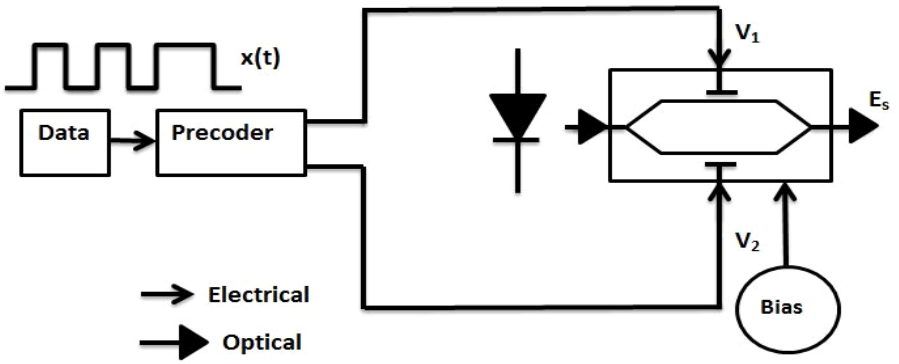

Figure 4.2: Dual-arm MZM

The use of optical duobinary transmitter with the dual-arm MZM is the usual choice in transmitter design at high data rate. However, dual arm configuration demands more stringent requirement of symmetry to be met in both the arms [182]. To get the optimum performance, in the present chapter duobinary transmitter is designed using dual arm MZM configuration. The block level architecture of the proposed design is shown in Figure 4.3. Optsim^{TM} platform has been used to simulate the system performance and measured in terms of BER-equivalent Q-factor. This transmitter design consists of a pseudo-random binary sequence generator, non-return-to-zero or return-to-zero modulation driver, electrical low pass Bessel filters, logical not gate, dual arm MZM and a laser source. The data source generating pseudo-random sequences at 40 Gbps feeds two modulation drivers, one directly

and the other through a not gate. These two electrical signals are then passed through an optimized LPF of order 4. The laser source has been chosen to emit continuous wave (CW) at a center frequency of 193.414THz with FWHM (Δν) of 10 MHz. The two filtered electrical signals and carrier optical signal from CW laser is fed to the dual arm MZM to achieve duobinary optical modulation. The transmitter thus produces 40 Gbps duobinary optical pulses which can be either NRZ duobinary or RZ-duobinary based on the type of modulation driver.

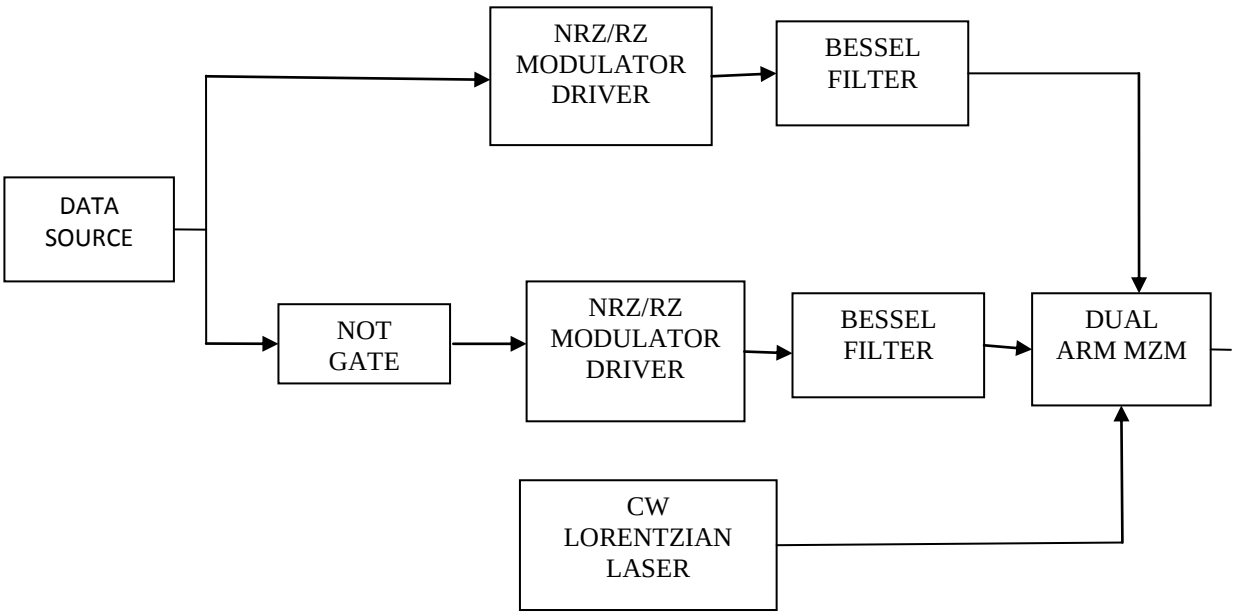

Figure 4.3: Duobinary transmitter module with Dual-arm MZM

After the transmitter design section 4.2.1 discusses the pulse shape optimization strategy to evaluate an optimum bandwidth for electrical LPF at the transmitter and an optical BPF at the receiver end.

4.2.1 Duobinary pulse shape optimization

An important consideration in optimizing the performance of a duobinary transmission is to investigate the optimum pulse shape. This can be achieved by deploying an electrical LPF at the transmitter end and an optical BPF at the receiver end. ASE noise is one of the important limiting factors in the design of the high speed optical system, therefore, needs proper addressing. As stated in the literature [183,184], to achieve optimal receiver performance in an ASE-noise-limited system, an optical duobinary system must employ a

matched optical filter in front of the photo-detector. The optimum duobinary pulse shape at input to the photo-detector should mathematically be represented as:

$$y(t) = \frac{\sin(\pi \frac{t}{T_b})}{\pi \frac{t}{T_b}(1 - \frac{t}{T_b})} \tag{4.3}$$

where, $T_b = 1/B$ is bit period and B is the bit rate

It is observed from the duobinary matched optical filter transfer function that the full-width at half-maximum (FWHM) bandwidth of the duobinary matched optical filter is ~0.67B. Theoretical ideal duobinary generating LPF transfer function shows that the optimum LPF bandwidth used in WDM systems with wide optical filters must be around 0.28B. As per the literature [183], for a duoninary matched filter at receiver end, the generating LPF can have even a wider bandwidth around ~ 0.42B. Therefore it is observed that the expected range of LPF bandwidth lies between 0.28B and 0.42B. It may be noted that wider bandwidth of LPF at the transmitter demands narrower bandwidth optical matched filter at the receiver. This theory of filter optimization is well applicable for NRZ duobinary pulses [185]. A closer look at the NRZ and RZ-duobinary spectrum as shown in Figure 4.4 shows that the RZ-duobinary spectrum has a central lobe accompanied by side-lobes in contrast with a single-lobe spectrum for NRZ duobinary case. The presence of spectral sidelobes in RZ-duobinary does not allow obtaining an optimum pulse shape and matched filter for this case.

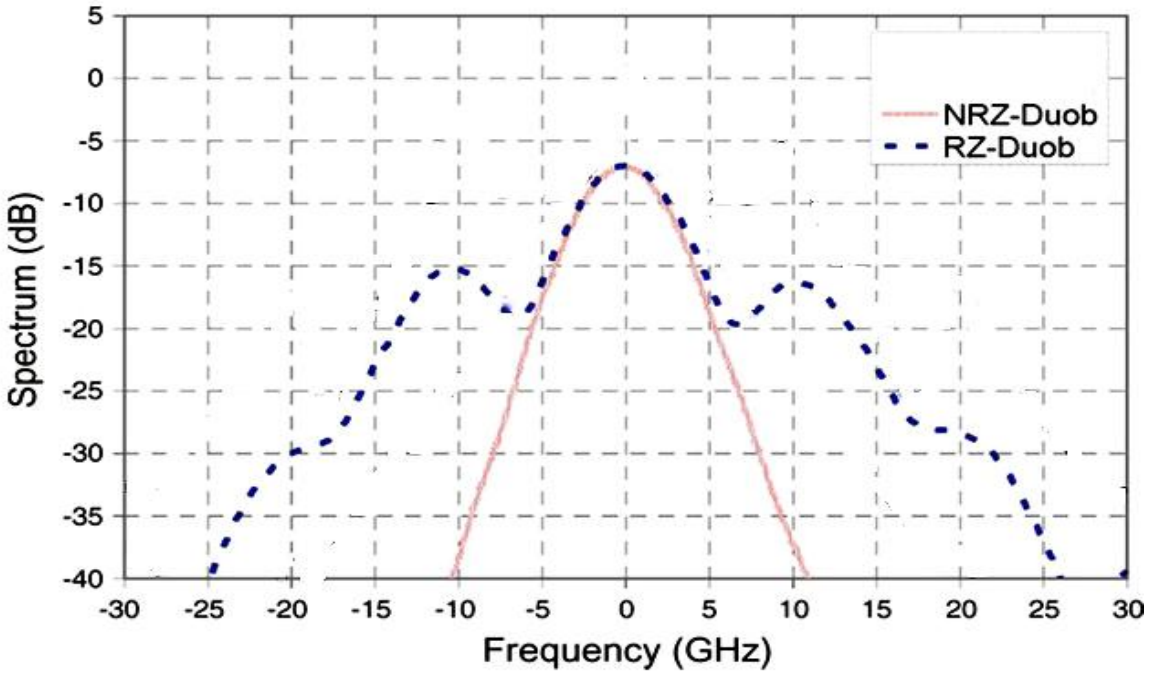

Figure 4.4: Spectrum of NRZ and RZ duobinary [183]

Thus better approximation for the optimum performance of RZ-duobinary can be achieved by filtering out these sidelobes. Now, conversion of the RZ-duobinary spectrum into an equivalent single-lobe spectrum matched with NRZ spectrum allows considering the optimum LPF in the similar fashion to that of NRZ case. Section 4.2.2 discusses the setup and the procedure used to shape the RZ and NRZ pulses.

4.2.2 Procedure for pulse shaping at 40Gbps

Figure 4.5 shows the setup used to select the LPF and optical filter (of order 4) bandwidth that optimizes the performance of the duobinary transmission link under limitations imposed by ASE noise. In this simulation model, optical spectrum analyzer (OSA) with a resolution bandwidth of 0.1nm to express the OSNR readings measured with respect to 0.1 nm noise bandwidth has been used. OSNR of 20dB/0.1nm is maintained by appropriate tuning of the variable optical attenuator (VOA).

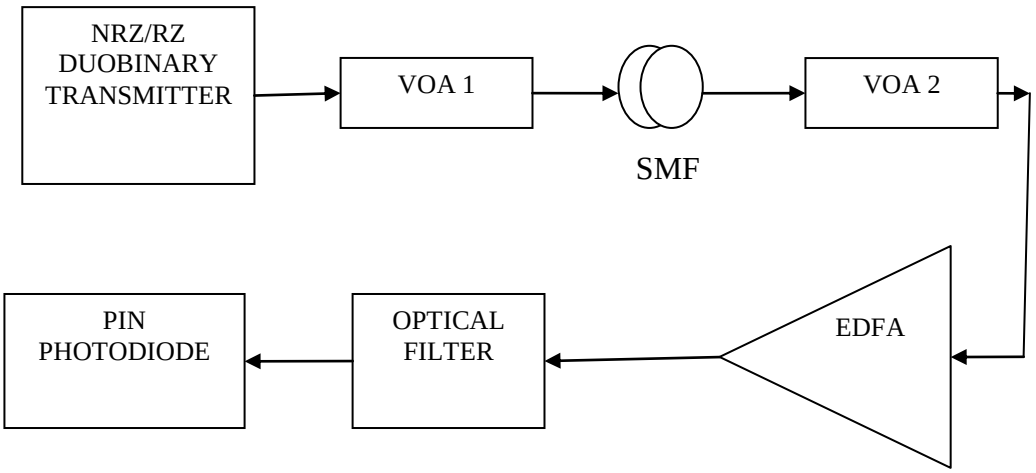

Figure 4.5: Simulation Setup for 40 Gbps RZ and NRZ duobinary transmission

Other parameters used in the analysis are 10 Km single mode fiber (SMF) with an attenuation (α) of 0.2 dB/km, dispersion (D) of 17 ps/km-nm and dispersion slope(S) of 0.07 ps/nm^2/Km at 1550nm, nonlinear refractive index(n_{nl}) of 2.5 x 10^{-20}m^2/W and core effective area of the fiber (A_{eff}) of 80 μm^2 . The MZIM has an offset voltage of 0.5V with 20dB extinction ratio providing 3dB average power reduction due to modulation. Direct detection method has been used at the receiver and utilizes the PIN photo-detector with the quantum efficiency of 0.63992, the responsivity of 0.8 A/W and dark current of 0.1nA. The RZ- or NRZ-duobinary optical signal from the duobinary transmitter is fed into VOA1 that controls the launch power into the SMF segment. VOA2 is used to set the input optical power into an erbium-doped fiber amplifier (EDFA). An OSA is been used to monitor the optical signal-to-noise ratio (OSNR) at the output of the EDFA. Using this setup electrical filter optimization and optical filter optimization at 40Gbps has been discussed in section 4.2.3 and 4.2.4 respectively.

4.2.3 Electrical filter optimization at 40Gbps

In duobinary modulation, filter limit depends critically on the pulse shape. This feature of duobinary makes it different from other modulation formats. A significant benefit from the duobinary pulse shaping has been reported [183] were narrow band optical filters have been used at the either end of the transmission link. Therefore, to verify this concept for 40Gbps systems a relatively wide optical filter of bandwidth 156 GHz and a narrow optical filter having 28 GHz bandwidths have been used in this analysis. Performances of NRZ duobinary (NRZ Duob) and RZ-duobinary (RZ Duob) are measured in terms of BER-

equivalent Q-factor for the varying LPF bandwidth as shown in Figure 4.6. It has been observed from these plots that with narrower optical filter better system performance can be achieved for both RZ- and NRZ duobinary transmission.

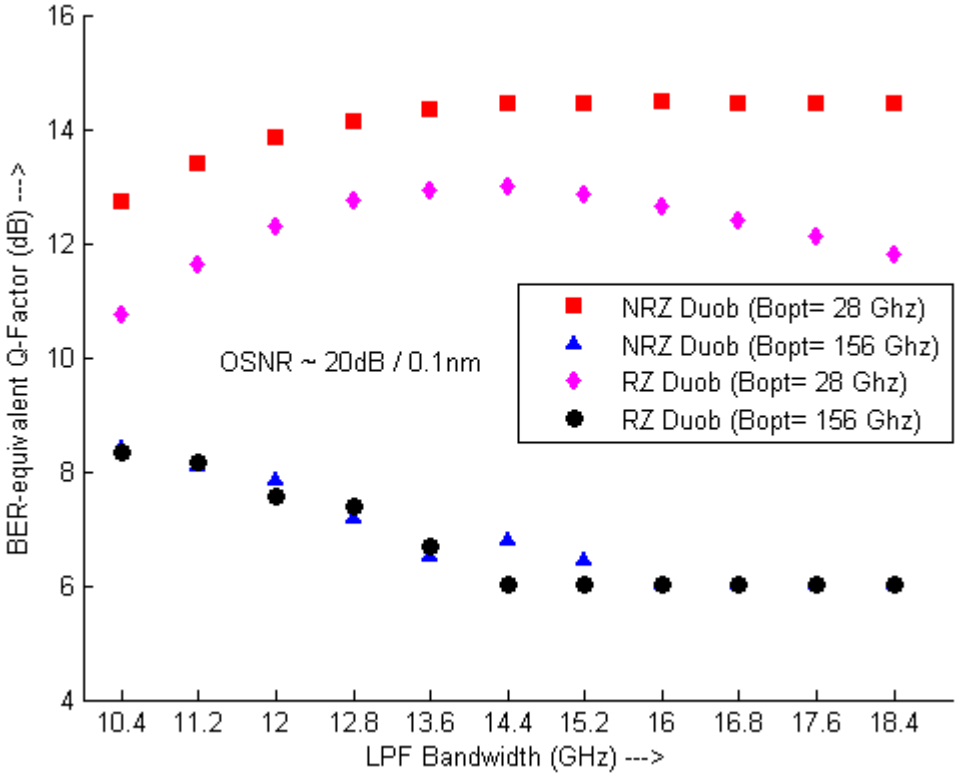

Figure 4.6: BER-equivalent Q-factor vs. LPF bandwidth with the optical filter bandwidth at 28 and 156 GHz for RZ- and NRZ-duobinary

Also in such ASE noise-loaded system NRZ duobinary outperforms RZ-duobinary by a significant margin when a narrow optical filter is employed as compared to a wider optical filter. From the obtained results, optimum LPF bandwidth for both RZ- and NRZ duobinary, which is obtained by deploying a nearly matched optical filter is approximately 14.4 GHz (i.e. 0.36B) and 16 GHz (i.e. 0.4B) respectively. The LPF bandwidths obtained here agree with the theoretical limits of $0.28\ B < \Delta f < 0.42\ B$. To obtain an optimum optical filter bandwidth, LPF bandwidth has been fixed at 14.4 GHz (0.36 B) and rest varying the optical filter bandwidth as discussed in section 4.2.4.

4.2.4 Optical filter optimization at 40Gbps

For the optical filter optimization, the performance of the system is measured in terms of BER-equivalent *Q*-factor versus receiver optical filter bandwidth and the same is plotted in Figure 4.7.

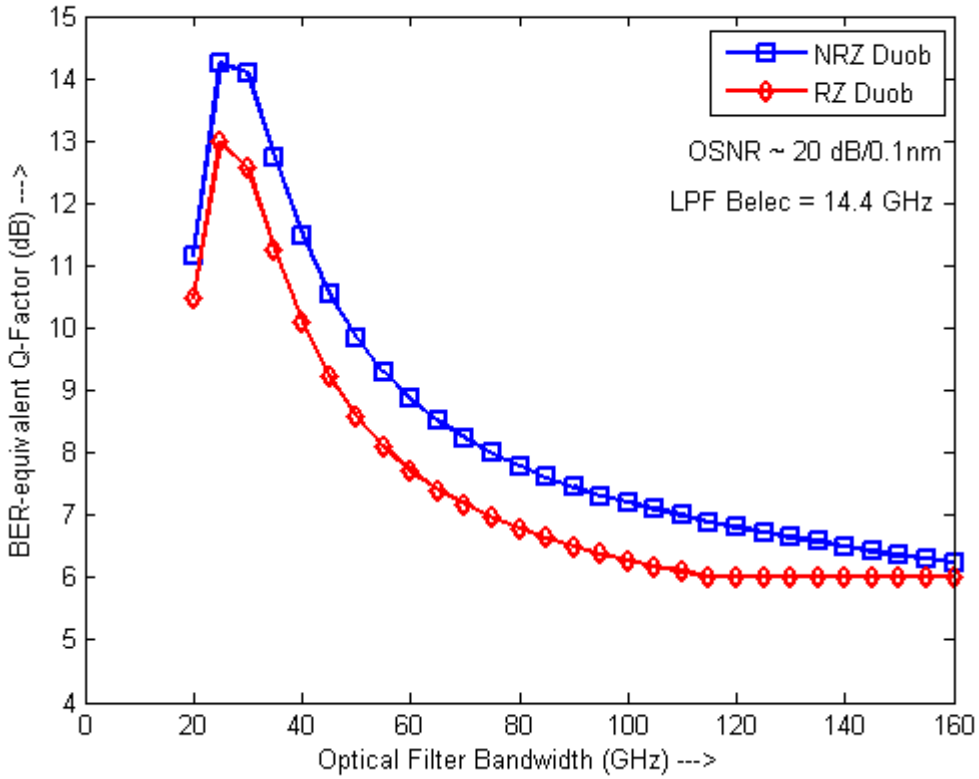

Figure 4.7: Optical filter bandwidth optimization for RZ- and NRZ duobinary systems

Here, along with keeping the RZ- and NRZ- duobinary LPF bandwidths at 14.4 GHz, OSNR is maintained at 20 dB with a noise bandwidth of 0.1nm by tuning VOA2. It can be interpreted from Figure 4.7 that both RZ- and NRZ duobinary pulses obtain their optimum ASE-noise-limited performance at the same value of optical filter bandwidth i.e. 28 GHz which is ~0.7B and is quite close to the FWHM bandwidth of ~0.67B as reported in the literature. The same value of optimum optical bandwidth is owing to the fact that the RZ-duobinary pulse spectrum is actually been converted into an equivalent NRZ-duobinary spectrum by the ultranarrow optical filtering process. This result proves the superiority of NRZ over RZ pulse shape for duobinary systems when the link performance is limited by ASE noise.

From this analysis it is clear that the optimum LPF bandwidth should be 14.4 GHz (0.36B) and 16GHz (0.4B) for RZ- and NRZ duobinary pulse shapes at 40Gbps respectively whereas, optimum optical filter for both duobinary pulse shapes should have 28GHz (0.7B) bandwidth for optimum performance in an ASE-noise limited system.

After obtaining the optimum bandwidths for both the filters in an ASE noise limited system the analysis has been further extended to observe the effect of dispersion for NRZ- and RZ-

duobinary on receiver sensitivity. For this, performance is measured for varying SMF distance while maintaining the fixed OSNR value of 20 dB/0.1 nm and results are reported in Figure 4.8. For the analysis 10km SMF is used and in order to avoid nonlinear impairments in the simulation, the launch power into the SMF segment has been reduced to a relatively low value of ~ -5 dBm using VOA1 (Figure 4.5). It is observed from the results of Figure 4.8 that the optimum NRZ duobinary system achieves receiver sensitivity of ~ -31.6 dBm (for BER of 10^{-9}), till 4 Km of SMF transmission which is better in comparison to the RZ-duobinary system. RZ-duobinary pulse suffers ~ 0.8 dB penalty in receiver sensitivity when compared with NRZ duobinary pulse, subjected to dispersion induced impairments.

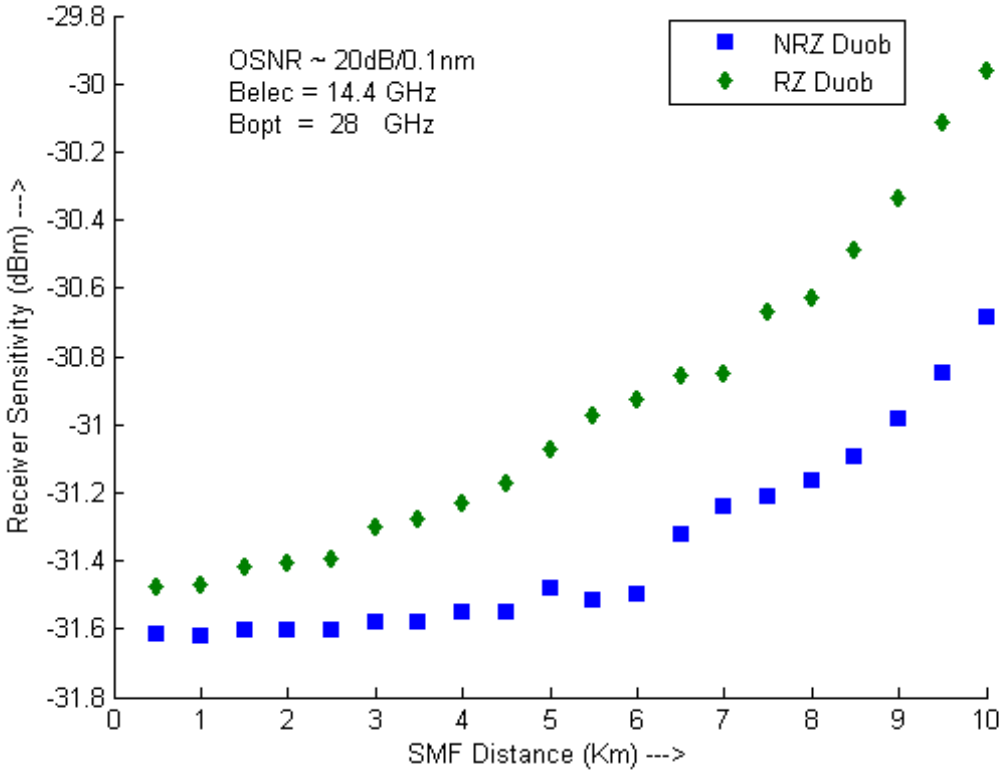

Figure 4.8: Receiver sensitivity of RZ- and NRZ duobinary pulses for varying SMF segment length

Therefore, it can be rightly said that NRZ duobinary shows better receiver sensitivity than RZ-duobinary and the superiority of NRZ- over RZ-duobinary increases with the increase in dispersive effects in longer fiber sections. OSNR is an important design parameter in optical link designs and therefore all the above analysis has been done at fixed OSNR value of 20dB/0.1nm. To better observe the effect of OSNR on the performance of duobinary link design the duobinary optical link has been designed by utilizing the

optimized parameters and then analyzed for GVD and SPM induced impairments for two different OSNR values in section 4.3.

4.3 Duobinary optical link design at 40Gbps

The bane of increasing the transmission capacity of the single channel optical link is GVD and SPM. Therefore, proposed transmission link is designed and analyzed for GVD and SPM effects for two different cases first, when either of the ones is present at a time in the link and second, when both of them are present at a same at fixed OSNR conditions.

Starting with the dispersion analysis, the setup is illustrated in Figure 4.9. In this model duobinary transmitter section is same, as discussed in section 4.2.2. Other parameters used in the design are as follows: 10 Km single mode fiber (SMF) with an attenuation (α) of 0.2 dB/km, dispersion (D) of 17 ps/km-nm and dispersion slope (S) of 0.07 ps/nm^2/Km at 1550nm, nonlinear refractive index (n_2) of 2.5 x 10^{-20}m^2/W and core effective area of the fiber (A_{eff}) as 80 μm^2. The MZM has an offset voltage of 0.5V with 20dB extinction ratio providing 3dB average power reduction due to modulation. PIN photodetector has a quantum efficiency of 0.63992, the responsivity of 0.8 A/W and dark current of 0.1nA. Optical spectrum analyzer with a resolution bandwidth of 0.1nm to express the OSNR readings with respect to 0.1nm noise bandwidth is used. OSNR is maintained by appropriate tuning of the variable optical attenuators.

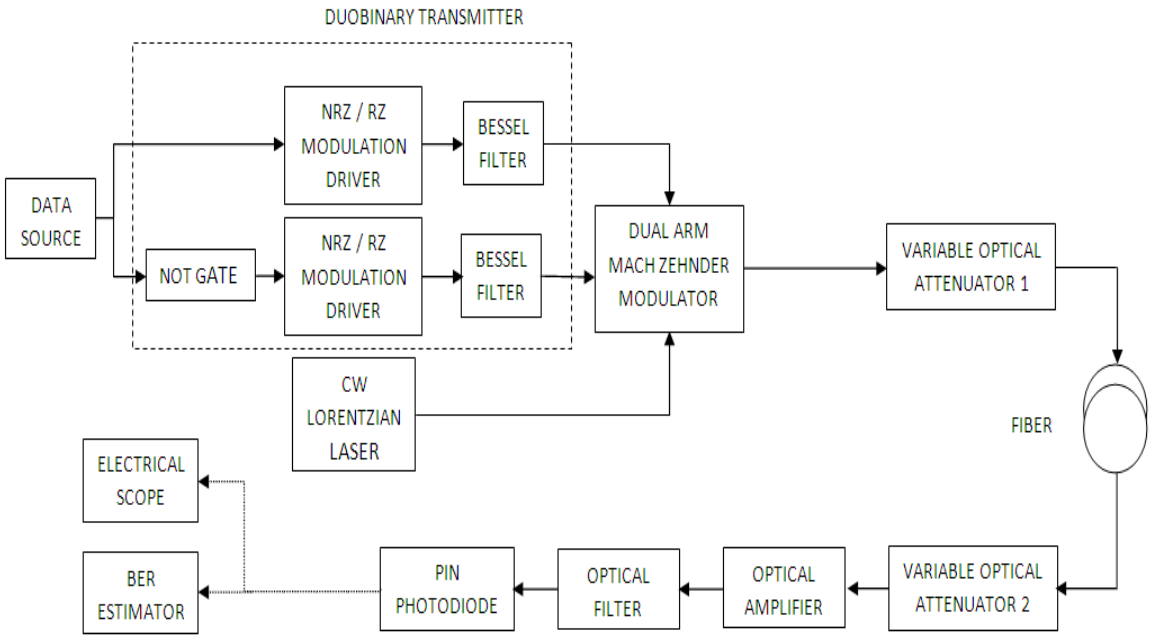

Figure 4.9: Simulation layout of 40 Gbps duobinary transmission

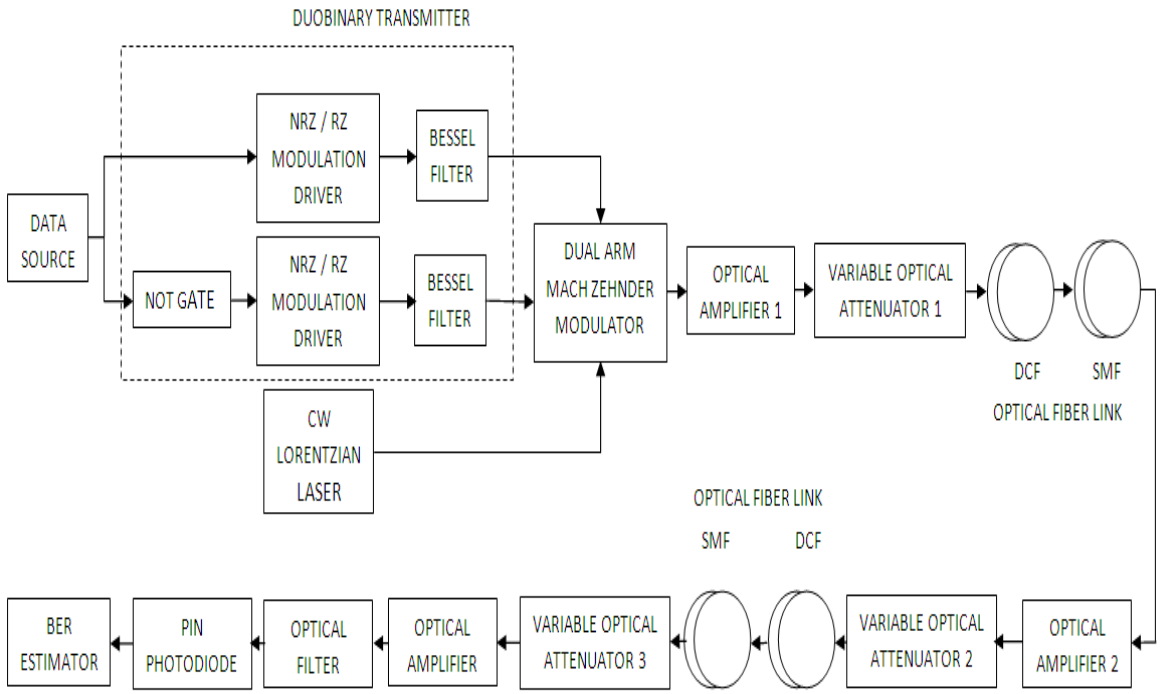

Figure 4.10: Simulation setup to study effects of SPM

Simulation setup used for the SPM analysis is as shown in Figure 4.10. A comparative study has been carried out for DB-NRZ and DB-RZ to figure out which modulation scheme has better tolerance to SPM. The setup uses similar components as used in Figure 4.9 except the fiber link. To study SPM effect, two spans of the identical optical channel made of dispersion compensating fiber (DCF) followed by single mode fiber (SMF) has been used to neglect the GVD induced effect. DCF segment used in each span for compensating GVD is of 1.202 Km length with α = 0.6 dB/km, D = -63.65 ps/km-nm and S = 0.07 ps/nm^2/Km at 1550nm, n_2 = 3.8 x 10^{-20} m^2/W and A_{eff} = 19.4 μm^2. SMF segment of 4.5 Km length with attenuation α = 0.2dB/km, D = 17 ps/km-nm and S = 0.07 ps/nm^2/Km at 1550nm, n_2 = 3 x 10^{-20} m^2/W and A_{eff} = 60.805 μm^2. LPF and optical filter bandwidths are maintained at their optimized value in both GVD and SPM analysis models.

After the complete duobinary link design for the 40Gbps data rate, section 4.3.1, 4.3.2 and 4.3.3 presents the GVD, SPM, and GVD along with SPM induced impairments on the performance of the transmitted pulses respectively.

4.3.1 GVD induced degradation

To analyze the degradations induced by GVD, degradation owing to nonlinear effects was managed to be negligible by ensuring low value of the power (~ -5 dBm) launched into SMF by tuning VOA 1 (Figure 4.9) and important findings are plotted in Figure 4.11 for

DB-NRZ and DB-RZ pulse shapes for both OSNR conditions. It is observed from these results that DB-NRZ encoded optical data shows better tolerance to GVD induced degradation as compared to DB-RZ at 40 Gbps data rate. Similar qualitative behavior is seen for both OSNR values i.e. 15/0.1nm and 20dB/0.1nm.

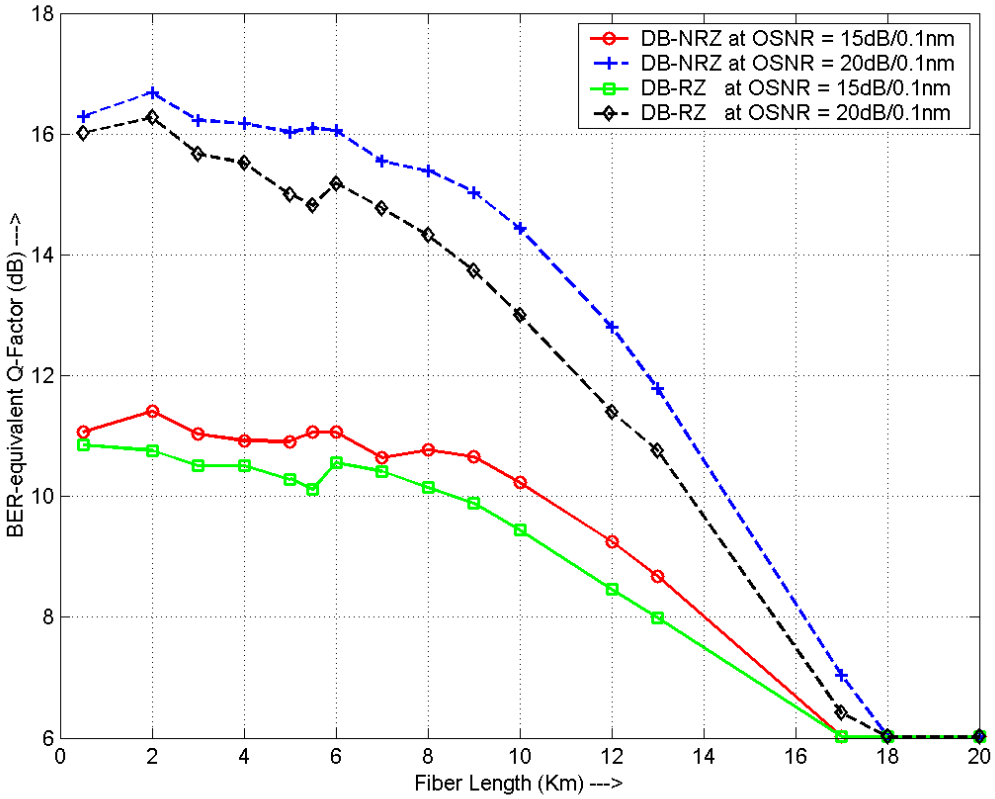

Figure 4.11: Dispersion limited BER-equivalent Q-factor for different OSNRs in RZ and NRZ duobinary system

As DB-RZ format has a wider spectrum with side lobes as compared to the DB-NRZ format. The high-frequency components present in the DB-RZ spectral sidelobes may penetrate into the optical filter bandwidth, which results in a higher BER, i.e. a lower equivalent Q value as compared with DB-NRZ. It is inferred that the GVD-induced power penalty influences the NRZ format significantly and brings its Q value close to the RZ case beyond 20km of length. These curves reveal a sharper deterioration of the Q value with propagation length due to the cumulative delay introduced by the fiber dispersion.

4.3.2 SPM induced degradation

To investigate SPM-induced nonlinear effects a typical launch power of 10mW has been considered. OSNR is maintained constant with the help of VOA3 (Figure 4.10). The SPM-induced impairments are more prominent at higher launch power; hence, to observe the link performance at the extreme case, 100mW launched power has considered. SPM-induced signal degradation and its influence over the BER-equivalent Q-factor of the system have been estimated with respect to optical bandwidth and shown in Figure 4.12 and Figure 4.13 for 20dB/0.1/nm and 15dB/0.1nm OSNR values respectively. The spectral side lobes present in the optical spectrum may be affected by SPM-induced nonlinearities. The SPM effect induces broadening in the signal spectrum which tends to make the side lobes broader. Thus, aliasing of high-frequency components from the sidelobes into the main spectral lobe produces severe degradation in the performance. Since higher optical filter bandwidth allows more side lobes to be aliased with the main spectrum and significant degradation can be noticed. The same procedure has been followed to compare the effect of SPM on DB-RZ and DB-NRZ pulses.

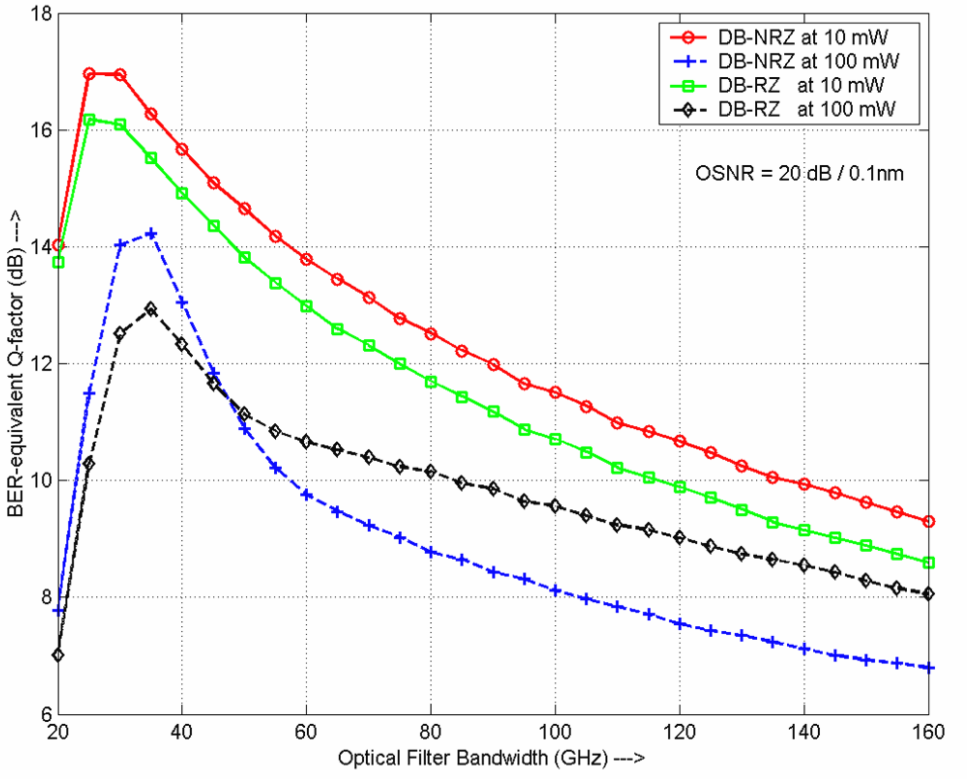

Figure 4.12: SPM effect on RZ and NRZ duobinary at 20dB/0.1nm

It can be interpreted from Figure 4.12 that at a launch power of 10mW DB-RZ underperforms DB-NRZ. The severe degradation for DB-RZ is due to the fact that the DB-RZ spectrum has wider side lobes as compared to DB-NRZ. It is observed that a 100mW curve shows a lower Q-factor as compared to the 10mW case, owing to greater deterioration of performance due to significant SPM-induced impairment at the higher power level. This also shows a higher optical bandwidth requirement for the optimum performance at the higher launch power level, because SPM-induced chirping broadens the spectrum since it adds high-frequency components to the side lobes and hence requires a larger bandwidth to maintain the performance. It is also noted that SPM-induced impairments deteriorate the DB-NRZ performance rapidly for 100mW launch power and after a crossover bandwidth it starts underperforming DB-RZ. This may be attributed to a larger energy in the case of DB-NRZ, which triggers severe deterioration due to SPM.

Figure 4.13 presents the limitations to system performance when the OSNR of the same system deteriorates to 15 dB/0.1 nm. A similar qualitative behavior can be observed in this case but with a quantitative difference in the Q value owing to degraded OSNR. It can be observed that DB-RZ outperforms DB-NRZ for both power levels after a crossover bandwidth. This is in contrast to the fact seen in Figure 4.12 where only at a higher power level DB-NRZ underperforms DB-RZ. At higher power level, the reduction observed in the value of the crossover bandwidth for the lower OSNR (Figure 4.13) in comparison to that seen in the case of the higher OSNR (Figure 4.12) can be interpreted as a fact that for lower OSNR, sidelobes contain less power; hence degradation due to side lobe aliasing in DB-RZ can be overcome at a lower optical bandwidth.

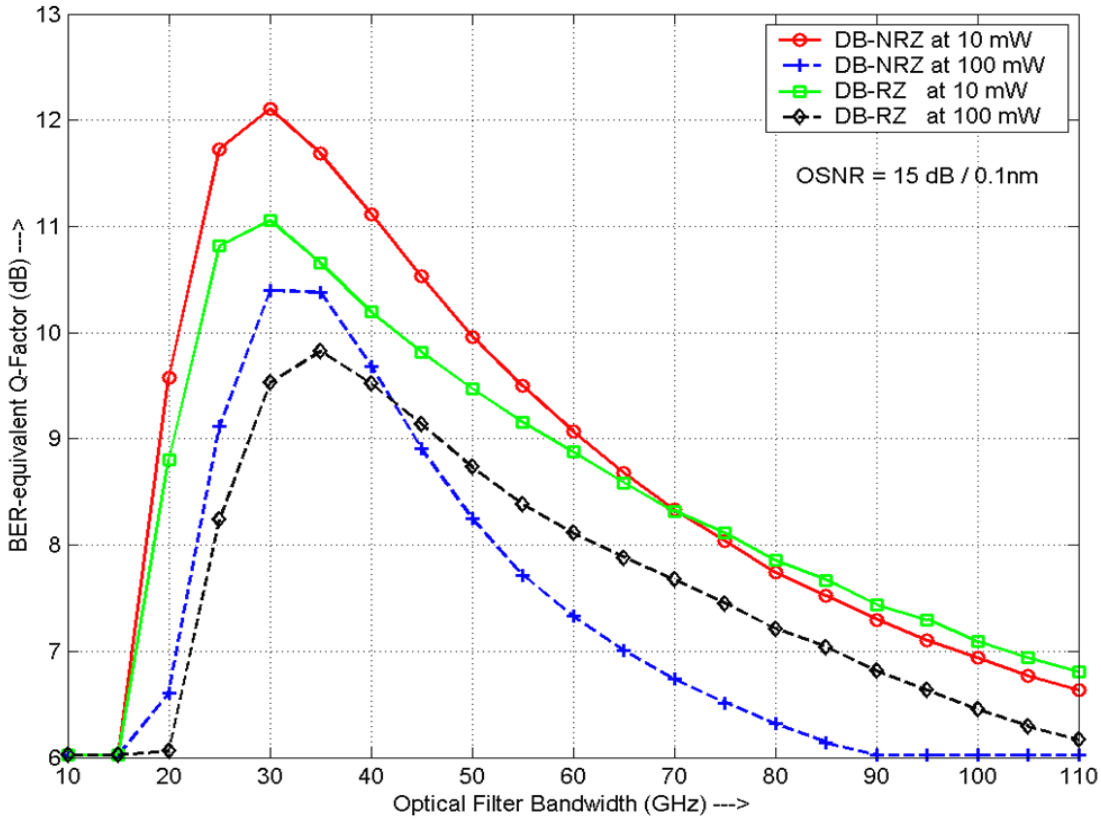

Figure 4.13: SPM Effect on RZ and NRZ Duobinary at 15dB/0.1nm

It can be inferred from Figures 4.12 and 4.13 that the crossover bandwidth at which DB-NRZ ceases to outperform DB-RZ depends on upon the system OSNR value. At lower OSNR, side lobes contain less power causing less degradation owing to side lobe aliasing for DB-RZ and hence require a lower crossover bandwidth as observed ~42GHz for 15 dB/0.1nm OSNR compared to ~48GHz for 20 dB/0.1 nm. It is vivid from the comparison that for 20 dB/ 0.1nm OSNR, DB-NRZ offers superior performance as compared to DB-RZ when an optical duobinary signal is launched into the fiber at 10mW power. For the 15 dB/0.1nm OSNR, DB-NRZ starts underperforming DB-RZ after a crossover bandwidth (~70 GHz) of the optical filter is reached.

After observing the link performance individually for GVD and SPM, section 4.3.3 consider a more realistic scenario where performance analysis has been done for the case when degradation induced due to the combined effect of GVD and SPM in an optical channel at OSNR value of 20dB/0.1nm.

4.3.3 Combined effect of GVD and SPM induced degradation

The simulation setup shown in Figure 4.9 has been used for this purpose. The setup remains the same as used for the case of GVD-induced degradation except for the fact that here a source power of 5mW has been considered to include the SPM effect. The length of the SMF has been varied and the corresponding results are plotted in Figure 4.14.

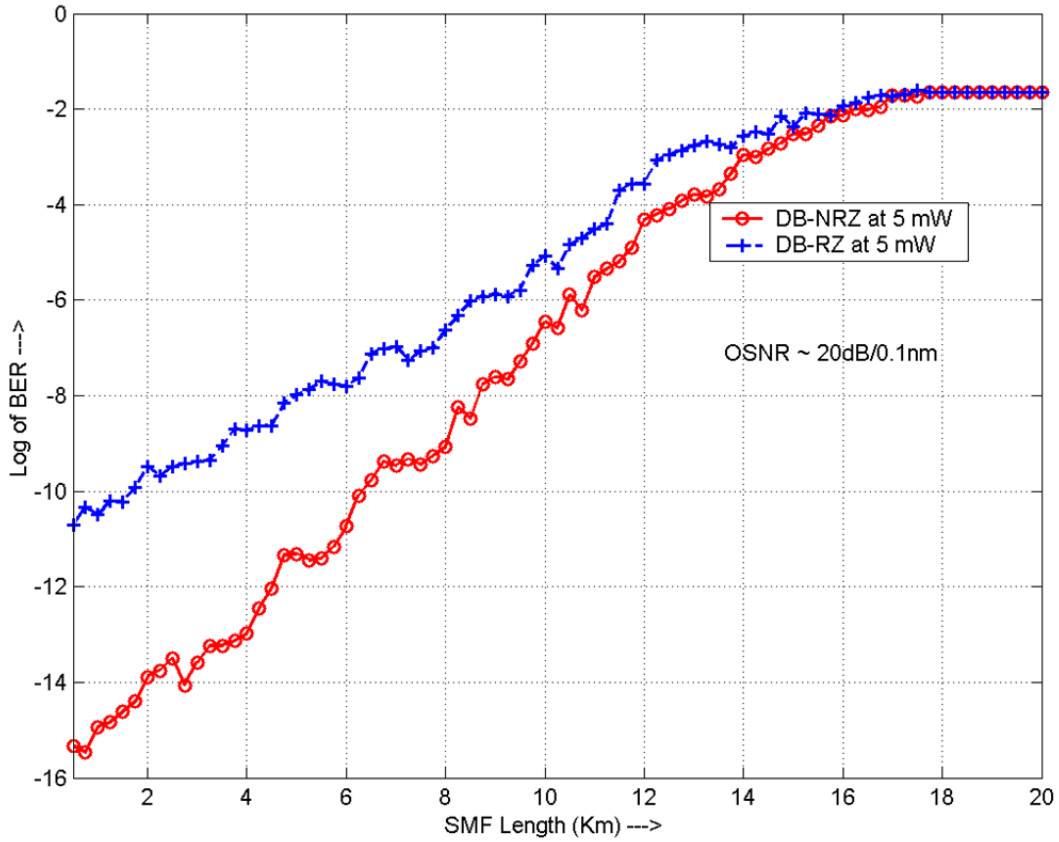

Figure 4.14: Study of combined effect of GVD and SPM on DB-RZ and DB- NRZ

It is observed from the plot that in a realistic model, where GVD and SPM both are degrading the performance, DB-NRZ offers better tolerance to these degradations as compared to DB-RZ pulses at a constant value of OSNR.

4.4 Conclusion

In this chapter, duobinary transmission at 40 Gbps data rate has been discussed. Link design starts with the proper selection of dual arm based MZM transmitter section. For the optimum transmission, the spectrum of RZ and NRZ pulses has been analyzed and modified with the use of suitable filters in ASE noise limited conditions. Results show that optimum LPF bandwidth is 0.36 of bit rate i.e. 14.4GHz and 0.4 of bit rate i.e. 16GHZ for RZ and NRZ duobinary pulse shapes respectively at 40Gbps. Optical filter bandwidth for both

duobinary pulse shapes should be 0.7 of bit rate i.e. at 28GHz. These optimized filters have been utilized for the design and analysis of link performance under constant OSNR conditions to investigate the limitations of GVD and SPM induced effects, individually and combined. From the obtained results it has been observed that for the higher OSNR performance of DB-NRZ is superior to the DB-RZ. However, for a lower OSNR value, a crossover optical filter bandwidth has been observed beyond which DB-RZ outperforms DB-NRZ pulse shapes.

CHAPTER 5

Optical Transmission Link Design: Multilevel Modulation Techniques

5.1 Introduction

Phase modulation formats such as differential phase shift keying (DPSK) and differential quadrature phase shift keying (DQPSK) are quite attractive and popular in the design of high-speed optical communication link. Both these formats are extensively studied because of their resilience to linear and nonlinear impairments [141-146]. In these modulation schemes information bits are encoded using the phase differences between two successive symbols rather than absolute phase, thus non-coherent detection is possible. In DPSK modulation, the symbol can take two different values of phase i.e. 0 and π between adjacent symbols. However, in DQPSK, information is encoded in both the quadrature components of the optical carrier and can take values as 0, $+\pi/2$, $-\pi/2$, π. DQPSK is true multi-level modulation format and is a promising technique to enhance the information carrying capacity of the channel [174]. This scheme also provides improved chromatic dispersion, PMD tolerance, and resilience to fiber nonlinearities in practical optical transmission links. One of the main advantages of DQPSK modulated transmission is that the intensity of the coded signals remains constant in time, except on the level of transition from one phase to another. All these features of DQPSK make it suitable for the high speed next-generation data transmission systems [153-155]. The exponential increase of the bit rate demand on geographical scales from the home network to worldwide multi-vendor business networks has resulted in deploying multichannel optical networks based on multi-protocol wavelength-division-multiplexing (WDM) technology [186].

The next generation long haul optical network will support 100G optical transport network with a defined Optical Transport Unit (OUT)-4 specification of the bit rate of 112Gbps per channel. It has been reported in the literature that polarization division multiplexing (PDM) of quadrature phase shift keying (QPSK) is one of the promising and emerging solutions for the implementation of WDM system for 100G network [187,188]. Consequently, dense wavelength-division-multiplexing (DWDM) systems working with

denser channel spacing of 50 GHz compared with the conventional WDM channel spacing of 100 GHz are becoming a prime area of interest in modern optical communication research [150-152].

However, the data transport capacity of a DWDM links is more severely limited by linear and nonlinear impairments compared to their single-channel counterparts. These impairments can be arises due to intrachannel and interchannel crosstalk. Intrachannel effects such as GVD and SPM whereas four-wave mixing (FWM) and cross phase modulation (XPM) are dominant in multichannel configuration [15,189].

This chapter presents the transmission link analysis firstly with DQPSK modulation format and secondly with dual polarization format of DQPSK i.e. DP-DQPSK in a single and multichannel configurations respectively. Appropriate pulse shape has been selected and used with these modulation formats based on the detailed literature survey. The rest of the chapter is organized as follow: Section 5.2 provides the RZ-DQPSK link design and the ASE noise analysis with three different commercially available single mode fiber types. To provide the proper comparison among these three single mode fibers, the presented analysis is carried out at 10 Gbps and 40 Gbps data rate. Section 5.3 provides the transmission link design using DP-DQPSK modulation format in a 9 channel DWDM configuration. The proposed DWDM transmitter has been designed for symbol aligned and symbol interleaved formats. Section 5.4 provides the performance analysis of the designed link for linear and nonlinear effects. Section 5.5 summarizes the important findings of the chapter.

5.2 RZ-DQPSK transmission link design

Both NRZ and RZ line-coding are possible with DQPSK modulation and can be used for the transmission of input data. Since the RZ coding is less susceptible to the nonlinear effects thus, is a more popular coding technique in long distance optical transmission [75]. As discussed in chapter 2, DQPSK is a phase modulation format and for detection modulated signal first converted from phase to amplitude before applying to the photodiodes.

Proposed simulation setup for RZ-DQPSK modulated optical signal transmission is shown in Figure 5.1. The link parameters are specifically designed to investigate the ASE-noise performance at 10Gbps data rate. In the given model DQPSK precoder encodes the data signals from PRBS sources (P) and (Q) to the phase difference of the carrier. Precoder is an essential block in DQPSK transmitter, which prevents the error transmission it ensures

that the received signals are properly matched to the transmitted one. RZ driver 1 and 2 convert the input logical data signal into an electrical signal and these electrical signals pass through LPF (P) and LPF (Q) with a center frequency of 15GHz for further processing. DQPSK modulator receives the electrical input data signal from LPF (P) and LPF (Q) and provides the modulated optical signal for further transmission. An elaborate view of DQPSK modulator is shown in Figure 5.2 (a). Incoming in-phase and quadrature components of electrical data signals denoted as V_inphase and V_quadrature pass to the MZM_P and MZM-Q and the third MZM which work as a phase modulator is used to generate the RZ pulse shaped DQPSK (RZ-DQPSK) modulated the optical signal. Laser source which provides the optical signal to the modulator is having the linewidth of 10MHz and center frequency of 194 THz.

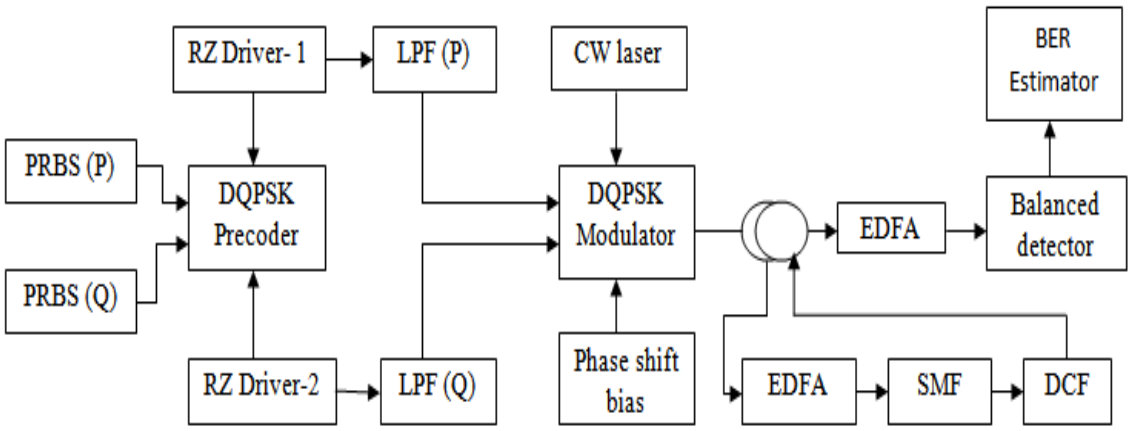

Figure 5.1: Simulation setup for RZ-DQPSK modulation transmission

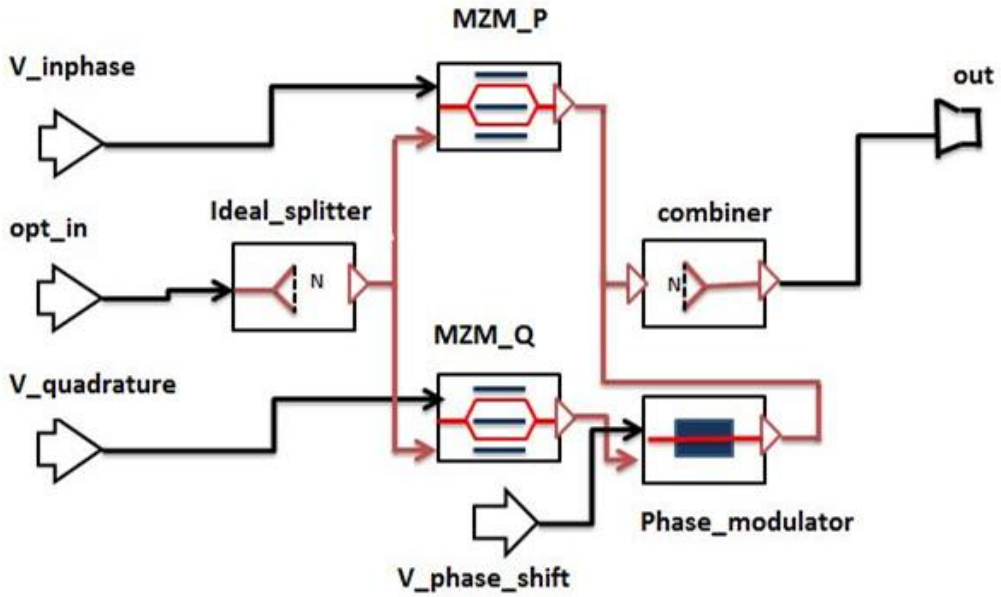

Figure 5.2(a): Inside view of DQPSK modulator [75]

Modulated optical signal is transmitted through the optical fiber loop. This fiber loop consist of an erbium-doped fiber amplifier (EDFA), single mode fiber (SMF) followed by dispersion compensation fiber (DCF). DCF is used to compensate the fiber dispersion along the length of the fiber. EDFA have the maximum gain of 30dB with the ASE noise of 4.5dB whereas power level in the link has maintained very low (-10dBm) to avoid nonlinear effects. Thus ASE noise is the most dominating factor for the degradation of the performance of this system.

In the literature, balanced detection scheme has been extensively studied and preferred for the demodulation of DQPSK signal [75, 121,122]. In this chapter, as well balanced detectors are used to demodulate the DQPSK modulated information. Balance detector consists of two photodiodes followed by an interferometer. Expanded version of demodulator subsection is as shown in Figure 5.2 (b). This is basically an incoherent differential detection scheme where one-bit delay line is used for the comparison of the phases of the carrier of the two consecutive bits. Delay interferometer configuration is used to retrieve both in-phase and quadrature phase outputs. From Figure 5.2 (b) it can observe that the filtered signal is applied to the asymmetric Mach-Zehnder (AMZ) interferometer and these two outputs of AMZ are applied to a balanced photodetector. Each arm of detector contains a phase shift of ± pi/4 and delay corresponding to twice the bit duration which corresponds to in-phase (P) and quadrature components (Q). The outputs are then passed through the LPF with cut off bandwidth of 15GHz to recover the required electrical information signal.

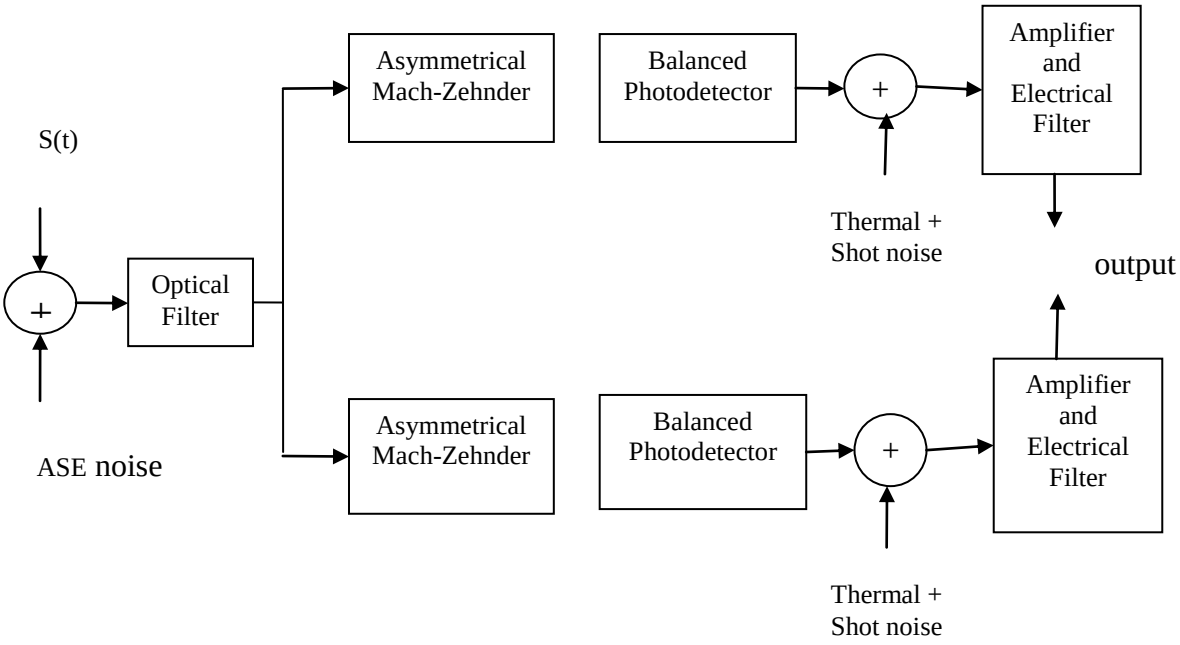

Figure 5.2(b): DQPSK Balanced detector configuration at the receiver [75]

After the transmission link design, section 5.2.1 provides the ASE noise analysis at 10Gbps data rate. For the comparative performance evaluation among different single mode fibers three different commercially available single mode fiber types are utilized. Transmission performance of these fibers is optimized with varying duty cycles in an ASE noise limited channel conditions. The aim of this analysis is to find the optimum fiber types for ASE dominated link which not only increases the performance of the link but also provides the economical solutions to the designers. Section 5.2.2 presents the 40Gbps data rate analysis.

5.2.1 Optimum duty cycle analysis with different fibers at 10Gbps

To observe the performance of smaller and wider pulse widths present simulative has been carried out for different duty cycle pulses with three different single mode fibers. For the same, duty cycles varying from 40% to 90% are considered for the analysis. Single mode fiber types used for the analysis are Standard Single Mode Fiber (SSMF), True Wave-Reduced Slope Fiber (TW-RS) and the Large Effective Area Fiber (LEAF). Specifications of these fibers are given in Table 5.1. During the analysis transmitter and receiver section remains same as discussed in section 5.2 with the channel corresponds to the used fiber type as mentioned in Table 5.1. Therefore, the first setup is design using an SSMF with an attenuation of 0.22dB/km and other corresponding parameters as mentioned in the table

along with an appropriate DCF (DCF_{SSMF}) with an attenuation of 0.55dB/km with all other specification as per the Table 5.1.

Table 5.1: Physical parameters of the fibers used for the analysis [190]

Fiber Type	**Fiber Attenuation** (dB/Km)	**Disp.** (ps/nm/km) @1550nm	**Disp. Slope** ($ps/nm^2/km$) @1550nm	**Nonlinear ref. index** (m^2/W)	**Effective core area** (μm^2)	**Length for Single Span** (km)
SSMF	0.22	17	0.016	3	80	25
DCF_{SSMF}	0.55	-80	-0.076	2.5	20	5.31
TW-RS	0.2	4.5	0.045	2.5	55	25
DCF_{TW-RS}	0.55	-80	-0.8	2.5	20	1.40
LEAF	0.2	4	0.1	2.5	72	25
DCF_{LEAF}	0.55	-80	-2	2.5	20	1.25

Similarly, the analysis has been expanded with the other mentioned fibers with their corresponding DCF fibers to evaluate the optimum duty cycles in an ASE-limited channel condition. Link performance has been measured in terms of BER-equivalent Q-factor (Q-factor) for the varying OSNR values illustrated in Figures 5.3, 5.5 and 5.5 for SSMF, TW-RS, and LEAF- based optical links respectively. Figure.5.3 shows the performance of RZ-DQPSK system with the standard single mode fiber (SSMF) followed by DCF_{SSMF}. It has been observed from the obtained results that the performance of 40% duty cycle pulse is largely influenced by the accumulated ASE noise in the channel, and not much improvement is observed even for the OSNR value of as high as 25dB.

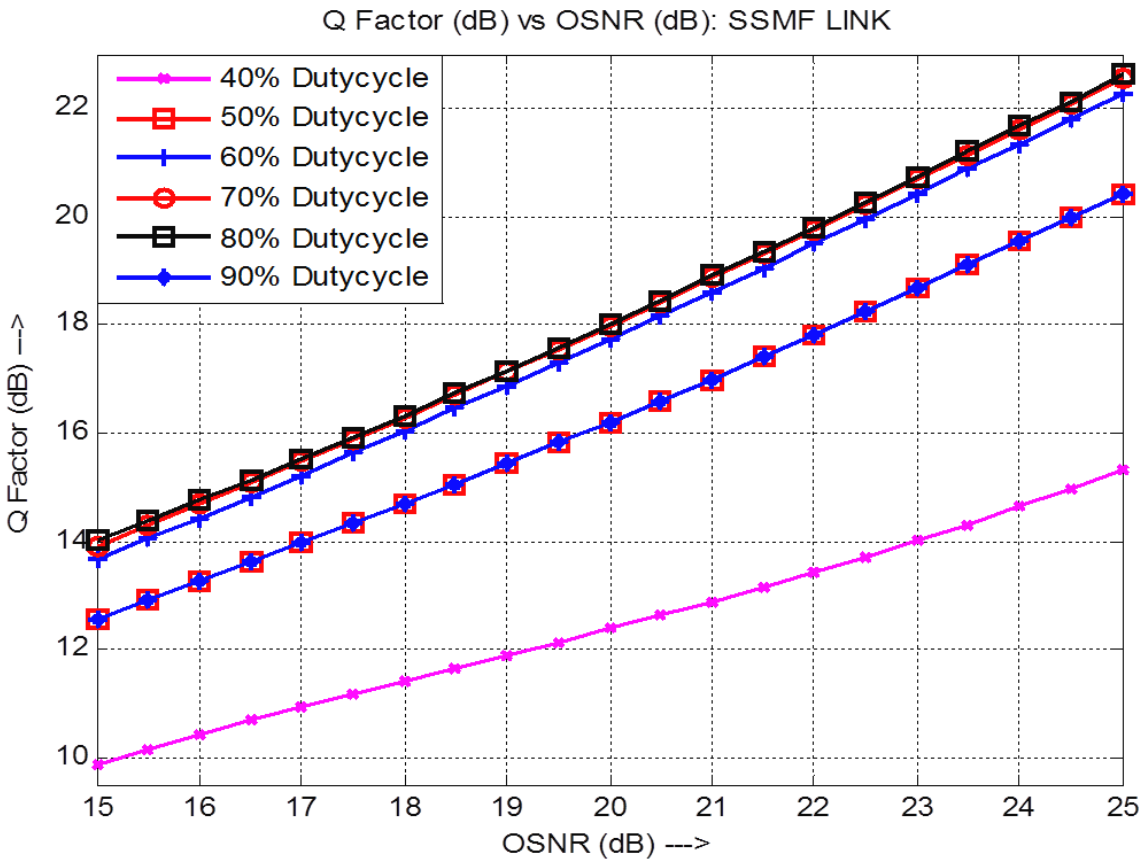

Figure 5.3: SSMF type single mode fiber followed by DCF $_{SSMF}$ for different duty cycle

Curves also reveal that the performance starts improving for higher duty cycle pulses i.e. from 50% to 80%, and a higher value of Q-factor can be obtained even at lower OSNR conditions. Another important finding visible from the graph is that the performance for the 90% duty cycle pulse again degrades. Therefore, it can be wisely said that the link performance cannot be improved simply by increasing the duty cycle of the input pulse.

Similar qualitative behavior can be observed with TW-RS and LEAF fiber channels as shown in Figure 5.4 and 5.5 respectively.

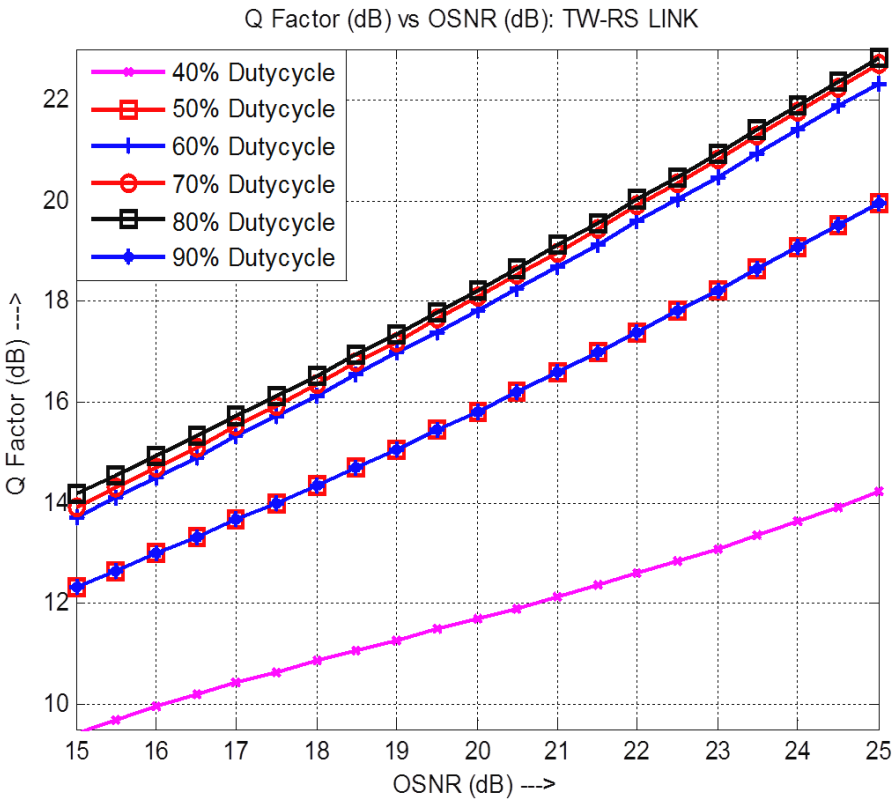

Figure 5.4: TW-RS type single mode fiber followed by DCF $_{\text{TW-RS}}$ for different duty cycles

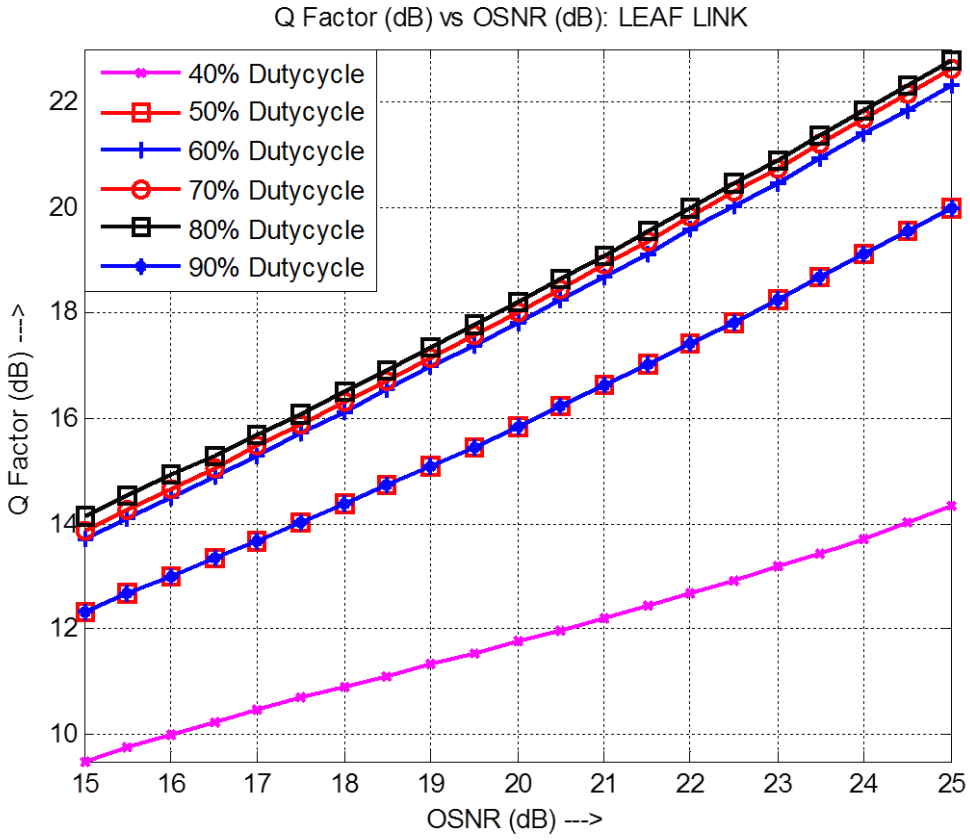

Figure 5.5: LEAF type single mode fiber followed by DCF $_{\text{LEAF}}$ for different duty cycles

These results clearly show that the duty cycles lower than 50% and higher than 90% are not a good choices to get the optimum performance. It has also been observed that the performance of 70% and 80 % pulses is almost identical and both are showing an almost similar pattern for three fiber types. Therefore, to identify the cause of performance deterioration at 90% pulse whereas higher Q-factor for 70% and 80% pulses, an optical power spectrum of these three duty cycles is plotted and shown in Figure 5.6.

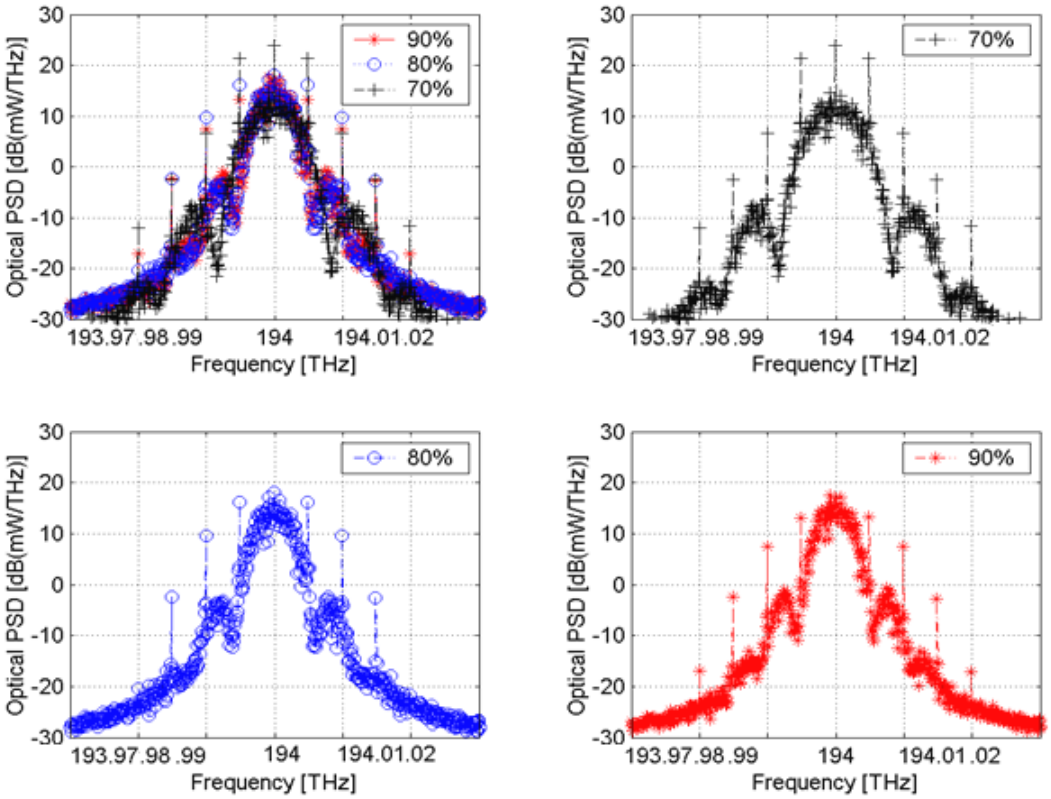

Figure 5.6: Comparison of spectrum of RZ-DQPSK signals having 70%, 80% and 90% duty cycle

From these power spectrum curves, it has been observed that the 70% duty cycle pulse has the widest main lobe and comparatively smaller side lobes. However, 80% and 90% pulses have very identical and close lying main lobes but the distribution of side lobes in both cases is different. It can also be noted with a closer look into the spectrums that 90% pulse has higher side lobes and hence more power inside lobes as compared to 80% and 70% duty cycle pulses, which cause SNR and performance degradation.

After the duty cycle optimization, in section 5.2.2 this optimized duty cycle is used in all three fibers to observe the performance of different fiber types for the long-haul, dispersion compensating optical transmission.

5.2.2 RZ-DQPSK transmission link for long haul applications

For the design of long haul RZ-DQPSK transmission link involves multiple identical spans ranging from 10 to 100 loops with each loop consisting of specific single mode fiber and an optimum length of DCF fiber to compensate the dispersion effect. The link analysis has been done with the optimum duty cycle of 80% and fixed OSNR value of 20dB/0.1nm. The findings of this analysis are presented in Figure.5.7. Obtained results shows that the performance of the link using LEAF as a channel is better than the other two fiber types for the 100 spans of the used link and this is maintained to even beyond this length. These results justified saying that LEAF is a good candidate for the ultra long-haul lightwave link designs.

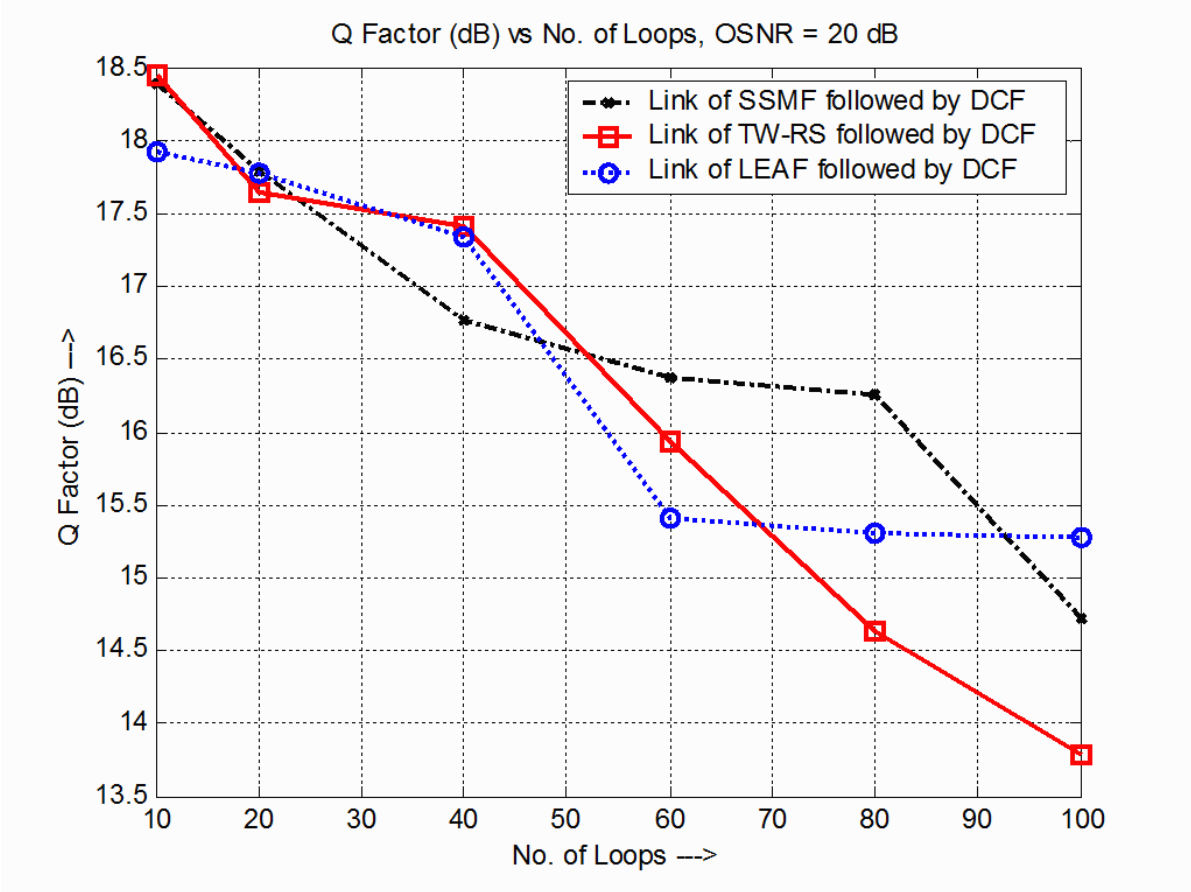

Figure 5.7: Performance of link for three different fibers with 80% duty cycle with different fiber spans

From the curves, it can also be interpreted that after the LEAF the performance of the SSMF as can be observed for up to 90 spans of fiber but after that it starts decreasing. Similar pattern is observed for TW-RS fiber but here this deterioration is more rapid.

Although LEAF provides the longer transmission distance but this definitely comes at higher installation cost, as LEAF is an expensive single mode fiber compared to SSMF and TW-RS fibers as can be seen from Table 5.2.

Table 5.2: Fibers and their commercial prices [191]

Fiber Type	Manufacturer	Price ($/meter)
SMF-28	Corning	0.02
LEAF	Corning	0.042
TW-RS	Lucent	0.032

From this performance analysis and the cost estimation for each of the fiber types it becomes clear that if one needs to design a link for a long haul applications where cost is not an issue than LEAF is a good choice whereas, if the link length is adequate than SSMF is better approach with a less cost of installation. Also, this analysis is useful for the system designers to choose the optimum duty cycle in the ASE noise limited conditions.

Since the objective of this thesis work is to increase the capacity of the link with the economical solutions, therefore, the present analysis is further extended for 40Gbps data rate with SSMF fiber in section 5.2.3.

5.2.3 RZ-DQPSK link analysis at 40Gbps

DQPSK modulation is popular and one of the desired modulation formats utilized to meet the ever increasing demand of data [192-196]. This section provides the simulative analysis of 40Gbps RZ-DQPSK modulated signal transmission in an ASE noise limited channel conditions. The dispersion in the propagation link is fully compensated using the suitable length of the fiber. A transmitter and receiver model remains same as discussed in section 5.2. Figure 5.8 presents the results obtained for various duty cycle pulses at the fixed value of OSNR i.e.20dB/0.1nm.

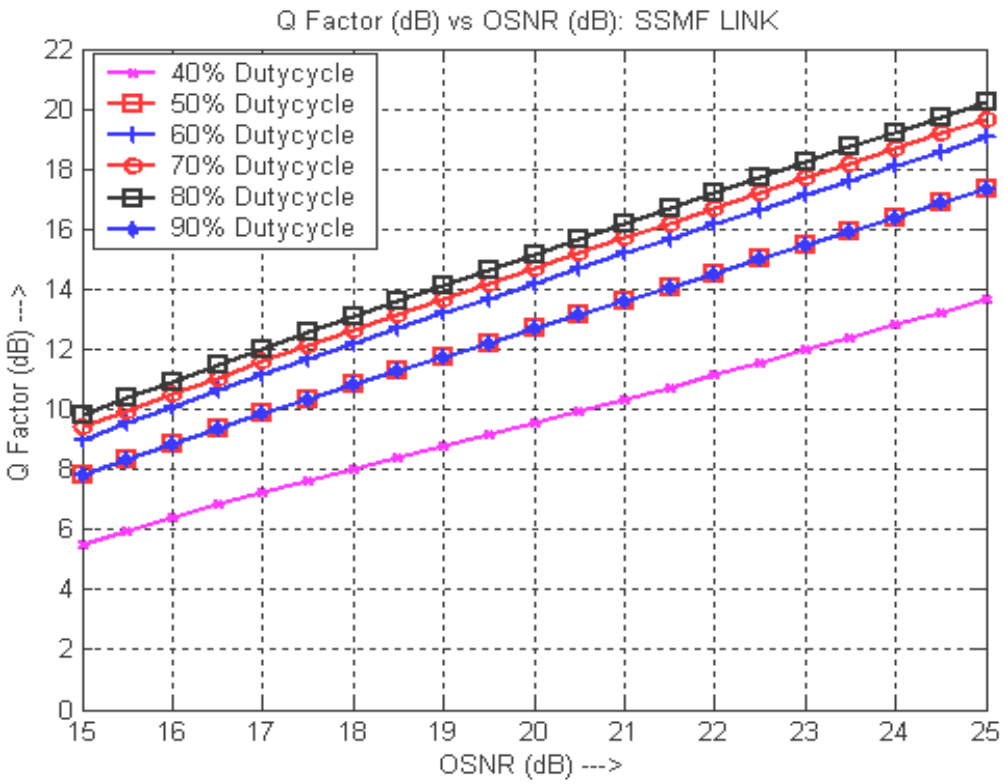

Figure 5.8: Performance of link at 40Gbps data rate

Similar qualitative behavior obtained at 40 Gbps but a significant quantitative difference in the Q values compared with 10Gbps data rate. Thus, at 40Gbps data rate as well 70% and 80% are the better performing pulses and the 80% is providing the best performance. It is also evident that the performance of all other duty cycle pulses degrades greatly with the increase in data rate. The superiority of the 80% duty cycle pulse comes from its spectral distribution with smaller main lobe and lesser spikes.

Design and analysis of single channel optical transmission link is a good approach to analyze the performance of the link for various modulation formats, filter optimizations, fiber types etc. But the implementation of single channel optical transmission is not an ideal approach from both economical as well as from optimum bandwidth utilization point of view. Also, there is a limit to increase the bit rate of a channel as higher data rate demand higher bandwidth and this greater bandwidth incorporates a larger noise power presents in the channel and thus decreases the sensitivity of the system.

Therefore, multichannel systems are required to further increase the data carrying capacity of the optical systems. Also, it has been observed that the new evolving high-speed optical communication systems utilize various multilevel modulation formats which reduce

the symbol rate or baud rate and eventually enhances the system tolerance to OSNR and nonlinear impairments. Moreover, the performance of such systems has been further boosted using polarization multiplexed modulation schemes. As disused in chapter 2 dual polarization modulation schemes are quite popular for future 100G applications. Along with various coherent detection schemes. As per the literature [153-154,156] non-coherent DQPSK modulation with RZ and CSRZ pulse shapes is a popular scheme for long haul high data rate applications. One of the most attractive features of dual polarized formats in a DWDM systems is the significant reduction in the required symbol rate [149]. Thus, if DQPSK modulation is used for 100G transmission then the required symbol rate would be 56Gbaud whereas for DP-DQPSK the symbol rate needed is 28Gbaud. Lower symbol rate gives better tolerance to linear and nonlinear effects and it allows the utilization of already matured lower speed components to be utilized in the link. Also, research has shown that NRZ and RZ pulse shape with symbol-interleaving significantly improves the system performance in presence of cross phase modulation reducing the signal-to-average-power ratio [197].

Therefore, the present analysis of DQPSK link transmission has been further extended for multichannel systems with dual polarized configuration of DQPSK i.e. DP-DQPSK in section 5.3 to further increase the data rate of the optical transmission links. Transmission link has been designed for symbol aligned and symbol interleaved formats and optimized for various fiber impairments.

5.3 DP-DQPSK transmission link design

OptSim^{TM} based DP-DQPSK transmitter model is shown in Figure 5.9. This transmitter is used to generate the NRZ and RZ pulses in symbol-aligned and symbol-interleaved formats. Two different duty cycles of RZ pulse has been considered for the transmission i.e. 50% duty cycle RZ (RZ50) and 67% duty cycle RZ (RZ67). Lower duty cycle pulses have not been considered for this analysis because the spectrum of those pulses is significantly wide for the 50GHz channel spacing.

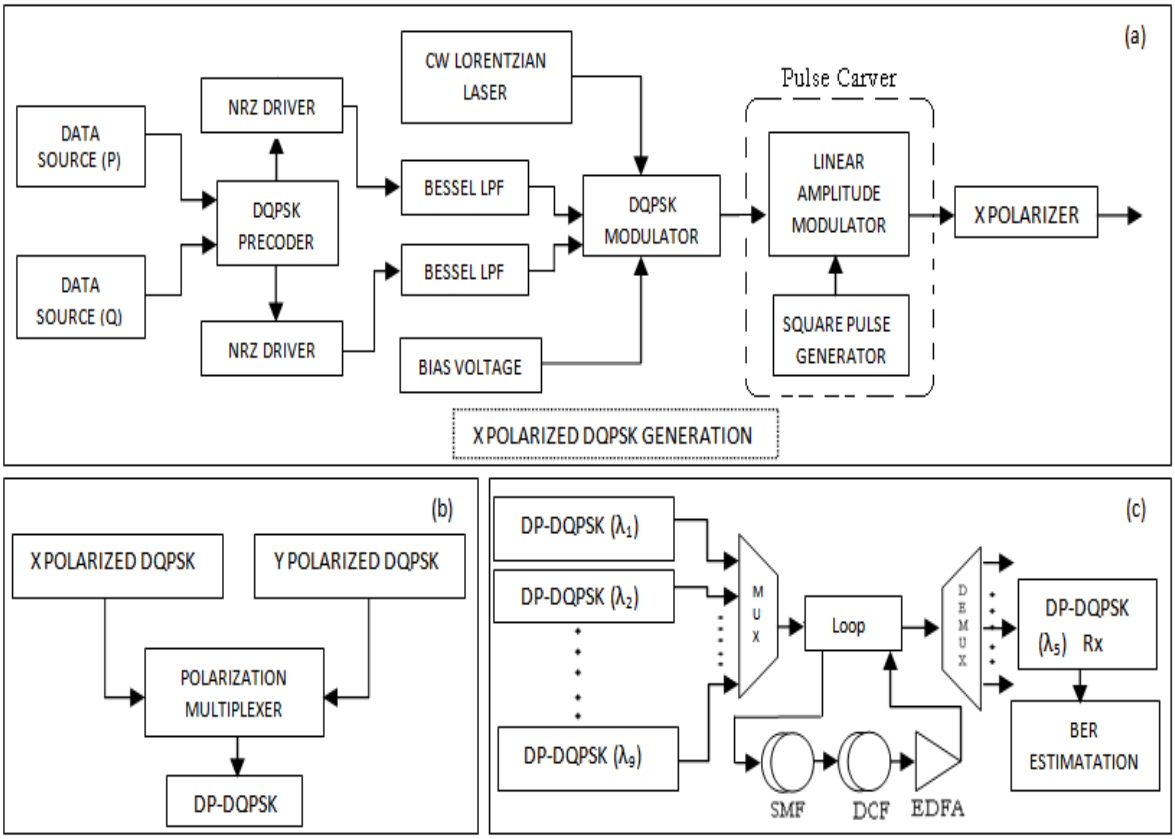

Figure 5.9: Simulation setup for 1Tbps DWDM transmission. (a) Setup for generation of X-polarized DQPSK transmitter comprising of NRZ-DQPSK module, Pulse Carver Module and X Polarizer module (b) Setup for generating DP-DQPSK (c) Simulation setup for 9 channel DP-DQPSK DWDM optical communication system

Figure 5.9 (a) shows the single channel DQPSK transmitter section which consists of I and Q modulators driven by independent data sources (pseudo- random binary sequence generator) with sequence length of 2^{16}-1 and symbol rate of 28Gbaud, DQPSK precoder, NRZ modulator drivers, electrical Bessel low pass filters (LPF), DQPSK modulator and bias voltage generator. CW laser is used as an optical source having a line width of 10MHz. Pulse carving circuit which is used to generate the RZ pulse shape with different duty cycle consists of the clock generator and linear amplitude modulator.

The generated DQPSK signal is followed by a linear polarizer with X-polarization to generate X-polarized component. The Y-polarized component is also generated using the similar model with a polarization rotator and polarizer to change the state of polarization and then these two components are multiplexed using polarization multiplexer to generate DP-DQPSK as shown in Figure 5.9 (b). In this design, delay devices in the Y-polarized arm are used to obtain symbol-interleaved formats from the conventional symbol-aligned

format. Bessel optical band pass filters with -3dB bandwidth of 64GHz are used as optical multiplexing filters within WDM multiplexer shown in Figure 5.9(c), which are deployed for removing the extra side lobes from the pulse and finally transmitting them through the optical fiber link. For the simulation LPF of order 5 and bandwidth equals to the baud rate have been used. This design is modeled for 9 WDM channels with channel spacing of 50GHz. The center WDM channel wavelength is 1550 nm and has been de-multiplexed using the optical de-multiplexer filter with specifications identical to that of optical multiplexer filter used at the transmitter side. At the receiver side, optical demultiplexing filters, electrical LPF (specifications same as used at the transmitter side) and DPSK receiver are used for the estimation of system performance in terms of BER-equivalent Q-factor.

Figure 5.9(c) shows the optical communication system for 9 channels NRZ/ RZ50/ RZ67 DP-DQPSK (symbol-aligned/ symbol-interleaved) leading to 1Tbps DWDM transmission. In the simulation model of optical link in Figure 5.9(c) a single mode fiber (SMF) with attenuation (α) of 0.2 dB/km, dispersion (D) of 16.5 ps/km-nm and dispersion slope(S) of 0.07 ps/nm^2/Km at 1550nm, nonlinear refractive index (n_2) of 2.5 x 10^{-20}m^2/W, nonlinear coefficient (γ) = 1.3 W^{-1}km^{-1} and core effective area of the fiber (A_{eff}) as 80 μm^2 has been considered. The dispersion compensating fiber segment used in each span for compensating GVD has α = 0.6 dB/km, D = -63.65 ps/km-nm and S = 0.07 ps/nm^2/Km at 1550nm, n_2 = 3.0 x 10^{-20} m^2/W, γ = 5.2238 W^{-1}km^{-1} and A_{eff} = 20 μm^2. The bandwidth of the optical multiplexing and demultiplexing filters are chosen after the careful analysis of these spectrums shown in Figure 5.10.

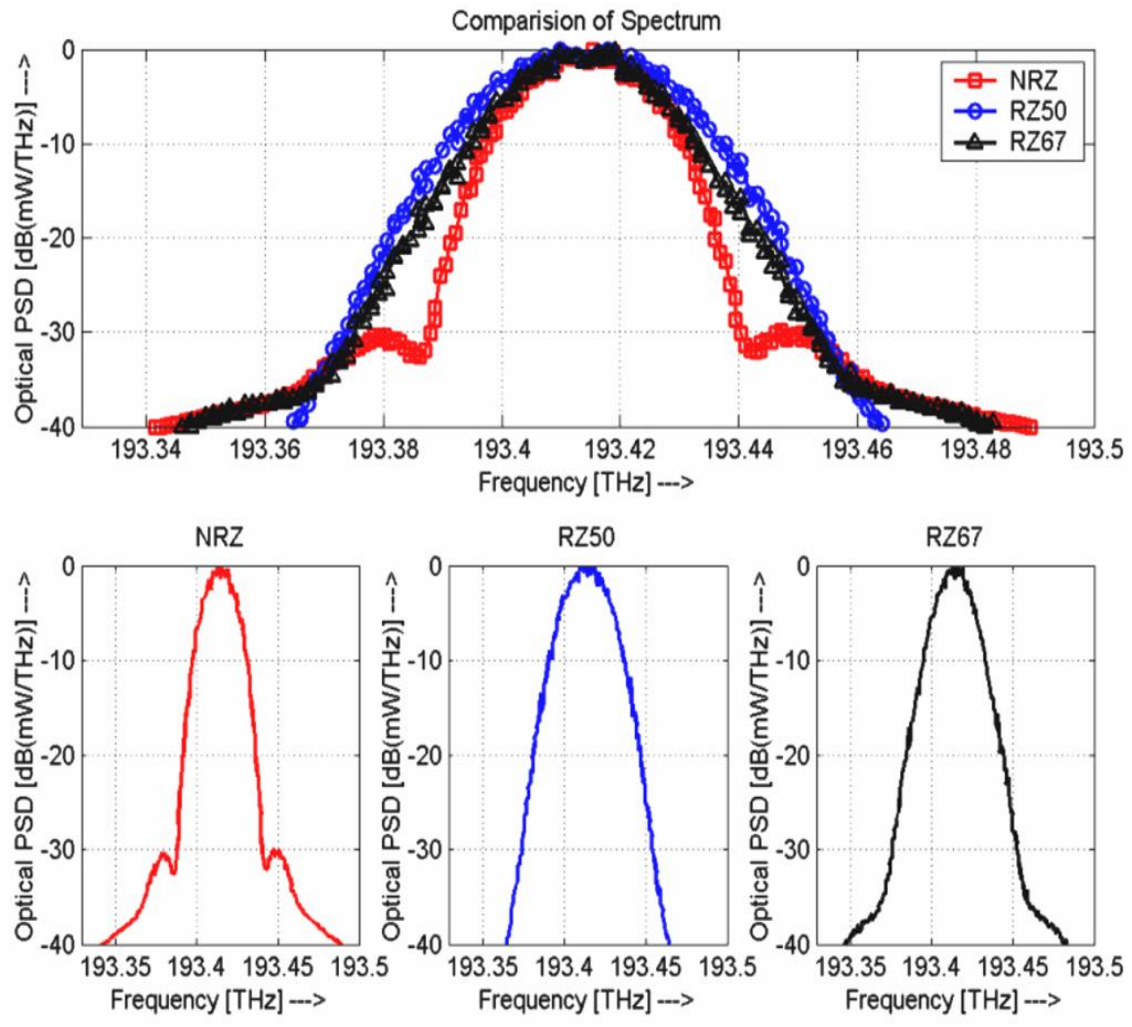

Figure 5.10: Optical Spectrum of NRZ, RZ50 and RZ67 pulse shapes

From the spectrum, it has been observed that the NRZ pulse have the narrower main beam but higher side lobes as compared to RZ50 and RZ67 pulse shapes. RZ50 pulse has the widest main lobe followed by the RZ67 pulse.

After the complete link design, section 5.4 provides the performance analysis for various linear and nonlinear fiber impairments for two different situations first when one of the effect is present at a time in the link and second for a more realistic situation when all are influencing the signal transmission at the same time.

5.4 Analysis of intrachannel and interchannel effects

This section provides the performance analysis of three pulse shapes mentioned above, For ASE, GVD, XPM, and PMD for the high-speed long haul optical transmission link.

5.4.1 ASE noise limited system

ASE is a critical issue to take care of high-speed WDM systems. The used amplifier noise figure (F_n) depends on the gain (G) and spontaneous noise factor (n_{sp}). General expression for the same can be written as [26]:

$$F_n = 2n_{sp}\,(G-1)/G \approx 2n_{sp} \qquad (5.1)$$

In the present analysis to consider only the ASE effect 3.5dB F_n has been considered. The dispersion effect is fully compensated using a DCF segment of length ~20.586km for the used SMF length of ~79.414 km. Degradation owing to nonlinear effects are negligible by ensuring a low value of launched power. The Length of the transmission link has been considered up to 1000km (10 spans of 100km each). System performance has been measured in terms of BER-equivalent Q-factor. In the link design EDFAs are placed after every span of 100km thus ASE noise gets accumulated during the propagation. This accumulated ASE effect deteriorates the SNR value at the receiver and eventually degrades the measured BER equivalent Q value.

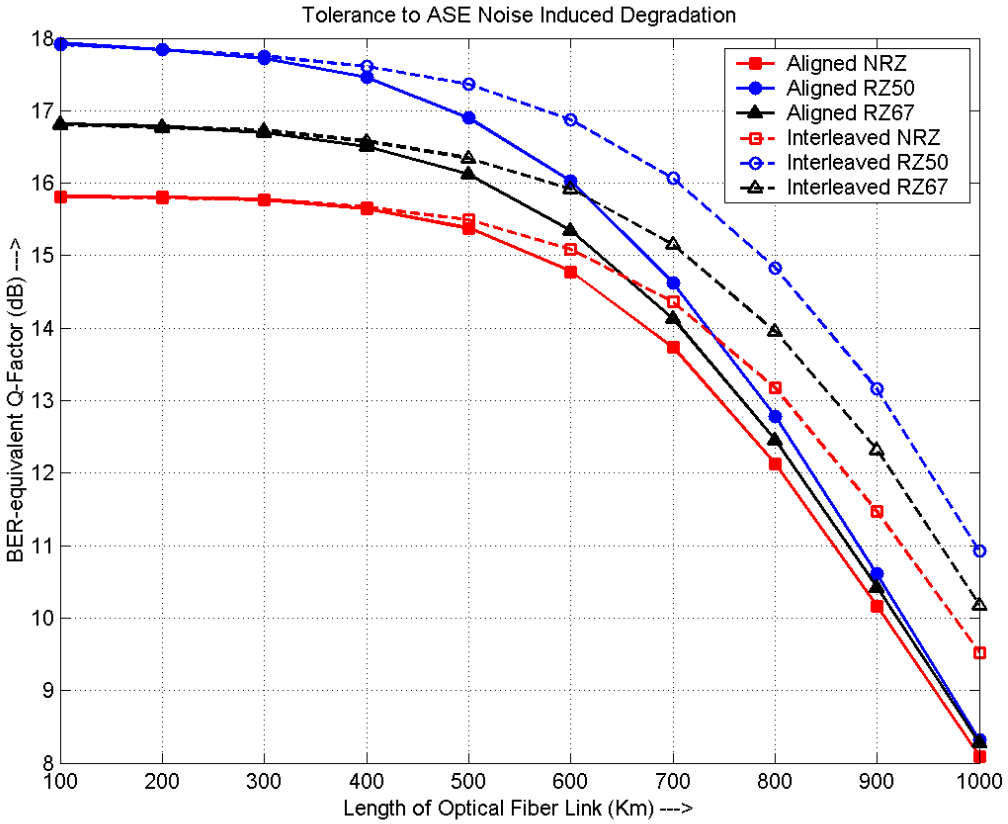

Figure 5.11: ASE noise limited system performance for various pulse shapes

Figure 5.11 reports a BER equivalent Q factor with the varying length of the fiber for symbol aligned and interleaved cases of NRZ and RZ pulse shapes. It can be observed from the curve that symbol- interleaved outperforms symbol- aligned format for both NRZ and RZ pulse shapes. It is also observed that RZ50 pulse shape provides the maximum advantage from the symbol interleaving case. The performances of symbol aligned NRZ, RZ50, and RZ67 show a significant difference for the shorter optical link up to 400km but they tend to follow each other for the longer length of the link and ultimately merging with each other for the longer fiber length i.e. 1000km. The symbol interleaved case also show the similar qualitative behavior with the quantitative difference to show a larger Q-value or a better performance. Although, for the symbol interleaved case curves are also converse as the distances increases but the effective distance is higher than the case of symbol aligned. These analyses appreciate the benefit of symbol interleaving over the symbol aligned case.

5.4.2 GVD limited system

For the GVD analysis, distributed dispersion along the length of the SMF fiber has been considered. In a distributed dispersion map a DCF segment is placed after an SMF segment for the proper management of the accumulated dispersion. In this simulation run, fiber dispersion of +10 ps/nm for every dispersion map period has been considered and the same is shown in Figure 5.12. This residual dispersion-per-span (RDPS) helps to reduce the impact of FWM and XPM for multichannel DWDM systems. Here, for the GVD induced degradation, same simulation setup is considered as shown in Figure 5.9 except the lengths of SMF and DCF fibers. These lengths are chosen to be ~79.53837km and 20.46163Km respectively to maintain an RDSP of +10 ps/nm in each dispersion map.

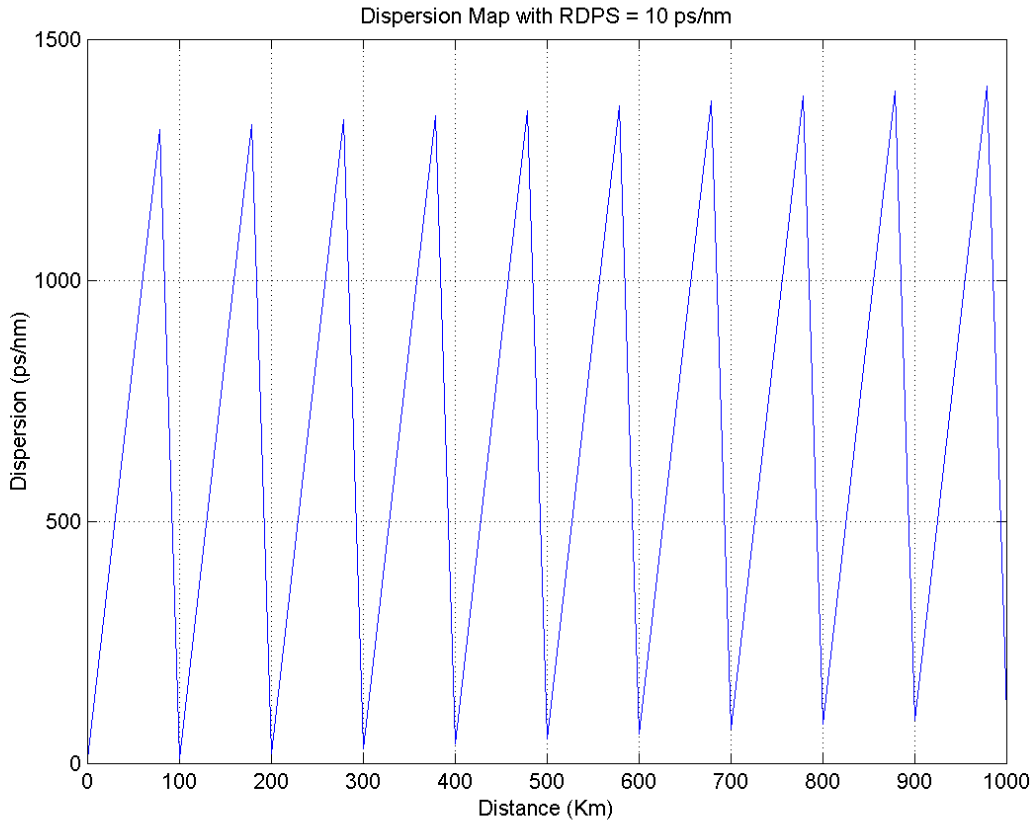

Figure 5.12: SMF-DCF based dispersion map with RDPS = + 10ps/nm.

ASE noise has been neglected in this simulation. Nonlinearities are kept at a minimum level by considering a small launched power. Dispersion effect has been observed up to 1000km (10 spans of 100km each). The performance of the link has been measured in terms of BER- equivalent Q and with respect to the fiber length and the same is plotted in Figure 5.13. From the careful analysis of the curves, it can be observed that here as well symbol-interleaving shows more tolerance towards the accumulated dispersion when compared with symbol aligned format. Also for the symbol aligned case RZ pulse shapes perform better than NRZ even for the shorter fiber lengths. Among the two RZ formats, RZ50 shows the better performance towards the accumulated dispersion in both symbol-aligned and interleaved formats.

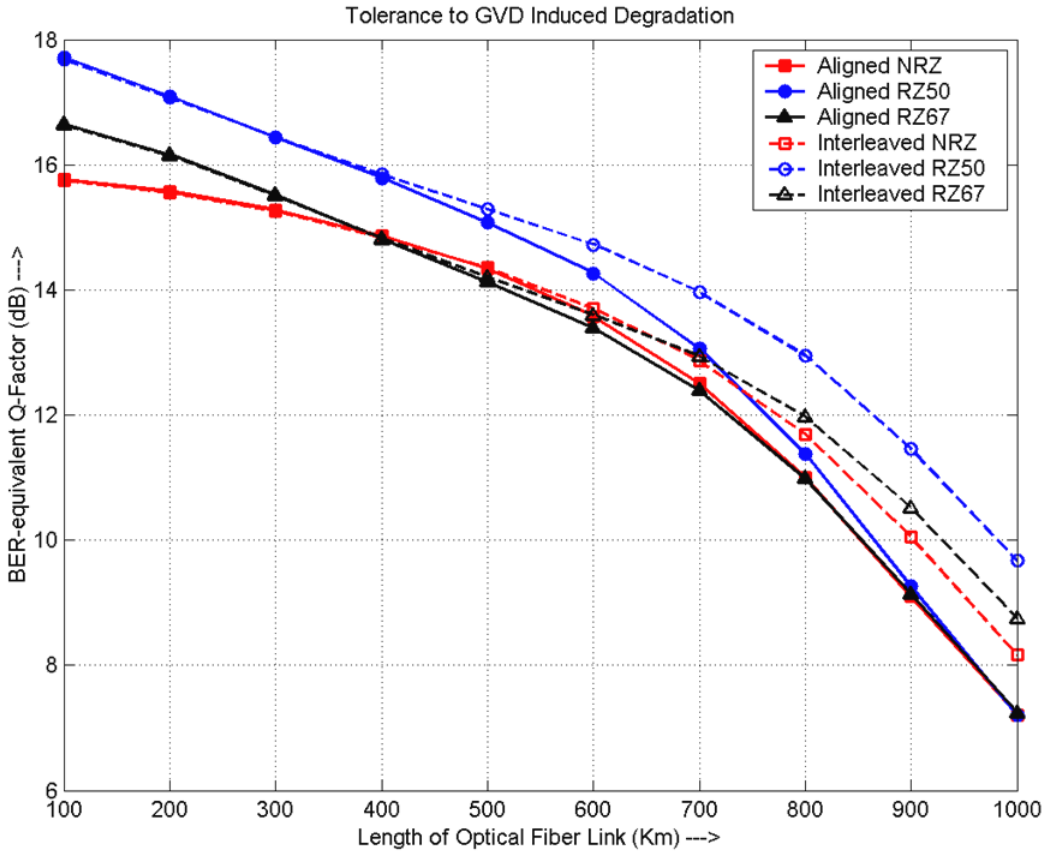

Figure 5.13: GVD limited system performance for different spans of optical fiber for various pulse shapes.

These results appreciate the benefits of symbol interleaving over symbol-aligned and can recommend RZ50 to be an optimum pulse shape for GVD induced impairments in DWDM transmission. This analysis helps in estimating the system performance degradation due to the accumulation of GVD induced impairments over multiple spans of fiber.

5.4.3 XPM limited system

In DWDM systems when two or more channels are transmitted simultaneously inside an optical fiber then because of the intensity dependence of the refractive index the cross-phase modulation (XPM) results. To limit the nonlinear effects launched power is kept at lower levels but as the number of channels increased in WDM systems then power has to be increased to get the desired SNR at the receiver. XPM is an important limiting factor for WDM systems and depends not only on the power of the channel but also on the power of the other neighboring channels [69]. Nonlinear phase change of the j^{th} channel ϕ_j^{NL} can be related to the power of the channel as:

$$\phi_j^{NL} = \gamma L_{eff}\left(P_j + 2\sum_{m \neq j} P_m \right) \quad (5.2)$$

where, γ is a nonlinear parameter in W^{-1}/km and α is an attenuation in dB/km. XPM vary with a bit to bit depending on the bit pattern of the neighboring channels and for equal channel powers, the phase shift in the worst case where all channels simultaneously carry 1 bits and all pulses overlap is given by.

$$\phi_j^{NL} = (\gamma / \alpha)(2M - 1)P_j \quad (5.3)$$

In equation (5.2) and equation (5.3) factor 2 is due to the nonlinear susceptibility and it shows that the XPM is twice as effective as SPM for the same amount of power. Therefore, to observe the effect of XPM induced impairments in presented DWDM model launched power is considered from ~5mW to ~80mW. GVD is fully compensated using the SMF of length ~ 79.414 km and DCF of length ~ 20.586km. Also for this analysis, ASE and PMD effects are not included. Findings of this analysis are measured in terms of BER-equivalent Q-factor corresponding to the launch power and the same are plotted in Figure 5.14. Since XPM induces the broadening of the pulse spectrum which tends to make the side lobes broader. These side lobes cause aliasing with the other pulses of adjacent channels and degrade the link performance.

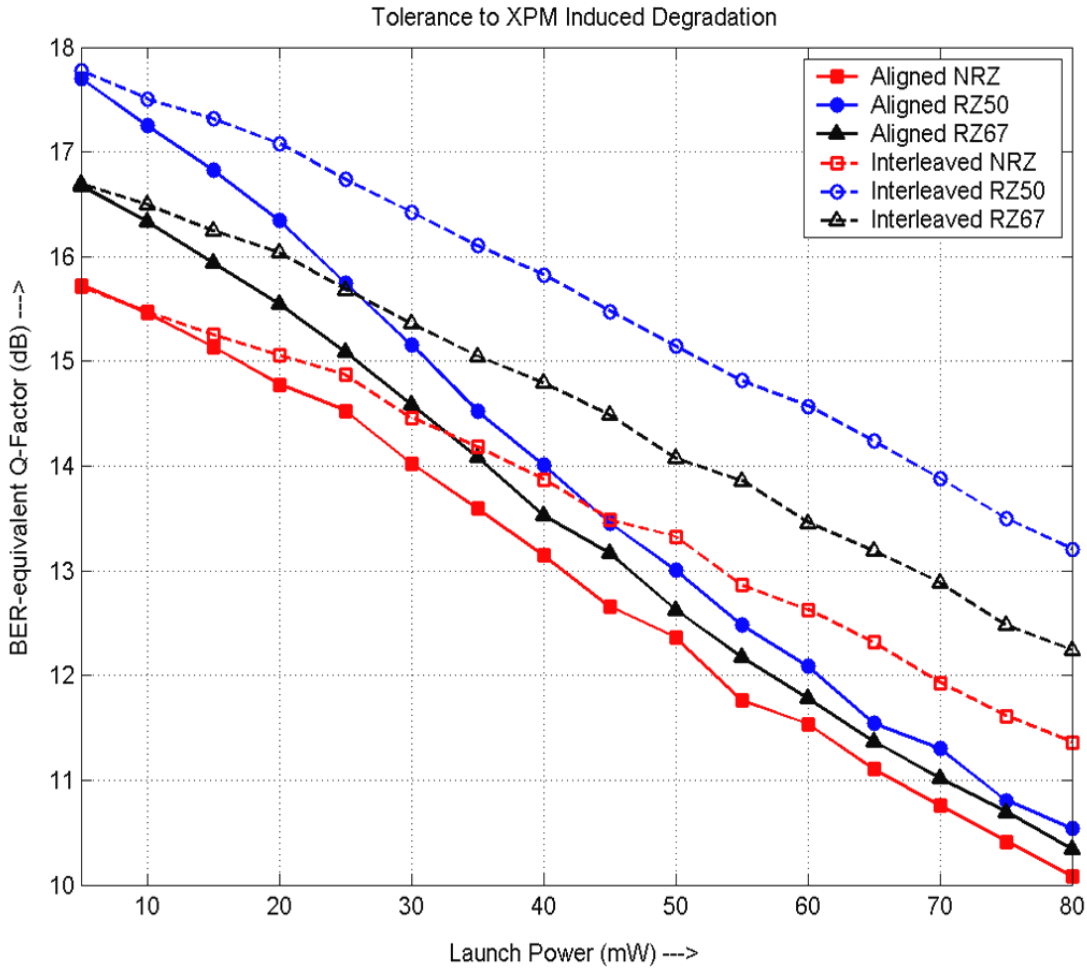

Figure 5.14: XPM limited system performance for various pulse shapes

From these results, it has been observed that for the smaller launch power the performance of the Aligned- RZ50 pulse shape is better than the other two pulse shapes. But the performance of all the three pulse shapes deteriorates when the XPM induced nonlinear impairments dominant with the increase of launch power. From these results, it has also been observed that in the case of interleaved format, RZ50 outperforms RZ67 and NRZ and their relative performance is maintained even for higher launch power levels. We can also observe that all the three pulse shapes obtain the benefit from the symbol interleaving format and amidst all RZ50 pulse shape acquire the maximum advantage.

5.4.4 PMD limited system

PMD-induced degradation limits the performance of the modern high-speed optical systems. Since birefringence of the fiber is not constant but changes randomly. As a consequence of this fact, light launched into the fiber with linear polarization quickly

reaches different random polarization state and results in pulse broadening. The degree of modal birefringence is defined as:

$$\sigma_T^2 = \left\langle (\Delta T)^2 \right\rangle \approx D_p^2 . L \tag{5.4}$$

where, ΔT is the time delay between two polarization components during propagation of an optical pulse and represents as:

$$\Delta T = \left| \frac{L}{v_{gx}} - \frac{L}{v_{gy}} \right| \tag{5.5}$$

L is the length of fiber, D_p is the PMD parameter typically ~0.1 to 1ps/√km, v_{gx} and v_{gy} are the group velocities of X and Y polarized components.

To observe the performance of the optical system under PMD induced degradation, PMD parameter (~0.1ps/√km) and fiber birefringence in both SMF and DCF fibers has been included. The system performance is again observed for 1000km (10 spans of 100km) and the same is presented in Figure 5.15. From the figure, it is observed that Aligned- RZ50, RZ67 and NRZ pulses are not able to show desired performance for longer length of the fiber but for shorter optical link i.e. up to 400km shows a significant difference and tend to follow each other when the system performance gets limited by PMD over longer fiber links of up to 1000 km. It can also observe from the graph that for symbol-aligned format RZ50 offers the best tolerance to PMD induced degradation. Similar behavior is observed for all the three pulse shapes in symbol-interleaved format.

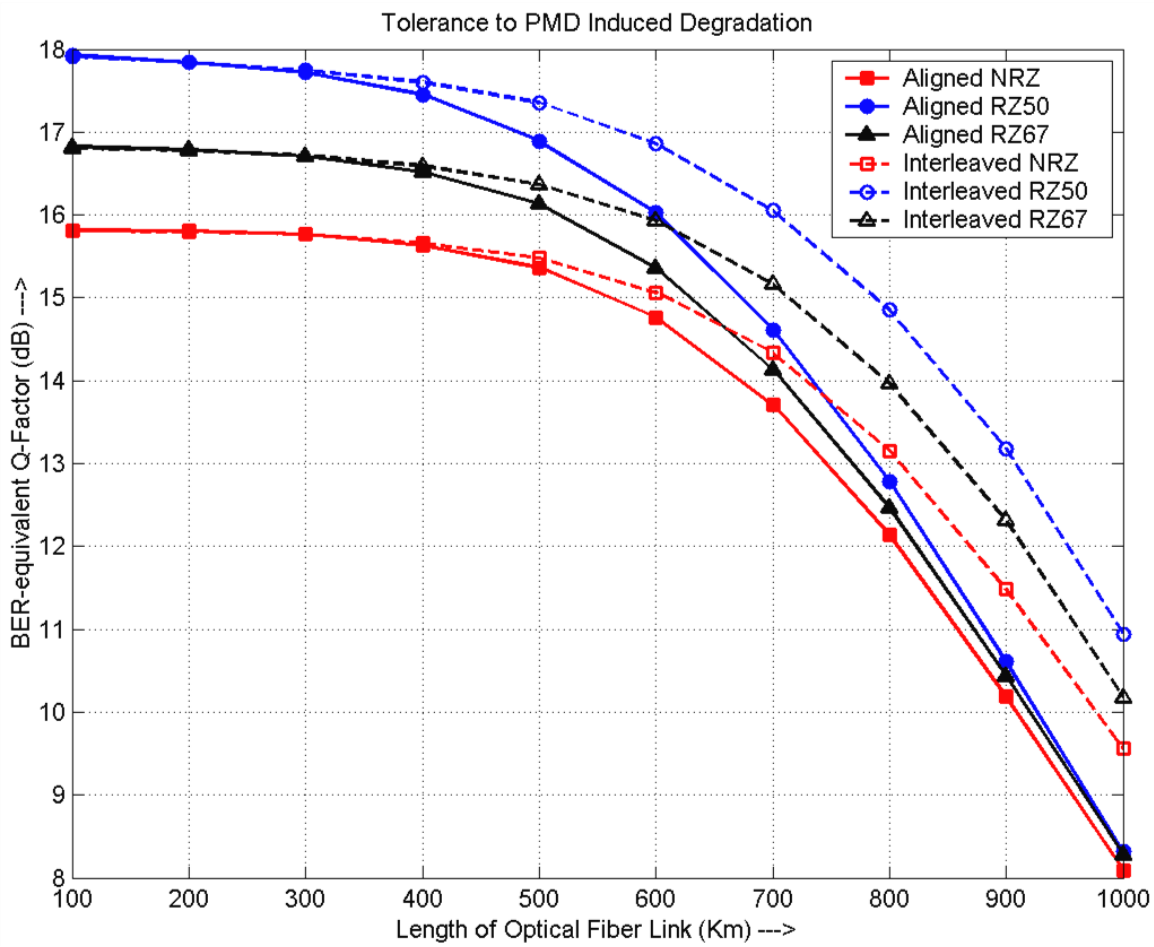

Figure 5.15: PMD limited system performance for various pulse shapes

After observing the individual behavior of each of these effects, present analysis has been carried out for the more realistic situation in section 5.4.5 when all the effects are present in the link at the same time.

5.4.5 Combined effect of ASE, GVD, XPM and PMD

For this analysis 3.5dB of noise figure in EDFA is included for the ASE effect, residual dispersion of +10ps/nm for the GVD effect, launch power of around ~5mW to include XPM effect and PMD parameter of ~0.1ps/√km in both SMF and DCF segment has been considered.

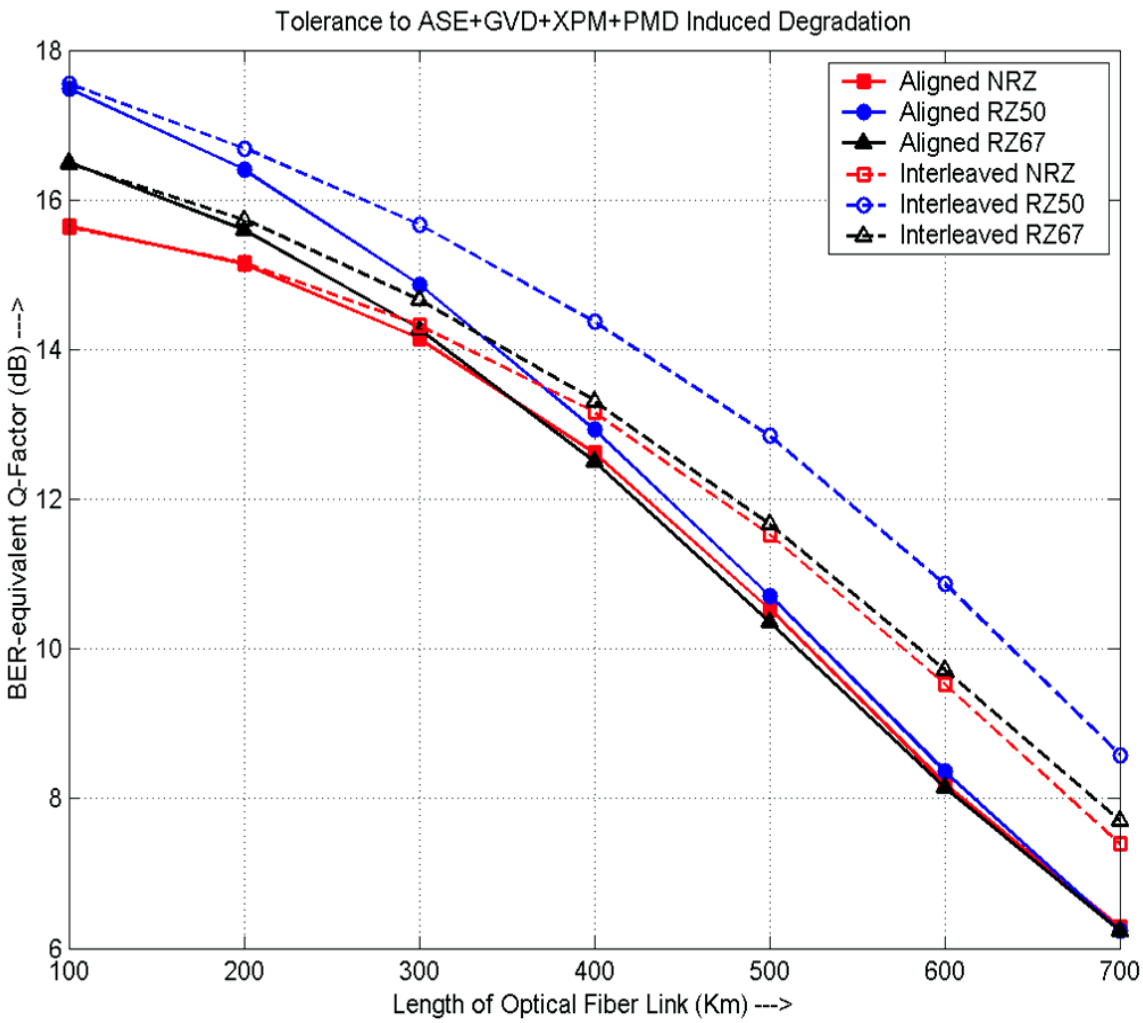

Figure 5.16: Effect of ASE, GVD, XPM and PMD on system performance for various pulse shapes

This analysis has been performed till 700km as after that the obtained Q-factor reaches to a minimum required value of 6. Results of this analysis are reported in Figure 5.16. The similar qualitative pattern has observed as found in previous analyses. It is clear from the results that for symbol aligned modulation format performance of the RZ50 pulse is better than RZ67 and NRZ pulse shapes. However, as the fiber length increases performances of these different pulse shapes follow each other. For symbol interleaved case, RZ50 outperforms RZ67 and NRZ pulse shapes and the superiority is maintained along the fiber link. The performance of Interleaved -NRZ is found to be inferior to -RZ67 for smaller fiber link but becomes comparable over longer propagation distance. Thus from the results, one can appreciate the benefits of symbol interleaving and can recommend RZ50 with symbol interleaving to be the optimum pulse shape when the performance of the high-speed DWDM transmission system is limited by linear and nonlinear impairments.

5.5 Conclusion

This chapter discusses the DQPSK modulated pulse transmission in a single channel link with RZ pulse shape (RZ-DQPSK). The transmission of the pulse is carried out for 10Gbps and 40Gbps data rates. The performance of the link has been optimized for different duty cycles in an ASE noise limited channel conditions. For the analysis, three different single mode fiber types have considered named SSMF, LEAF, and TW-RS. The analysis shows that the performance of all the fiber types is optimum at 80% duty cycle. Also, it has been observed that LEAF and SSMF are good performing fibers for long distance optical communication, whereas, LEAF is the best candidate for the ultra long haul link designs. Although, the transmission link design using LEAF is a costly affair compared to the other two fiber types. The presented analysis is useful in selecting the specific fiber type and the optimum duty cycle as per the requirement and the available cost budget. The second part of the chapter i.e. section 5.3 deals with further enhancement of data carrying capacity using DP-DQPSK modulated format in a 9 channel DWDM configuration. DP-DQPSK transmitter was designed for symbol-aligned and symbol-interleaved formats. Transmission link analysis shows that RZ50 pulse shape outperforms the RZ67 and NRZ pulses in the presence of various fiber impairments. However, the performance of the link has improved for symbol interleaving compared to symbol aligned format for all the three pulses.

CHAPTER 6

Optical Long Haul Link Design: Dispersion Map Approach

6.1 Introduction

The current explosion of data traffic in communication networks is driven by an unquenchable appetite for internet connectivity on a geographical scale from intra-building to worldwide multi-vendor networks employing multiprotocol wavelength-division multiplexing (WDM) technology [198-199]. To improve the overall capacity of the optical systems various techniques such as the use of advanced modulation formats, different types of fibers, dispersion and nonlinearity compensation has been explored and adopted by system designers. Implementation of advanced modulation formats to carry more number of bits per symbol is an attractive solution to increase the spectral efficiency, but at the cost of higher installation charges due to the requirement of relatively complex receivers.

Although, in optical links, amplifiers compensate the losses but at the same time increases the amount of dispersion accumulated over a transmission link and limit the effective transmission distance. Proper implementation of dispersion management technique such as pre-chirping, dispersion compensating fibers, optical filters etc helps to increase the transmission distance to some extent [15]. But at the same time, implementation of dispersion management for the long haul applications where distance is several thousands of kilometers has been a matter of research. For the shorter distances, dispersion management techniques mentioned above performs well since the nonlinearities do not accumulate over lengths. But nonlinear effects dominate the transmission if the signal remains in the optical domain over the larger link length. For the long distance links, the performance is gradually degraded thus it becomes much more challenging to compensate the errors caused due to these distortions. Therefore, for these applications only dispersion compensation is not sufficient but suitable strategies are required to reduce the accumulated effect and to achieve the optimum performance.

Implementation of periodic dispersion where two different fibers with positive and negative GVD parameters have been used in a periodic manner such that total dispersion

over each map period is approximately zero emerges as a key solution. In this technique of dispersion management effective dispersion is compensated over each map period. Variation of fiber dispersion in this combination leads towards quasi-periodic breathing effect in pulse propagation. Dispersion management (DM) technology has evolved over past few decades and has proved to be very effective in various lightwave applications [200,201]. The effect of GVD in a dispersion managed links along with the fiber nonlinearities enables a stable propagation of pulse where the transmitted pulse undergoes periodic evolution and thus forming dispersion managed soliton known as DM soliton [202,203]. Hence, DM optical links for high data rate long-haul soliton based communication has been an active area of research for last few decades [204].

In dispersion managed link, fiber GVD varies between normal and anomalous values periodically, to yield either positive, negative, or even zero average GVD over a map period. Such propagating pulses in a properly dispersion managed link, enjoy few advantages over solitons in optical links with constant GVD [205]. The designed dispersion managed link also offers reduced Gordon-Haus timing jitter, the lesser influence of FWM, improved signal-to-noise ratio (SNR) at the receiver [206]. Four wave mixing (FWM) in WDM system can be managed to be negligible by ensuring that the dispersion managed link offers large value of local GVD and almost zero average GVD value over the map[207]. However, unlike conventional soliton system where the soliton pulse maintains its shape during propagation in a constant GVD link, the width of a dispersion managed soliton pulse oscillates periodically along the link and it regains its shape after each dispersion managed link span known as Dispersion Map (L_{Map}) [202-207].

As deployment of the DM scheme in optical link forces each soliton pulses to propagate through normal dispersion regime followed by another segment of fiber with anomalous dispersion. Generally, normal-GVD fibers do not support bright solitons and they lead to substantial broadening and chirping of pulse [26]. However, intensive theoretical studies cited in the literature [26,201] have supported the survival of solitons in a DM link, when L_{Map} is kept as a fraction of the nonlinear length (L_{NL}), this ensures negligible nonlinear effects and enables the pulse to propagate in a linear fashion over one map period. Thus DM solitons survive in such a link in an average sense provided their peak power along with width and pulse shape is permitted to undergo periodic oscillations. This chapter presents the numerical analysis mainly concentrates with various dispersion map profiles and eventually investigates the critical fraction i.e. the ratio of L_{Map} to L_{NL} for

each of these profiles. This analysis helps in identifying the best suitable dispersion map profile for DM soliton propagation. The present chapter aims to find the dispersion map profile which offers the maximum length of $L_{Map.}$ This analysis has been further explored for the effect of negative residual dispersion from zero residual dispersion and initial pulse chirp. The Last section of this chapter provides the collision dynamics of the dispersion managed soliton. The organization of this chapter is as follows:

Mathematical modeling of DM link to analyze the pulse propagation has been discussed in section 6.2; Section 6.3 provides dispersion management strategies in fibers suitable for DM soliton propagation. Section 6.4 attempts to maximize the propagation length in such cases with the use of negative dispersion and initial chirp. This section also provides the collision dynamics of these DM solitons. Important findings of the chapter are summarized in section 6.5.

6.2 Mathematical modeling of dispersion managed link

In anomalous dispersion coefficient fibers with a positive value of GVD parameter, β_2 the propagating pulse gets broaden due to dispersive behavior, however, the presence of nonlinear effects induces a counter balance effect to this dispersion. Also, another fiber with a negative value of dispersion parameters β_2 is required to recover the original pulse shape forms a dispersion map (L_{Map}). Therefore this analysis starts with the evaluation of critical fraction (L_{Map}/L_{NL}) for a simple dispersion managed link comprising of alternation spans of two fibers with positive and negative values of GVD parameter β_2 forming the dispersion map. Propagation of an optical pulse inside a dispersion managed link is governed by the Nonlinear Schrödinger equation (NLSE) given as (6.1):

$$i\frac{\partial A}{\partial z}-\frac{\beta_2}{2}\frac{\partial^2 A}{\partial t^2}+\gamma|A|^2A=-\frac{i\alpha}{2}A \tag{6.1}$$

Here A is the pulse envelope, γ is nonlinear coefficient and α is fiber attenuation constant It may be noted in equation (6.1) that β_2, γ, and α are periodic functions of z as these parameters vary periodically and obtain different values in two or more fiber segments deployed to form the dispersion map. Compensation of attenuation at lumped amplifier can be included by tactfully changing the loss parameter suitable at the amplifier locations. Equation (6.1) has been solved numerically to study the performance of DM systems

[208,209]. The last term on the right-hand side in equation (6.1) is further eliminated using the following transformation.

$$A(z,t) = B(z,t)\exp\left[-\frac{1}{2}\int_0^z \alpha(z)dz\right] \tag{6.2}$$

Equation (6.1) then evolves to

$$i\frac{\partial B}{\partial z} - \frac{\beta_2(z)}{2}\frac{\partial^2 B}{\partial t^2} + \bar{\gamma}(z)|B|^2 B = 0 \tag{6.3}$$

The power variations of the pulse propagating along the dispersion managed link are included through a nonlinear parameter

$$\bar{\gamma}(z) = \gamma\exp\left[-\int_0^z \alpha(z)dz\right] \tag{6.4}$$

The variational method used in solving equation (6.3) provides a substantial insight to the design of dispersion managed links [26]. It has been observed that despite variations in amplitude, width, and chirp during propagation, a chirped Gaussian pulse is able to maintain its functional form in a linear regime (γ = 0). Therefore, in dispersion managed link where the nonlinear effects are relatively weak compared to the dispersive effects in each fiber sections, the pulse shape is likely to retain its Gaussian shape defined in equation (6.5)

$$B(z,t) = a\exp[-\frac{(1+iC)t^2}{2T^2} + i\phi] \tag{6.5}$$

where a is the amplitude, T is the width, C is the chirp and ϕ is the phase of the pulse. All these four parameters vary with z because of perturbations produced by periodic variations of $\beta_2(z)$. Equation (6.3) can be derived from the Euler-Lagrange equation using the following Lagrangian density:

$$L_{den} = \frac{i}{2}\left(B\frac{\partial B^*}{\partial z} - B^*\frac{\partial B}{\partial z}\right) + \frac{1}{2}\left[\bar{\gamma}(z)|B|^4 - \beta_2(z)\left|\frac{\partial B}{\partial t}\right|^2\right] \tag{6.6}$$

The evolution equations of the four parameters a, T, C and ϕ in equation (6.5) are found using variational approach. The phase equation is ignored as it is not coupled to other three equations. It is found by integrating the amplitude equation that the combination a^2

T does not vary with z, which leaves the following two coupled equations to be solved [26].

$$\frac{dT}{dz} = \frac{\beta_2 C}{T} \tag{6.7}$$

$$\frac{dC}{dz} = \frac{\bar{\gamma} E_0}{\sqrt{2\pi} T} + (1 + C^2)\frac{\beta_2}{T^2} \tag{6.8}$$

For the linear condition with γ = 0, the ratio $\frac{1+C^2}{T^2}$ is related to the spectral width of the pulse that remains constant and maintain the initial value of the pulse as $\frac{1+C_0^2}{T_0^2}$, where C_0 and T_0 are the chirp and width of input pulses before launched into the dispersion managed link. The solution to equation (6.7) and (6.8) has been found analytically [26] and expressed as:

$$T^2(z) = T_0^2 + 2\int_0^z \beta_2(z) C(z) dz \tag{6.9}$$

and

$$C(z) = C_0 + \frac{1 + C_0^2}{T_0^2} \int_0^z \beta_2(z) dz \tag{6.10}$$

Using equations (6.9) and (6.10) the values of T and C at the end of first map period (z = L_{Map}) are found to be

$$T_1 = T_0 \left[(1 + C_0 d)^2 + d^2 \right]^{1/2} \tag{6.11}$$

and

$$C_1 = C_0 + (1 + C_0^2) d \tag{6.12}$$

where $d = \frac{\overline{\beta_2} L_{Map}}{T_0^2}$ and $\overline{\beta_2} = \frac{\beta_{2n} l_n + \beta_{2a} l_a}{l_n + l_a}$ (6.13)

It is clear from equation (6.13) that for dispersion managed link with $\overline{\beta}_2 = 0$, both T and C returns to their initial input values at the end of each map period. For a dispersion managed link with some residual dispersion i.e., $\overline{\beta}_2 \neq 0$ T and C change after each map period and

the pulse evolution thus is not periodic. For the weakly nonlinear system, an initially chirped pulse satisfying $\overline{\beta}_2 C < 0$ can result in a final pulse narrower than the initial pulse. If dispersion managed link is designed in a fashion that the pulse broadens in the first fiber section and compresses in the second section then the impact of nonlinearities on pulse propagation can be reduced significantly. For such quasi-linear dispersion managed links periodic solutions for T and C can be found by imposing periodic boundary conditions as mentioned below:

$$T(L_{Map}) = T_0 \text{ and } C(L_{Map}) = C_0 \tag{6.14}$$

The conditions in equation (6.14) ensure that the pulse recovers its initial shape at the end of each map period. Thus, such Gaussian pulses propagating through dispersion managed link gives rise to soliton-like behavior, essentially called as dispersion managed (DM) Soliton [26, 205]. Literature reports that the shape of such DM soliton is typically closer to "Gaussian" profile rather than "sech" profile associated with standard solitons [26].

In this chapter, Nonlinear Schrödinger equation has been solved numerically using split-step Fourier method [210-212] implemented in MATLAB for dispersion managed optical link for soliton propagation with Gaussian pulse approximation. Section 6.3 presents the different dispersion map profiles for dispersion managed pulse propagation.

6.3 Different dispersion map profiles for dispersion managed pulse propagation

In this section, four different dispersion profiles resulting in four different dispersion maps with zero residual GVD have been investigated first. The fibers are assumed to be lossless in the simulation.

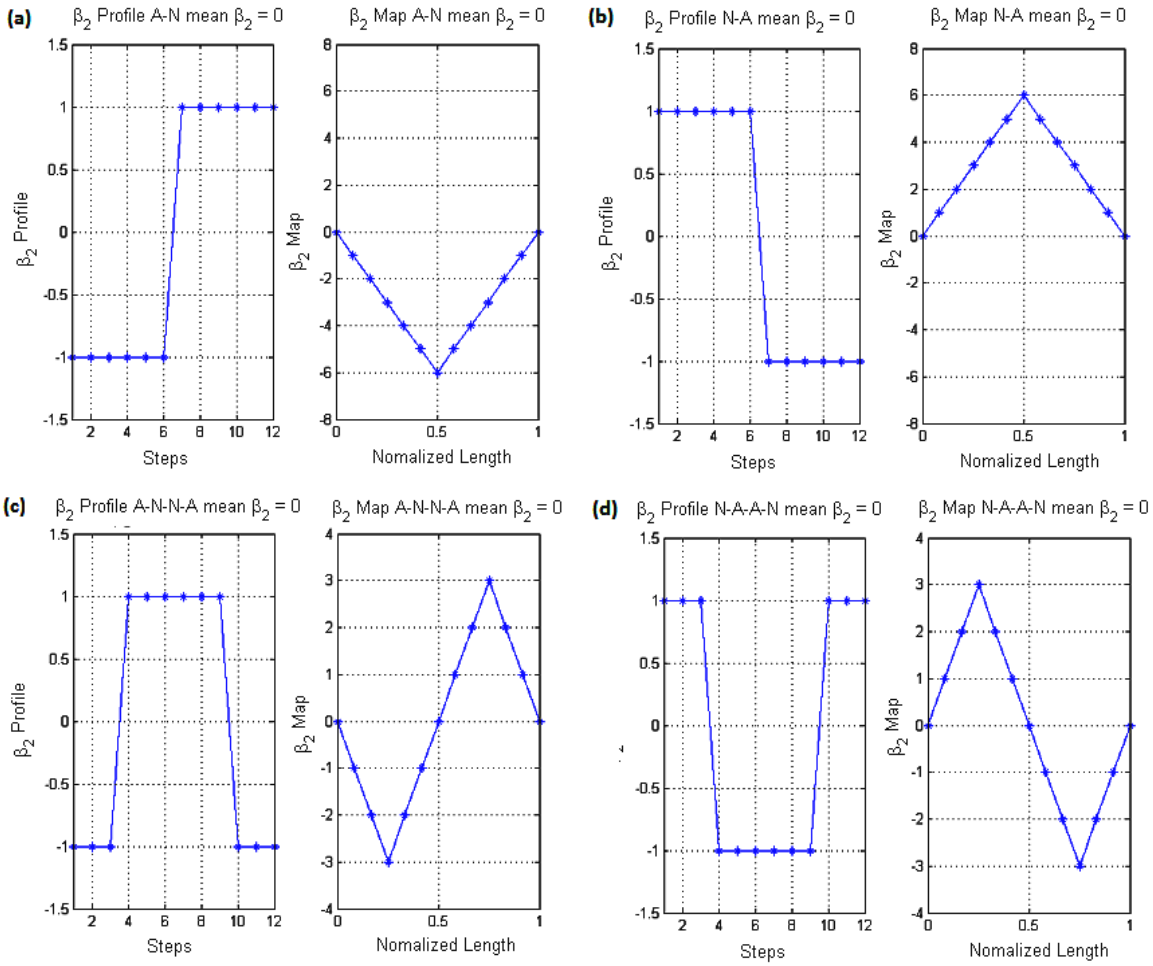

Figure 6.1: (a) A-N dispersion profile and dispersion map (b) N-A dispersion profile and dispersion map (c) A-N-N-A dispersion profile and dispersion map (d) N-A-A-N dispersion profile and dispersion map.

Figure 6.1 shows the four dispersion map profiles viz. Anomalous-Normal (A-N), Normal-Anomalous (N-A), Anomalous-Normal-Normal-Anomalous (A-N-N-A), Normal-Anomalous-Anomalous-Normal (N-A-A-N) considered in this analysis to find out the critical fraction (hereafter called as n where $n = L_{Map}/L_{NL}$) for which DM pulse propagates in a linear fashion over each L_{Map}. It can be seen from Figure 6.1 that all these different dispersion map profiles have zero residual dispersion over a map period. Figure 6.2 shows the pulse propagation in each of these dispersion map profiles when dispersion map length is comparable to the nonlinear length i.e. for the case when n =1.

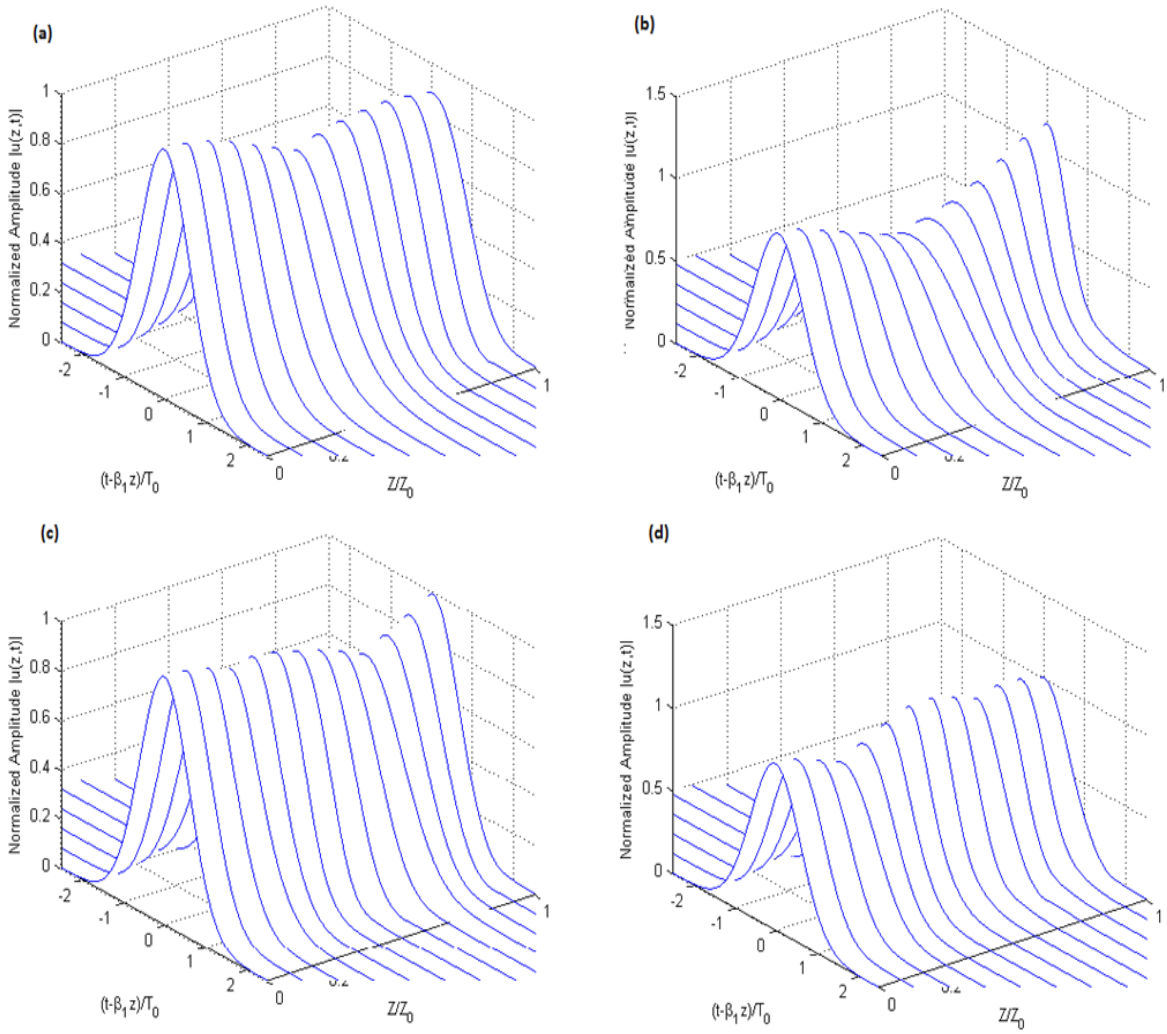

Figure 6.2: Pulse propagation and evolution in (a) A-N dispersion map (b) N-A dispersion map (c) A-N-N-A dispersion map (d) N-A-A-N dispersion map.

It can be observed from Figure 6.2 that DM soliton formation and evolution varies with the dispersion managed scheme deployed in the fiber link. A-N and N-A dispersion map leads towards pulse broadening and pulse compression respectively resulting in a broadened and compressed pulse at the end of a L_{Map} as shown in Figure 6.2 (a) and 6.2(b) . A-N-N-A and N-A-A-N profiles prove to be more suitable for DM soliton formation and evolution as can be seen from Figure 6.2 (c) and 6.2(d) where pulse width in terms of full-width at half maxima (FWHM) at the end of L_{Map} closely follows the pulse initial FWHM .

Further numerical simulations have been carried out to find the critical fraction *n* in these dispersion map profiles having zero residual dispersion to ensure stable DM soliton propagation. This *n* factor can be a design guideline which indicates that, for a particular

dispersion map profile, L_{Map} can be increased maximum up to n^{th} fraction of L_{NL} to ensure DM soliton stability. These findings are graphically presented in Figure 6.3.

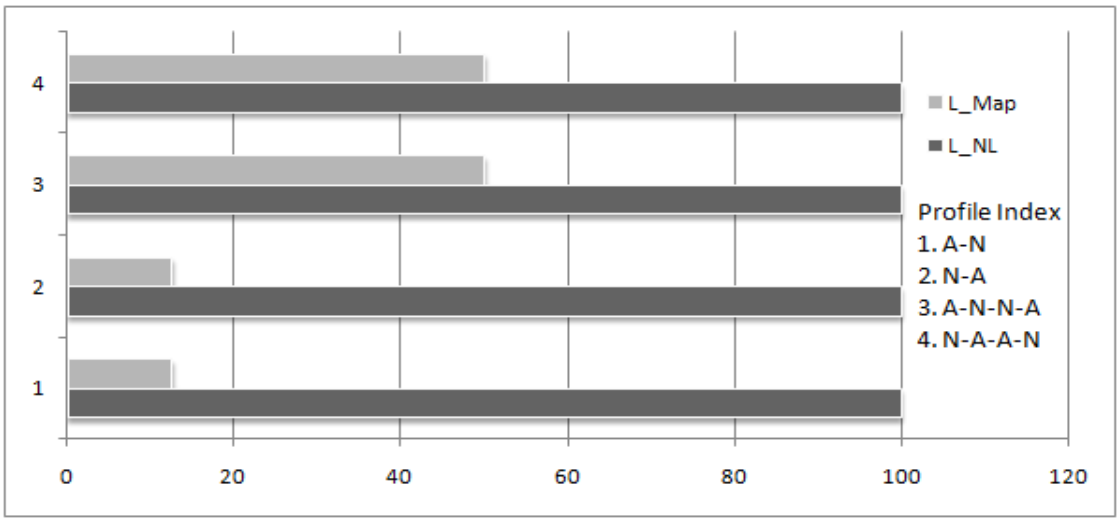

Figure 6.3: L_{Map} shown as percentage of L_{NL} for four different dispersion map profiles

From Figure 6.3 it is observed that, for A-N and N-A profile, the critical fraction *n* is 1/8 i.e. L_{Map} can be maximum up to 12.5% of L_{NL}, whereas for A-N-N-A and N-A-A-N profile the critical fraction *n* is 1/2 i.e. L_{Map} can be extended maximum up to 50% of L_{NL}. So, to maximize the length of dispersion map one should prefer either A-N-N-A or N-A-A-N dispersion map profile to deploy the dispersion managed optical link. Basically, Anomalous (A) regime of β_2 essentially refers to standard single mode fiber (SSMF) with the positive value of dispersion (D) and negative value of β_2 , whereas Normal (N) regime of β_2 essentially refers to the dispersion compensating fiber (DCF) with the negative value of dispersion (D) and positive value of β_2.

Figure 6.4 shows DM soliton pulse evolution with L_{Map} designed according to the critical factor *n* found in the above simulation i.e. from the findings highlighted in Figure 6.3.

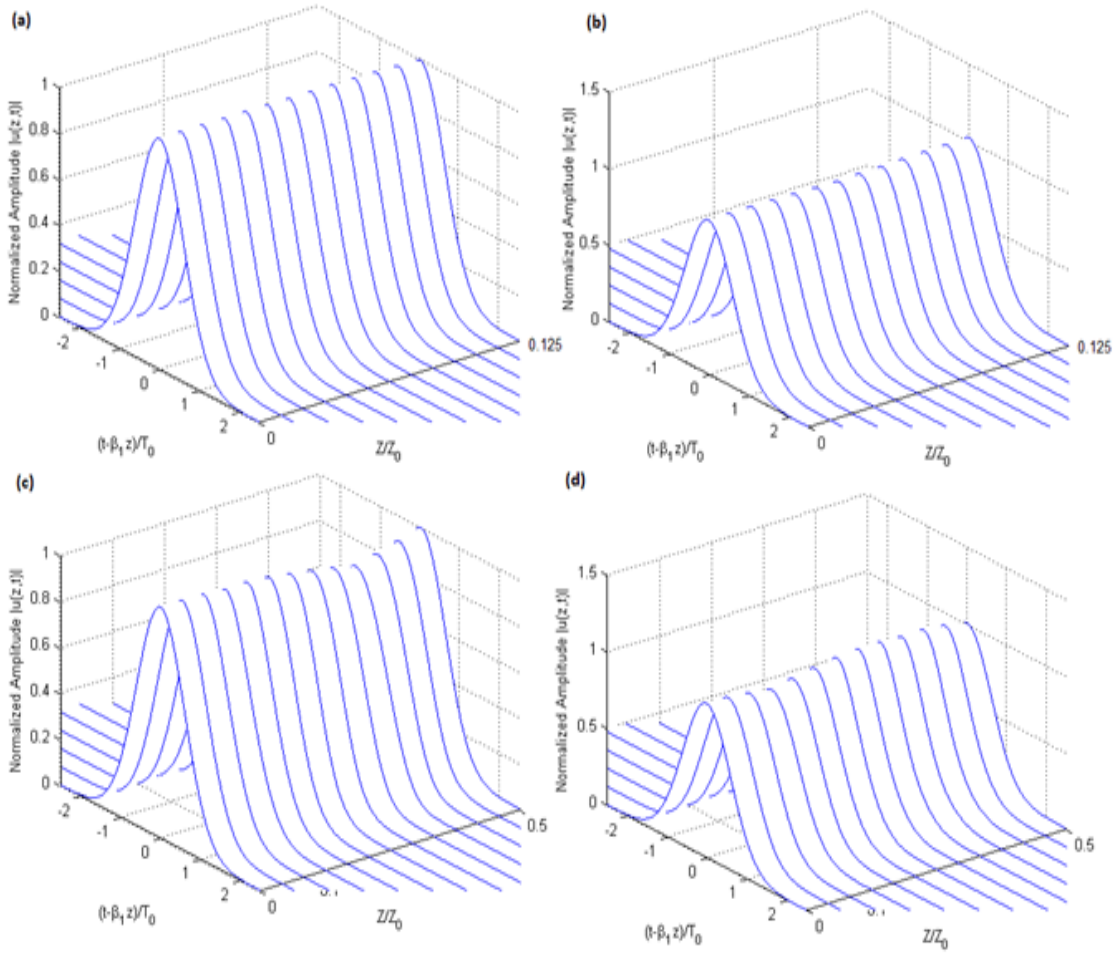

Figure 6.4: Pulse propagation and evolution in (a) A-N dispersion map with n = 1/8 = 0.125 (b) N-A dispersion map with n = 1/8 = 0.125 (c) A-N-N-A dispersion map with n = 1/2 = 0.5 (d) N-A-A-N dispersion map with n = 1/2 = 0.5

Thus, as A-N-N-A and N-A-A-N profile have the same requirement in terms of critical fraction n, to further investigate which profile supports DM soliton pulse propagation in a more favorable way over multiple loops of L_{Map}. The total propagation distance L_{Total} normalized to L_{NL} has been found for these two profiles and as theoretically expected, with the increase of L_{Total} the critical factor n has to be further reduced to ensure a quasi-linear propagation of DM soliton pulse. Needless to say that, with increasing distance nonlinear impairments accumulates to distort the shape of the propagating pulse. Thus n should be accordingly reduced to ensure that DM soliton pulse regains its shape and width every map period in a long distance propagation link made up of multiple identical dispersion maps. Figure 6.5 shows the comparative analysis between A-N-N-A and N-A-A-N profile for 200 loops of L_{Map}.

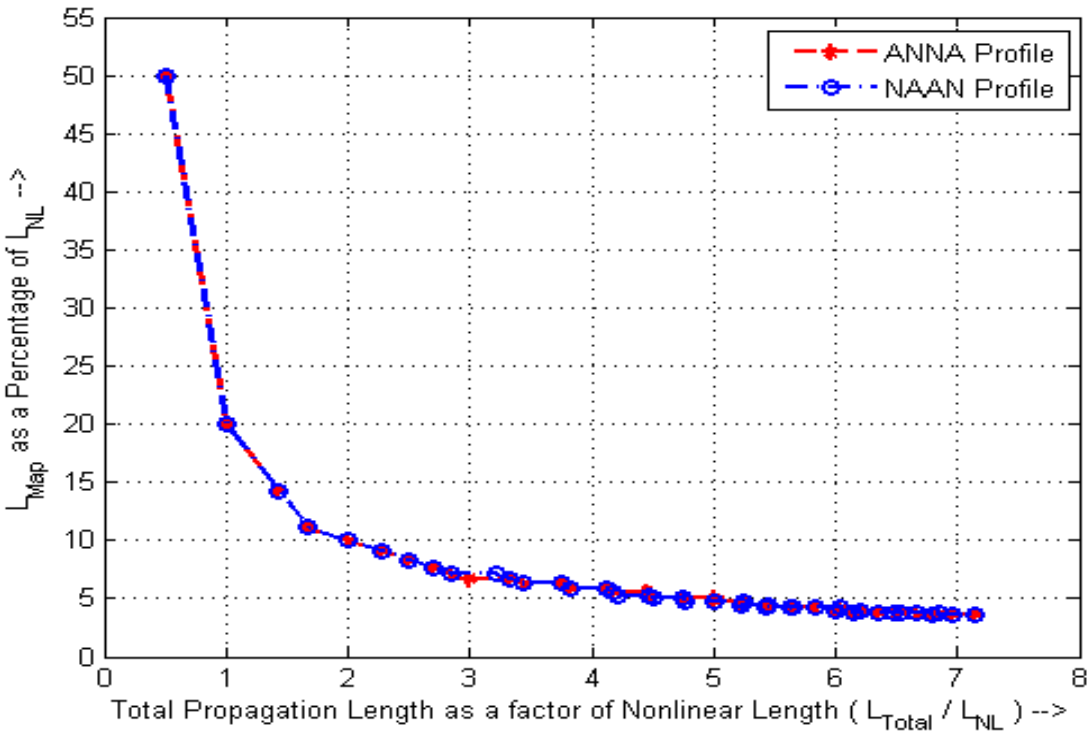

Figure 6.5: Comparative analysis of A-N-N-A and N-A-A-N Profile over 200 loops of L_{Map}

The important facts extracted from Figure 6.5 have been summarized as:

- With the increase in L_{Total}, the critical fraction *n* decreases. It means L_{Map} becomes a smaller fraction of L_{NL} to ensure quasi-linear propagation of DM soliton pulse when nonlinearities accumulate with increasing propagation distance which is calculated as L_{Total} / L_{NL}.
- A-N-N-A and N-A-A-N dispersion map profiles behave almost identically for pulse evolution but a closer look at the graph reveals that A-N-N-A profile is a better choice for the designer.

To be precise, for A-N-N-A profile, critical factor *n* comes out to be 1/20 when 100 loops of L_{Map} are considered as propagation length. Therefore, L_{Total} = 100 x L_{Map} = 100x1/20 L_{NL} = 5 L_{NL} and thus L_{Total} / L_{NL} is 5. Whereas, for N-A-A-N profile, the critical factor *n* comes out to be 1/21 for the same propagation distance. Therefore, L_{Total} = 100x L_{Map} = 100x1/21 L_{NL} = 4.76 L_{NL} which means L_{Total} / L_{NL} is 4.76 in this case. So, selection of A-N-N-A profile allows longer propagation distance for stable DM soliton. This confirms that A-N-N-A profile is the best dispersion map profile to deploy dispersion managed optical link.

After finding the optimum dispersion map for DM soliton propagation where average dispersion was zero, this analysis is further extended with some residual dispersion and initial chirp in section 6.4.

6.4 Analysis with negative average dispersion

Extending the above-mentioned analysis further, propagation distance improvement for DM soliton in an A-N-N-A dispersion profile is investigated where average dispersion value is considered to be slightly negative i.e. $\overline{\beta_2} < 0$. In this case, some initial chirp of the Gaussian pulse shall be useful to ensure DM soliton pulse regaining its shape and width at each map period. A comparative analysis has been thus provided between A-N-N-A fully-compensated profile with $\overline{\beta_2} = 0$ and A-N-N-A undercompensated profile with $\overline{\beta_2} < 0$. The findings of these analyses are presented graphically in Figure 6.6. Some positive initial chirp in Gaussian pulse proves very handy in increasing the propagation distance for DM soliton in an A-N-N-A undercompensated profile with $\overline{\beta_2} \approx -0.1$ which is shown in Figure 6.6(a). It can also be seen that for A-N-N-A fully-compensated profile DM soliton sustains for only one map period and then no negative or positive value of chirp allows DM soliton formation and evolution over multiple loops of L_{Map}.

So, for an A-N-N-A undercompensated profile with n = 1/2 i.e. L_{Map}= 50% of L_{NL}, DM soliton can propagate over increased distance represented as L_{Total} / L_{NL} with the appropriate value of initial chirp as shown in Figure 6.6 (b). This gives a better view to support undercompensated A-N-N-A profile where total propagation distance has been plotted for a number of loops of L_{Map}. In the case of A-N-N-A fully-compensated profile, where initial chirp does not help towards DM soliton stability, critical factor n is needed to be lowered as discussed previously, to support DM soliton formation and stability. On the other side, A-N-N-A undercompensated profile with n = ½, supports DM soliton evolution for much longer distance by proper adjustment of the initial chirp of the Gaussian pulse. This feature seen in the case of A-N-N-A undercompensated profile needs to be analyzed more critically.

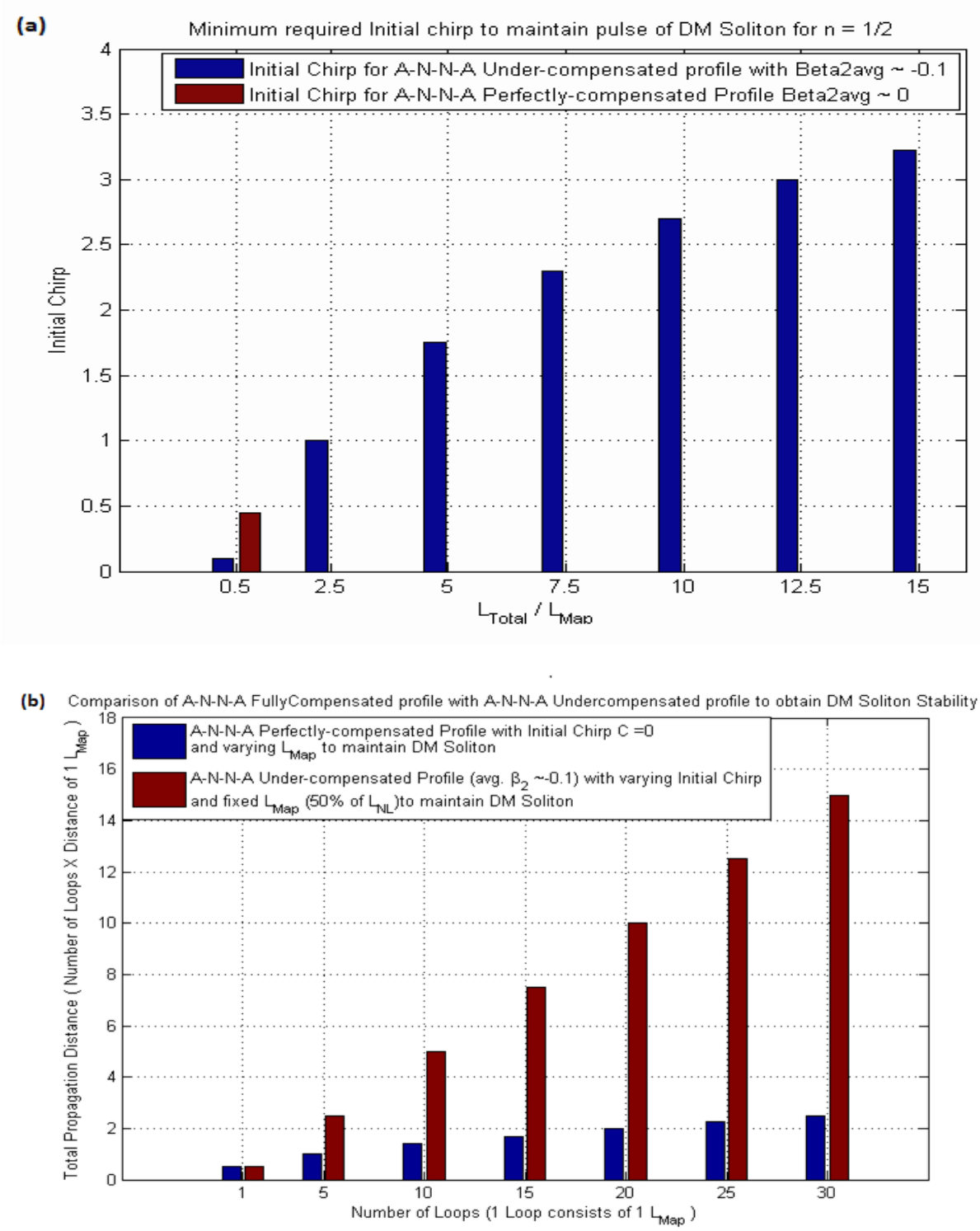

Figure 6.6: a) Comparison of minimum required chirp to maintain DM soliton for A-N-N-A fully-compensated and undercompensated profile (L_{Map}= 50% of L_{NL}) b) Comparison of Total propagation distance supported by A-N-N-A fully-compensated and undercompensated profile for different chirp and critical factor *n*

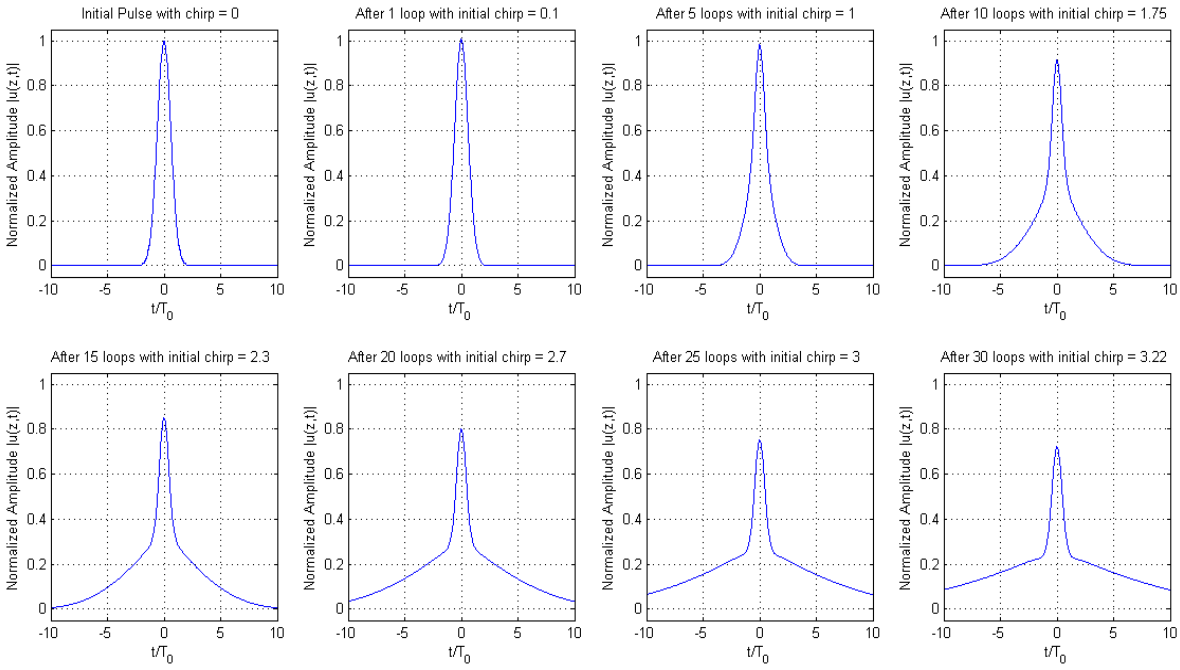

Figure 6.7: Pulse shape after different number of loops of L_{Map} (where L_{Map} is 50% of L_{NL}) with appropriate initial chirp.

Figure 6.7 thus, reports the pulse shape after different propagation distance with appropriate initial chirp to maintain pulse FWHM same as that of the initial Gaussian pulse. It is interesting to note that, with increasing positive values of initial chirp, this profile can support increased propagation length. The pulses are shown here (all having FWHM = 1) are able to regain their initial FWHM after propagating multiple loops but with dispersed tails. This indicates that, though, with initial chirp, L_{Total} can be increased but with a compromise with the bit rate. This implies that pulse repetition rate needs to be decreased to compensate for the impairments caused by the highly dispersive energy of the pulse tail.

This analysis has been further extended for different values of residual dispersion in an undercompensated A-N-N-A link to observe the effect of residual dispersion on DM soliton stability. Figure 6.8 thus, shows the stability region of DM soliton in different undercompensated profiles and their corresponding requirement of initial chirp values.

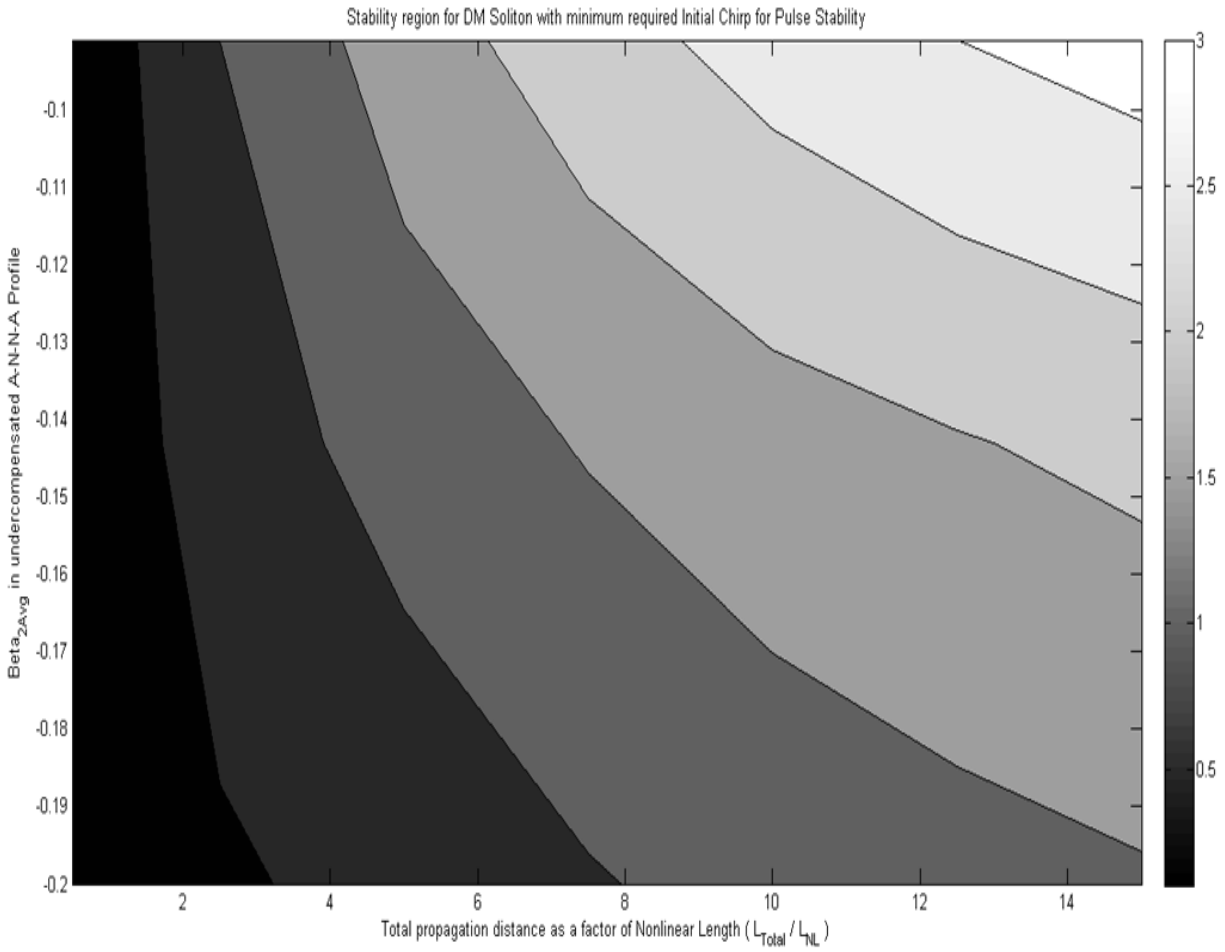

Figure 6.8: Stability region for DM soliton with n = ½ in the parametric space of $\overline{\beta_2}$ and Chirp (C)

The numerical analyses, performed so far, have investigated the suitable dispersion map profile and parametric space for DM soliton formation, propagation and stability. While in the transmission only single pulse doesn't exist thus, it is now important to study also the collision dynamics of two DM soliton pulses co-propagating in such an undercompensated A-N-N-A dispersion profile to observe the behavior of DM soliton propagation and interaction in a realistic situation.

6.5 Collision of dispersion managed soliton pulses

Dispersion managed soliton offers benefit of reduced impact of two-pulse interaction under weak dispersion management, over the conventional solitons in a constant GVD link [15]. Thus, in an undercompensated A-N-N-A profile, stationary two-pulse DM soliton solutions can be found which essentially leads towards the reduction in soliton interaction. Conventional solitons also show similar qualitative behavior as a result of some perturbations reported in the literature [15, 213-214].In soliton communication, the

dispersive waves accumulated through multiple in-line amplifiers, adds timing jitter to impair the system performance at high speed [215]. To visualize the soliton system performance, the influence of normalized pulse separation parameter (q_0) is studied to estimate the interaction of adjacent soliton pulses. In the present analysis, undercompensated A-N-N-A dispersion map profile has been considered to predict the suitable q_0 value for minimum DM soliton pulse-pair interaction. Soliton interaction and collision dynamics have been numerically simulated by solving NLS equation given in equation (6.3) considering the Gaussian pulse pair shown below:

$$u(0,\tau) = \text{gaussian}(\tau - q_0) + r.\text{gaussian}[r(\tau + q_0)]\exp(i\theta) \qquad (6.15)$$

where r is the relative amplitude of the two soliton pulses, θ is the relative phase and $2q_0$ is the initial (normalized) separation. Figure 6.9 shows the evolution of a DM soliton pulse-pair with $q_0 = 2$ for an A-N-N-A undercompensated profile with $\overline{\beta_2} \approx -0.1$ where L_{Map} is 50% of L_{NL}. From Figure 6.9 it is observed that for case (a) DM solitons get attracted and eventually collide with each other whereas in case (b) DM solitons start propagating with initial attraction and then eventually start repelling each other. In case (c) DM solitons repel each other even more strongly to lead to a significant separation between them as distance increases, whereas in case (d), though the pulses undergo perturbations while propagation but they are experiencing minimum interaction.

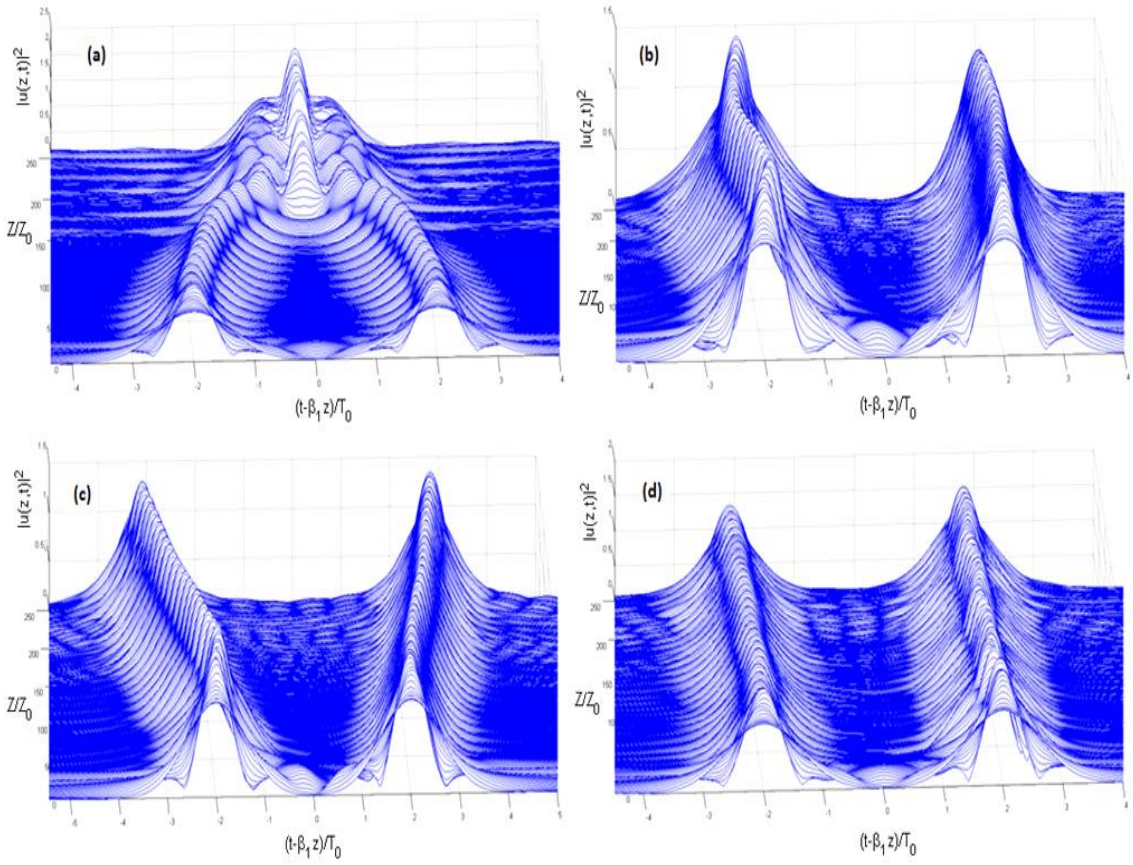

Figure 6.9: Evolution of DM soliton pair over 500 loops of L_{Map} (i.e. L_{Total}/L_{NL} = 250 as L_{Map} = 50% of L_{NL}). Case: a) $\theta = 0$ and r = 1 b) $\theta = \pi/4$ and r = 1 c) $\theta = \pi/2$ and r = 1 and d) $\theta = 0$ and r = 1.1

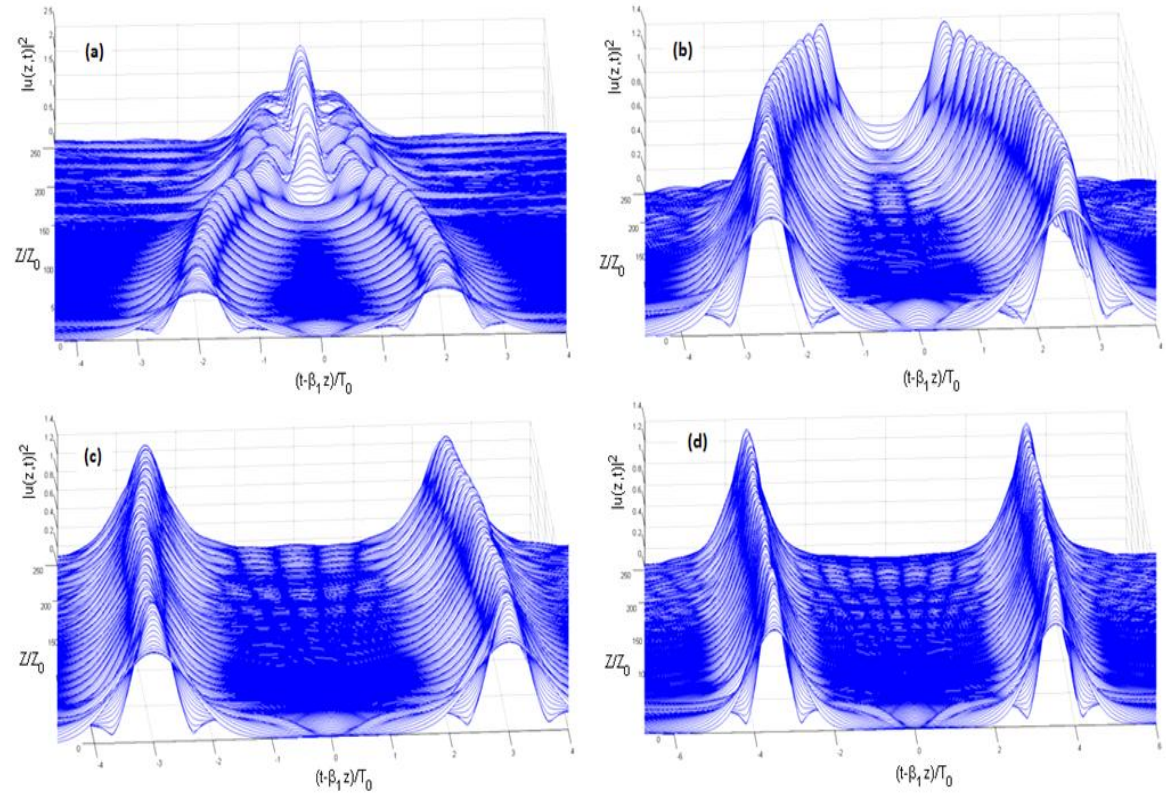

Figure 6.10: DM soliton collision dynamics for different initial spacing between pulse pair. Case: a) $q_0 = 2$, b) $q_0 = 2.5$, c) $q_0 = 3$, and d) $q_0 = 3.5$

Further, to achieve the optimum pulse separation i.e. the best spectral efficiency, the minimum value of q_0 has been estimated for a DM soliton pulse-pair under case (a) which is the most usual case of soliton propagation. The propagation dynamics depicted in Figure 6.10 shows that DM soliton pulse pair propagating in undercompensated A-N-N-A profile experience negligible interaction even for case (c) in Figure 6.10 for $q_0 = 3$ which relaxes the '$q_0 = 3.5$' constraint as applicable for fundamental soliton [15]. Thus, a system designer can design more spectrally efficient scheme deploying DM solitons in A-N-N-A undercompensated profile with proper adjustment of initial chirp value to achieve much longer propagation distance.

6.6 Conclusion

This chapter presented the detailed numerical analysis which will help in suggesting the best-suited dispersion map profile for DM soliton propagation. It has been observed that A-N-N-A dispersion map profile, having a certain amount of residual dispersion in uncompensated DM link; with initially chirped Gaussian pulse supports stable DM soliton formation and propagation over the larger number of dispersion map loops. Stability region for such DM solitons has been found in the parametric space of residual dispersion and initial chirp. Even the analysis of collision dynamics suggests that initially chirped DM soliton in undercompensated A-N-N-A dispersion map profile exhibit superior spectral efficiency as compared to the fundamental solitons.

CHAPTER 7

Conclusions and Future Directions

To fulfill the increasing demand of bandwidth and capacity in networks, optical fiber transmission becomes the favorable mode of communication. This thesis addresses various cost-effective solutions to enhance the data carrying capacity or the transmission distance of the optical links. For the same, 40 Gbps and 100 Gbps data rate per channel was the main focus of the designed optical links. At higher data rates i.e. 40Gbps and 100Gbps nonlinearities plays more crucial role, thus require proper spectral management techniques and strategies to achieve the desired optical link performance. The aim of the present work is to explore the various spectral management techniques to enhance the performance of the pulse propagating through the optical fiber in single and multichannel optical systems. The performance characteristics have been measured in terms of BER-equivalent Q factor. Apparently, there are various methods to increase the overall capacity of lightwave transmission link. The present chapter summarizes the major findings of the thesis and also discusses the future scope of the work.

In chapter 2, the literature review on the various aspects involving the design and development of high speed optical transmission link was presented. A topic covered in the review chapter includes the concepts involved in the design of modulation and demodulation used in the optical communication. Various data modulation formats starting from the conventional RZ/NRZ to duobinary and multilevel modulations formats have also been discussed. For the performance improvement of the long haul optical transmission links, periodic dispersion management techniques are the popular approaches. In consequence of the detailed literature review, it is observed that some of the preferred and widely accepted techniques to improve the overall performance of the high-speed optical communication links are: use of spectrally efficient modulation formats and pulse shaping schemes, use of different fiber types, design of WDM or DWDM system, and the implementation of periodic dispersion maps along the length of the optical fiber links.

In the present thesis, first, spectral management techniques have been used to improve the performance of the transmission link. One of such technique is pre-chirping of the input transmitting pulse to make it robust towards fiber impairments. Chapter 3 of the thesis

presents the analysis of the SPM and ASE noise induced impairments and their effect on the transmission of chirped Gaussian pulse propagating through the single mode fiber channel. The proposed transmission link has been designed at 40Gbps data rate for RZ modulated pulse shape employing a direct detection configuration at the receiver end. For the analysis different duty cycles and chirp values have been considered. Obtained results reveal that the higher duty cycle pulse with the negative chirp conditions performs better than lower duty cycle pulses for both SPM and ASE-limited channel conditions.

Duobinary is a 3-level modulation format and very efficient pulse shaping technique. It is very popular in wireless as well as in optical transmission link designs. Advantages of duobinary modulation format for the optical transmission links and its implementation at 40Gbps data rate with fixed OSNR conditions have been presented in chapter 4. This chapter also presented the filter bandwidth optimizations which are used at the transmitter and receiver side of the link under the ASE noise limited channel conditions to get the optimum performance for the duobinary NRZ and duobinary RZ pulses. The designed link has been subjected to SPM and GVD effects for two different situations first when they were acting one at a time and second, when both the effects are present at the same time. Dispersion compensating fibers are used to nullify the effect of dispersion when analyzing the SPM effect alone. The presented analysis shows the superiority of duobinary NRZ over duobinary RZ pulse at higher OSNR value however, for a typical OSNR value a crossover optical filter bandwidth has been observed beyond which duobinary RZ outperforms duobinary NRZ.

Multilevel modulation formats are popular and widely used modulation formats for the high speed optical link designs because of their higher tolerance towards linear and nonlinear effects. Optical link design using RZ-DQPSK in single channel configuration is discussed in chapter 5 of the thesis. Comparative analysis has performed for the three different single mode fiber types under ASE noise channel conditions. Single mode fibers used for the analysis are SSMF, TW-RS, and LEAF. Initially, this link analysis is performed at the 10Gbps data rate and then extended for the 40Gbps data rate. An obtained result shows the superiority of LEAF followed by SSMF and TW-RS fiber types especially for long haul applications but that comes at the higher installation cost.

Since DQPSK is a true multilevel modulation format which provides spectral efficiency compared to QPSK format but at the same time with the less complex transmitter and receiver designs. Therefore, the analysis in chapter 5 is further extended with the dual

polarization format of DQPSK (DP-DQPSK). Dual polarization modulation formats are very effective in increasing the data rate and transmission distance when used in WDM and DWDM configuration. Therefore, the proposed DP-DQPSK optical link has been designed for 9 channels in with 112Gbps data rate per channel and 50GHz channel spacing. Pulse transmission in symbol-aligned and symbol interleaved formats is analyzed for various linear and nonlinear fiber impairments. Obtained results show the superiority of symbol-interleaving format over their symbol-aligned counterparts when the link is subjected to various intrachannel and interchannel effects.

During this thesis, it has been observed that various techniques such as spectrally efficient modulation formats, different fiber types, and dispersion management schemes at various stages of the link are useful to improve the overall performance of the transmission system to some extent. But these techniques are useful for improving the performance of short and metro transmission links. For the long haul transmission link designs nonlinearities influence the overall system performance and for those applications, local GVD compensation is not sufficient to get the original signal back. As the design of optical long haul transmission links is required for providing the communication between long distance links and there is a continuous need for new techniques to improve the link length. Deployment of dispersion managed links along the length of the fiber is an effective solution to retain the shape of the propagating pulse. Therefore, in long distance links, it is important and beneficial to use both loss and dispersion management techniques simultaneously.

To keep this in mind chapter 6 of the thesis provides the mathematical modeling of periodic dispersion management for the propagation of dispersion managed pulse popularly known as dispersion managed soliton. Chapter 6 provides the analysis of different dispersion map profile to find the best suitable profile for the dispersion managed soliton pulse propagation. Periodic maps are formed with the combination of normal and anomalous fiber sections. The dispersion map profiles considered for the analysis are Anomalous-Normal (A-N), Normal-Anomalous (N-A), Anomalous-Normal-Normal-Anomalous (A-N-N-A) and Normal-Anomalous-Anomalous-Normal (N-A-A-N). Unlike normal soliton pulse propagation where the shape of the pulse remains constant because of fixed value of GVD, in dispersion managed links width of the propagating dispersion managed soliton oscillate periodically and regain its shape after each dispersion map. After

obtaining the suitable dispersion map, work has been further extended to increase the propagation length with the use of negative dispersion and initial chirp.

Analysis performed in this chapter shows that the A-N-N-A dispersion map along with negative dispersion and initial chirp support the dispersion managed soliton pulse for comparatively longer length. In soliton communication interaction between two neighboring solitons is an important aspect of system design. To achieve maximum spectral efficiency solitons are packed as tightly as possible. However, perturbation occurs in soliton transmission due to the presence of neighboring pulses. Chapter 6 also provides the analysis of dispersion managed soliton interaction analysis shows that more spectrally efficient scheme can be implemented using DM solitons in A-N-N-A undercompensated map with proper adjustment of initial chirp value to achieve much longer propagation distance.

Future Directions

Major challenges with the optical simulation tools are that they have to perform well for the wider optical bandwidth of tens of THz while incorporating the slow dynamics of amplifiers. In future, the proposed transmission links need further optimization with more sophisticated tools in terms of power budget, gain flattening, OSNR conditions etc. to provide the results at different abstraction levels.

The main focus of the present thesis is to improve the data transmission capacity of the optical transmission systems with the simple and low cost direct detection receivers. Therefore, another aspect of future work includes the implementation of coherent receiver schemes for improved receiver sensitivity. As all the information of the optical field is preserved during coherent transmission thus it offers various advantages. Also, several spectrally efficient optical modulation formats such as M-PSK and M-ary quadrature amplitude modulation (QAM) require coherent detection schemes at the receiver. In QAM schemes with the increase of the number of M, higher SNR is required under the same BER, thus, forward error correction (FEC) makes these schemes possible. Therefore, the implementation of advanced modulation formats along with FEC coding is one of the aspects of future work. Coherent detectors have their own complexity and stability issues. Therefore, another direction is homodyne detection schemes. For homodyne detection, with the availability of the high speed digital integrated circuits allows the use of electrical signal pre-processing and stable detection of in-phase and quadrature components of the signal is possible. Also, in DSP based systems as the carrier phase of coherent modulation formats is

recovered after homodyne detection with the use of digital signal processing, is a faster, stable and simpler approach compare to the conventional coherent detection schemes using optical phase-lock loops.

Numbers of new technologies have been introduced in recent years to fulfill the demand of ever increasing data for the future 100G systems. Multilevel modulation formats with a large number of bits per symbol will offer the essential ingredients for high-speed next generation lightwave systems. The presented work has explored only one types of modulation format for 100G systems. Implementation of various other 100G modulation formats and the link optimization is again a good approach to further extend the work.

For long haul optical link designs soliton communication is considered to be more robust approach as nonlinearities do not affect it although the existence of solitons depends on them. Most of the soliton communication is rely on binary coding and they are performing well till now, but to fulfill the demands of future high data applications it becomes extremely important to accommodate more number of bits per clock period.

In normal soliton communication, two pulses can co-propagates together depending on their relative phase. In conventional soliton transmission, pulses can either collide or repel each other whereas for dispersion managed solitons, stable separation exists between two pulses. Therefore, dispersion managed solitons are the good candidate for the future lightwave systems and the work in this area can be further extended to explore them for the future next generation optical transmission systems.

References

[1] G.Keiser optical fiber communication McGraw-Hill Companies, 1991 ed2

[2] Pratt, William K. "Laser Communication Systems." (1969).

[3] T. H. Maiman, “Stimulated optical radiation in ruby,” Nature 187, 493–494 (1960).

[4] Seidel, Robert W. "How the military responded to the laser." *Physics and Nuclear Arms Today* 4 (1991): 302.

[5] Faltas, Sami. "The invention of fibre-optic communications." *History and Technology, an International Journal* 5.1 (1988): 31-49.

[6] Cattani, Gino. "Technological pre-adaptation, speciation, and emergence of new technologies: how Corning invented and developed fiber optics." *Industrial and Corporate Change* 15.2 (2006): 285-318.

[7] Coffman, Kerry G., and Andrew M. Odlyzko. "The size and growth rate of the Internet." *First Monday* 3.10 (1998): l-25.

[8] Odlyzko, Andrew M. "The economics of the Internet: Utility, utilization, pricing, and Quality of Service." (1998).

[9] Odlyzko, Andrew. "Internet pricing and the history of communications." *Computer networks* 36.5 (2001): 493-517.

[10] Nosu, Kiyoshi. "Introduction to coherent lightwave communications" *Coherent Lightwave Communications Technology*. Springer, Netherlands, 1995. 1-11.

[11] Hill, Godfrey R. "Wavelength domain optical network techniques." *Proceedings of the IEEE* 78.1 (1990): 121-132.

[12] Borella, Michael S., et al. "Optical components for WDM lightwave networks." *Proceedings of the IEEE* 85.8 (1997): 1274-1307.

[13] Berthold, Joseph, et al. "Optical networking: past, present, and future." *Journal of lightwave technology* 26.9 (2008): 1104-1118.

[14] Mukherjee, Biswanath. "WDM optical communication networks: progress and challenges." *IEEE Journal on Selected Areas in communications* 18.10 (2000): 1810-1824..

[15] Agrawal, Govind P. "Optical fiber communication systems." *New York: A Wiley* 2 (2003).

[16] Miller, Steward E., Enrique AJ Marcatili, and Tingye Li. "Research toward optical-fiber transmission systems." *Proceedings of the IEEE* 61.12 (1973): 1703-1704.

[17] VALENTINE SR, G. A. R. Y., et al. "Fiber Optic.".

[18] David Goff fiber optic reference guide CRC press.

[19] DeCusatis, Casimer. *Fiber Optic Data Communication: Technology Advances and Futures*. Academic press, 2002.

[20] B.Mukherjee 1997] B. Mukherjee, "*Optical Communications Networks"*, McGraw-Hill, New York, 1997

[21] Okoshi, Takanori, and Kazurō Kikuchi. *Coherent optical fiber communications*. Vol. 4. Springer Science & Business Media, 1988.

[22] Zhuge, Qunbi, et al. "Spectral efficiency-adaptive optical transmission using time domain hybrid QAM for agile optical networks." *Journal of Lightwave Technology* 31.15 (2013): 2621-2628.

[23] Cvijetic, Milorad, and Ivan Djordjevic. "*Advanced optical communication systems and networks"*. Artech House, 2013.

[24] Idachaba, Francis, Dike U. Ike, and Orovwode Hope."Future Trends in Fiber Optics Communication." *World Congress on Engineering London July*. 2014.

[25] Romaniuk, Ryszard S. "Optical fiber transmission with wavelength multiplexing: faster or denser?" *Photonics Applications in Astronomy, Communications, Industry, and High-Energy Physics Experiments II*. International Society for Optics and Photonics, 2004.

[26] Agrawal, Govind P. *Nonlinear fiber optics*. Academic press, 2007.

[27] Jopson, Bob, and Alan Gnauck. "Dispersion compensation for optical fiber systems." *Communications Magazine, IEEE* 33.6 (1995): 96-102.

[28] Sano, Akihide, et al. "Ultra-high capacity WDM transmission using spectrally-efficient PDM 16-QAM modulation and C-and extended L-band wideband optical amplification." *Journal of Lightwave Technology* 29.4 (2011): 578-586.

[29] Fukuchi, Kiyoshi, et al. "10.92-Tb/s (273 x 40-Gb/s) triple-band/ultra-dense WDM optical-repeatered transmission experiment." *Optical Fiber Communication Conference*. Optical Society of America, 2001.

[30] Winzer, Peter J. "Modulation and multiplexing in optical communication systems." *IEEE Leos Newsletter* 23.1 (2009): 4-10.

[31] Ramaswami, Rajiv, Kumar Sivarajan, and Galen Sasaki. *Optical networks: a practical perspective*. Morgan Kaufmann, 2009.

[32] Turitsyn, Sergei K., and Elena G. Shapiro. "Variational approach to the design of optical communication systems with dispersion management." *Optical Fiber Technology* 4.2 (1998): 151-188.

[33] Hasegawa, Akira, Yuji Kodama, and Akihiro Maruta. "Recent progress in dispersion-managed soliton transmission technologies." *Optical Fiber Technology* 3.3 (1997): 197-213.

[34] Zhao, L. M., et al. "Bound states of dispersion-managed solitons in a fiber laser at near zero dispersion." *Applied optics* 46.21 (2007): 4768-4773.

[35] Akhmediev, N. N., et al. "Phase locking and periodic evolution of solitons in passively mode-locked fiber lasers with a semiconductor saturable absorber." *Optics letters* 23.11 (1998): 852-854.

[36] Biondini, Gino, and Sarbarish Chakravarty. "Nonlinear chirp of dispersion-managed return-to-zero pulses." *Optics letters* 26.22 (2001): 1761-1763.

[37] Betti, S., M. Giaconi, and M. Nardini. "Effect of four-wave mixing on WDM optical systems: a statistical analysis." *Photonics Technology Letters, IEEE* 15.8 (2003): 1079-1081.

[38] Smith, Nicholas J., et al. "Soliton transmission using periodic dispersion compensation." *Journal of lightwave technology* 15.10 (1997): 1808-1822.

[39] Abdullaev, F. Kh, and B. B. Baizakov. "Disintegration of a soliton in a dispersion-managed optical communication line with random parameters." *Optics letters* 25.2 (2000): 93-95.

[40] Lakoba, T. I., et al. "Conditions for stationary pulse propagation in the strong dispersion management regime." *Optics communications* 149.4 (1998): 366-375.

[41] Kumar, Shiva, and Falk Lederer. "Gordon–Haus effect in dispersion-managed soliton systems." *Optics letters* 22.24 (1997): 1870-1872.

[42] Nakazawa, M., and H. Kubota. "Optical soliton communication in a positively and negatively dispersion-allocated optical fibre transmission line." *Electronics Letters* 31.3 (1995): 216-217.

[43] Shapiro, Elena G., and Sergei K. Turitsyn. "Theory of guiding-center breathing soliton propagation in optical communication systems with strong dispersion management." *Optics letters* 22.20 (1997): 1544-1546.

[44] Chraplyvy, Andrew R. "Limitations on lightwave communications imposed by optical-fiber nonlinearities." *Journal of Lightwave Technology* 8.10 (1990): 1548-1557.

[45] Chraplyvy, A. R. "Impact of nonlinearities on lightwave systems." *Optics and Photonics News* 5.5 (1994): 16.

[46] Tiwari, B. B., et al. "Nonlinear effects in optical fiber transmission system." *IETE Technical Review* 16.5-6 (1999): 461-479.

[47] Lee, E-H., K. H. Kim, and H. K. Lee. "Nonlinear effects in optical fiber: Advantages and Disadvantages for high capacity all-optical communication application." *Optical and quantum electronics* 34.12 (2002): 1167-1174.

[48] Agrawal, Govind P. "Nonlinear fiber optics." *Nonlinear Science at the Dawn of the 21st Century*. Springer Berlin Heidelberg, 2000. 195-211.

[49] Poole, Craig D. "Chromatic dispersion compensated optical fiber communication system." U.S. Patent No. 5,261,016. 9 Nov. 1993.

[50] Payne, David N., and W. A. Gambling. "Zero material dispersion in optical fibers." *Electronics Letters* 11.8 (1975): 176-178.

[51] Gisin, N., and B. Huttner. "Combined effects of polarization mode dispersion and polarization dependent losses in optical fibers." *Optics Communications* 142.1 (1997): 119-125.

[52] Wai, P. K. A., and C. R. Menyak. "Polarization mode dispersion, decorrelation, and diffusion in optical fibers with randomly varying birefringence." *Lightwave Technology, Journal of* 14.2 (1996): 148-157.

[53] Gisin, Nicolas, and Jean-Paul Pellaux. "Polarization mode dispersion: time versus frequency domains." *Optics communications* 89.2-4 (1992): 316-323.

[54] Boyd, Robert W. *Nonlinear optics*. Academic press, 2003.

[55] Luís, Ruben S., and Adolfo VT Cartaxo. "Analytical characterization of SPM impact on XPM-induced degradation in dispersion-compensated WDM systems." *Journal of Lightwave Technology* 23.3 (2005): 1503-1513.

[56] Kim, Hoon. "Cross-phase-modulation-induced nonlinear phase noise in WDM direct-detection DPSK systems." *Journal of lightwave Technology* 21.8 (2003): 1770.

[57] Yadin, Y., M. Shtaif, and M. Orenstein. "Nonlinear phase noise in phase-modulated WDM fiber-optic communications." *Photonics Technology Letters, IEEE* 16.5 (2004): 1307-1309.

[58] Hui, R., et al. "Frequency response of cross-phase modulation in multispan WDM optical fiber systems." *Photonics Technology Letters, IEEE* 10.9 (1998): 1271-1273.

[59] Sano, A., et al. "A 40-Gb/s/ch WDM transmission with SPM/XPM suppression through prechirping and dispersion management." *Journal of Lightwave Technology* 18.11 (2000): 1519-1527..

[60] Tao, Zhenning, et al. "Simple fiber model for determination of XPM effects." *Journal of Lightwave Technology* 29.7 (2011): 974-986.

[61] Tipsuwannakul, Ekawit, et al. "Influence of self-and cross-phase modulation on 40 Gbaud dual polarization DQPSK/D8PSK signals in 10 Gbit/s OOK WDM systems." *Optics express* 18.23 (2010): 24178-24188.

[62] Stolen, R. H., and E. P. Ippen. "Raman gain in glass optical waveguides." Applied Physics Letters 22.6 (1973): 276-278.

[63] Toulouse, Jean. "Optical nonlinearities in fibers: review, recent examples, and systems applications." *Lightwave Technology, Journal of* 23.11 (2005): 3625-3641.

[64] Ippen, E. P., and R. H. Stolen. "Stimulated Brillouin scattering in optical fibers." *Applied Physics Letters* 21.11 (1972): 539-541.

[65] Tkach, R. W., et al. "Four-photon mixing and high-speed WDM systems." *Journal of Lightwave Technology* 13.5 (1995): 841-849.

[66] Singh, Sunil Pratap, and Nar Singh. "Nonlinear effects in optical fibers: Origin, management and applications." *Progress In Electromagnetics Research* 73 (2007): 249-275.

[67] Numai, Takahiro, and Ouichi Kubota. "Analysis of repeated unequally spaced channels for FDM lightwave systems." *Journal of Lightwave Technology* 18.5 (2000): 656.

[68] Forghieri, Fabrizio, et al. "Reduction of four-wave mixing crosstalk in WDM systems using unequally spaced channels." *IEEE Photonics Technology Letters* 6.6 (1994): 754-756.

[69] L. N.Binh Optical Fiber Communication System: Principle, Practices and MATLAB Simulink Models CRC Press, Taylors and Francis Group, 2009.

[70] John G. Proakis and Masoud Salehi,Digital Communication, McGraw-Hill, 5th Edition

[71] Stephen B. Alexander Optical Communication Receiver Design, Technology and Engineering, IET, 1997

[72] Essiambre, René-Jean, and Govind P. Agrawal. "Timing jitter analysis for optical communication systems using ultrashort solitons and dispersion-decreasing fibers." *Optics communications* 131.4 (1996): 274-278.

[73] Linn F. Mollenauer, James P. Gordon **"**Fundamentals and Applications**"** Academic Press, 2006.

[74] Chraplyvy, A.R., "The coming capacity crunch" *ECOC Plenary Talk* 2009.

[75] Le Nguyen Binh "digital optical communication" CRC press, 2008.

[76] Tkach, Robert W. "Scaling optical communications for the next decade and beyond." *Bell Labs Technical Journal* 14.4 (2010): 3-9.

[77] Kamiya, Takeshi, Tetsuya Miyazaki, and Fumito Kubota. "Social Demand of New Generation Information Network: Introduction to High Spectral Density Optical Communication Technology." *High Spectral Density Optical Communication Technologies*. Springer Berlin Heidelberg, 2010. 3-10.

[78] Sano, Akihide, and Yutaka Miyamoto. "Performance evaluation of prechirped RZ and CS-RZ formats in high-speed transmission systems with dispersion management." *Journal of lightwave technology* 19.12 (2001): 1864.

[79] Suzuki, Masatoshi, and Noboru Edagawa. "Dispersion-managed high-capacity ultra-long-haul transmission." *Journal of Lightwave Technology* 21.4 (2003): 916.

[80] The fifth-generation optical network - flexibility, orchestration, and openness http://www.huawei.com/en-AE/publications/communicate/74/HW_414991.

[81] Cisco Visual Networking Index: Forecast and Methodology, 20014-2019. Available:https://www.cisco.com/c/en/us/solutions/collateral/service-provider/visual-networking-index-vni/vni-hyperconnectivity-wp.html

[82] Cisco Visual Networking Index: Forecast and Methodology, 2015-2020. Available:http://www.cisco.com/c/en/us/solutions/service-provider/visual-networking-index-vni/index.html

[83] Deployment & service Activation at 100G & beyond: White paper http://www.viavisolutions.com/sites/default/files/technical-library files/HR_JDSU_100G_Deployment_0.pdf

[84] Fukuchi, Kiyoshi, et al. "10.92-Tb/s (273 x 40-Gb/s) triple-band/ultra-dense WDM optical-repeatered transmission experiment." *Optical Fiber Communication Conference*. Optical Society of America, 2001.

[85] Xu, Xiaogeng, et al. "Advanced modulation formats for 400-Gbps short-reach optical inter-connection." *Optics express* 23.1 (2015): 492-500.

[86] Zhang, Liang, et al. "Beyond 100-Gb/s transmission over 80-km SMF using direct-detection SSB-DMT at C-band." *Journal of Lightwave Technology* 34.2 (2016): 723-729.

[87] Poole, C. D., and R. E. Wagner. "Phenomenological approach to polarisation dispersion in long single-mode fibres." *Electronics Letters* 22.19 (1986): 1029-1030.

[88] Foschini, G. J., and C. D. Poole. "Statistical theory of polarization dispersion in single mode fibers." *Lightwave Technology, Journal of* 9.11 (1991): 1439-1456.

[89] Kai, Yutaka. "Dispersion compensation apparatus." U.S. Patent No. 6,154,588. 28 Nov. 2000.

[90] Ramaswami, Rajiv, Kumar Sivarajan, and Galen Sasaki. *Optical networks: a practical perspective*. Morgan Kaufmann, 2009.

[91] Eckardt, Robert C., Chi H. Lee, and James N. Bradford. "Effect of self-phase modulation on the evolution of picosecond pulses in a Nd: glass laser." *Opto-electronics* 6.1 (1974): 67-85.

[92] Alfano, R. R., and P. P. Ho. "Self-, cross-, and induced-phase modulations of ultrashort laser pulse propagation." *Quantum Electronics, IEEE Journal of* 24.2 (1988): 351-364.

[93] Tomlinson, W. J., R. H. Stolen, and C. V. Shank. "Compression of optical pulses chirped by self-phase modulation in fibers." *JOSA B* 1.2 (1984): 139-149.

[94] Mollenauer, Linn F., et al. "Extreme picosecond pulse narrowing by means of soliton effect in single-mode optical fibers." *Optics letters* 8.5 (1983): 289-291.

[95] Sunnerud, Henrik, et al. "Polarization-mode dispersion in high-speed fiber-optic transmission systems." *Journal of Lightwave Technology* 20.12 (2002): 2204.

[96] Technical Digest, Workshop on high spectral Density Optical Communication for New Generation Network (HDOC-WS 2008) http://www2.nict.go.jp/w/w112/ WS080523

[97] Paoli, Thomas L., and José E. Ripper. "Direct modulation of semiconductor lasers." *Proceedings of the IEEE* 58.10 (1970): 1457-1465.

[98] S. Jongthammanurak, J. Liu,D.Cannon, D. Danielson, C.Y. Hong, D. Pan, K. Wada, J. Michel, and L. Kimerling, "Franz–Keldysh effect in strained Ge on Si for light modulation," presented at the Fall Meet. Mater. Res. Soc., Boston, MA, Dec. 1, 2005, Paper EE 12.7.

[99] Binh, Le Nguyen. "Lithium niobate optical modulators: Devices and applications." *Journal of crystal growth* 288.1 (2006): 180-187.

[100] Hikami, Toshiya, et al. "External modulator for optical communication." U.S. Patent No. 5,506,721. 9 Apr. 1996.

[101] Kimura, Tatsuya. "Coherent optical fiber transmission." *Lightwave Technology, Journal of* 5.4 (1987): 414-428.

[102] Goldstein, Robert. "Pockels cell primer." *Laser Focus Magazine* (1968).

[103] Sharp, Richard. "Method for achieving improved transmission performance over fiber using a Mach-Zehnder modulator." U.S. Patent No. 6,741,761. 25 May 2004.

[104] Gronbach, Siegfried. "Method and apparatus for controlling a bias voltage of a Mach-Zehnder modulator." U.S. Patent No. 7,075,695. 11 Jul. 2006.

[105] Ding, Jianfeng, et al. "Ultra-low-power carrier-depletion Mach-Zehnder silicon optical modulator." *Optics express* 20.7 (2012): 7081-7087.

[106] Chung, Hwan Seok, et al. "Direct detection based optical transceiver for 100 Gb/s systems." *Opto-Electronics and Communications Conference (OECC), 2012 17th*. IEEE, 2012.

[107] H. S. Chung, et al., "Dual-Carrier DQPSK based 112 Gb/s Signal Transmission over 480 km of SMF Link Carrying 10 Gb/s NRZ Channels," in *OFC/NFOEC*, LA, CA, 2012, paper JW2A.3.

[108] Kim, Kwangjoon, et al. "Field Trial of Direct-Detection and Multi-Carrier based 100G Transceiver." *Optical Fiber Communication Conference*. Optical Society of America, 2014.

[109] Cox, Charles, et al. "Techniques and performance of intensity-modulation direct-detection analog optical links." *IEEE Transactions on Microwave theory and techniques* 45.8 (1997): 1375-1383.

[110] DeLange, O. E. "Some optical communications experiments." *Applied optics* 9.5 (1970): 1167-1175.

[111] Okoshi, Tadashi, and Kazuro Kikuchi. "Frequency stabilisation of semiconductor lasers for heterodyne-type optical communication systems." *Electronics Letters* 16.5 (1980): 179-181.

[112] Favre, F., and D. Le Guen. "High frequency stability of laser diode for heterodyne communication systems." *Electronics Letters* 16 (1980): 709.

[113] Yamamoto, Yoshihisa, and Tatsuya Kimura. "Coherent optical fiber transmission systems." *Quantum Electronics, IEEE Journal of* 17.6 (1981): 919-935.

[114] Imai, Tetsuro, et al. "Field demonstration of 2.5 Gbit/s coherent optical transmission through installed submarine fibre cables." *Electronics Letters* 26.17 (1990): 1407-1409.

[115] Mears, Robert J., et al. "Low-noise erbium-doped fibre amplifier operating at 1.54 μm." *Electronics Letters* 23.19 (1987): 1026-1028.

[116] Tsukamoto, Satoshi, et al. "Coherent Demodulation of 40-Gbit/s Polarization-Multiplexed QPSK Signals with16-GHz Spacing after 200-km Transmission." *Optical Fiber Communication Conference*. Optical Society of America, 2005.

[117] Sun, Han, Kuang-Tsan Wu, and Kim Roberts. "Real-time measurements of a 40 Gb/s coherent system." *Optics Express* 16.2 (2008): 873-879.

[118] Taylor, Michael G. "Phase estimation methods for optical coherent detection using digital signal processing." *Journal of Lightwave Technology* 27.7 (2009): 901-914

[119] Laperle, Charles, and Maurice O'Sullivan. "Advances in high-speed DACs, ADCs, and DSP for optical coherent transceivers." *J. Lightw. Technol* 32.4 (2014): 629-643.

[120] Khilo, Anatol, et al. "Photonic ADC: overcoming the bottleneck of electronic jitter." *Optics Express* 20.4 (2012): 4454-4469.

[121] Wree, Christoph, et al. "Experimental investigation of receiver sensitivity of RZ-DQPSK modulation format using balanced detection." *Optical Fiber Communication Conference*. Optical Society of America, 2003.

[122] Lyubomirsky, Ilya, Cheng-Chung Chien, and Yi-Hsiang Wang. "Optical DQPSK receiver with enhanced dispersion tolerance." *IEEE Photonics Technology Letters* 7.20 (2008): 511-513.

[123] Humblet, Pierre A., and Murat Azizoğlu. "On the bit error rate of lightwave systems with optical amplifiers." *Lightwave Technology, Journal of* 9.11 (1991): 1576-1582.

[124] Du Boff, Richard B. "Business Demand and the Development of the Telegraph in the United States, 1844–1860." *Business History Review* 54.04 (1980): 459-479.

[125] Ennser, K., and K. Petermann. "Performance of RZ-versus NRZ-transmission on standard single-mode fibers." *Photonics Technology Letters, IEEE* 8.3 (1996): 443-445.

[126] Breuer, D., and K. Petermann. "Comparison of NRZ-and RZ-modulation format for 40-Gb/s TDM standard-fiber systems." *Photonics Technology Letters, IEEE* 9.3 (1997): 398-400.

[127] Djordjevic, Ivan B., et al. "Achievable information rates for high-speed long-haul optical transmission." *Journal of lightwave technology* 23.11 (2005): 3755.

[128] Miyamoto, Y., et al. "320 Gbit/s (8× 40 Gbit/s) WDM transmission over 367 km with 120 km repeater spacing using carrier-suppressed return-to-zero format." *Electronics Letters* 35.23 (1999): 2041-2042.

[129] Hirano, A., et al. "40 Gbit/s L-band transmission experiment using SPM-tolerant carrier-suppressed RZ format." *Electronics Letters* 35.25 (1999): 2213-2215.

[130] Sano, Akihide, and Yutaka Miyamoto. "Performance evaluation of prechirped RZ and CS-RZ formats in high-speed transmission systems with dispersion management." *Journal of lightwave technology* 19.12 (2001): 1864.

[131] Sekiya, K., et al. "Flexible 40 Gbit/s WDM transmission beyond 1000 km enabled by 195 μm 2 A eff PSCF and AC-RZ signal format." *Electronics Letters* 39.4 (2003): 386-388.

[132] Lender, Adam. "Correlative digital communication techniques." *Communication Technology, IEEE Transactions on* 12.4 (1964): 128-135.

[133] Dutton, Harry JR. *Understanding optical communications*. New Jersey: Prentice Hall PTR, 1998.

[134] Price, A. J., and N. Le Mercier. "Reduced bandwidth optical digital intensity modulation with improved chromatic dispersion tolerance." *Electronics Letters* 31.1 (1995): 58-59.

[135] Yonenaga, Kazushige, and Shigeru Kuwano. "Dispersion-tolerant optical transmission system using duobinary transmitter and binary receiver." *Lightwave Technology, Journal of* 15.8 (1997): 1530-1537.

[136] Gu, X., et al. "Duobinary technique for dispersion reduction in high capacity optical systems-modelling, experiment and field trial." *IEE Proceedings-Optoelectronics* 143.4 (1996): 228-236.

[137] Lyubomirsky, Ilya, and Bharath Pitchumani. "Impact of optical filtering on duobinary transmission." *Photonics Technology Letters, IEEE* 16.8 (2004): 1969-1971.

[138] Anderson, John B., Tor Aulin, and Carl-Erik Sundberg. *Digital phase modulation*. Springer Science & Business Media, 2013.

[139] Miyazaki, Tetsuya, and Fumito Kubota. "PSK self-homodyne detection using a pilot carrier for multibit/symbol transmission with inverse-RZ signal." *IEEE photonics technology letters* 17.6 (2005): 1334-1336.

[140] Chien, Cheng-Chung. "Optical Modulation and Detection Techniques for High-Spectral Efficiency." (2008).

[141] M. Ohm and J. Speidel, "Quaternary optical ASK-DPSK and receivers with direct detection," *IEEE Photon. Technol. Lett.*, vol. 15, pp. 159–161, 2003.

[142] Kim, Hoon, and Alan H. Gnauck. "Experimental investigation of the performance limitation of DPSK systems due to nonlinear phase noise." *Photonics Technology Letters, IEEE* 15.2 (2003): 320-322.

[143] J.-X. Cai, et al. "RZ-DPSK field trial over 13 100 km of installed non slope-matched submarine fibers," in *Proc. OFC 2004*, Los Angeles, CA, 2004.

[144] Chikama, Terumi, et al. "Modulation and demodulation techniques in optical heterodyne PSK transmission systems." *Lightwave Technology, Journal of* 8.3 (1990): 309-322.

[145] A. H. Gnauck, P. J. Winzer, "Optical Phase Shift Keyed Transmission", J. of Lightwave Technology, Vol. 23, No. 1, Jan 2005

[146] Griffin, R. A., et al. "10 Gb/s optical differential quadrature phase shift key (DQPSK) transmission using GaAs/AlGaAs integration." *Optical Fiber Communication Conference*. Optical Society of America, 2002.

[147] Zhao, Lian,et al. "40G QPSK and DQPSK modulation." *Inphi Corporation, Sunnyvale, CA, USA, Tech. Rep* (2007).

[148] Kim, Hoon, and Peter J. Winzer. "Robustness to laser frequency offset in direct-detection DPSK and DQPSK systems." *Journal of Lightwave Technology* 21.9 (2003): 1887.

[149] Lach, Eugen, and Wilfried Idler. "Modulation formats for 100G and beyond." *Optical Fiber Technology* 17.5 (2011): 377-386.

[150] Roberts, Kim, et al. "100 G and beyond with digital coherent signal processing." *IEEE Communications Magazine* 48.7 (2010): 62-69.

[151] T. J. Xia *et al*., "End-to-end native IP data 100G single carrier real time DSP coherent detection transport over 1520-km field deployed fiber," in OFC/NFOEC2010, PDP4 (2010).

[152] Chung, Hwan Seok, Sun Hyok Chang, and Kwangjoon Kim. "Mitigation of imperfect carver-induced phase distortions in a coherent PM-RZ-QPSK receiver." *Lightwave Technology, Journal of* 28.24 (2010): 3506-3511.

[153] H. Wernz *et al*., "Nonlinear behavior of 112 Gb/s polarization-multiplexed RZ-DQPSK with direct detection in a 630 km field trial," presented at the Eur. Conf. Optic. Communication Vienna, Austria, 2009.

[154] Chung, Hwan Seok, et al. "Transmission performance comparison of direction detection-based 100-Gb/s modulation formats for metro area optical networks." *ETRI Journal* 34.6 (2012): 800-806.

[155] ITU-T Rec. G.694.1, Spectral Grids for WDM Applications: DWDM Frequency Grid, June 2002.

[156] Tiwari Vinita, et al. "Investigation of optimum pulse shape for 112Gbps DP-DQPSK in DWDM transmission." *Optik-International Journal for Light and Electron Optics* 124.22 (2013): 5567-5572.

[157] Chraplyvy, Andrew, et al. "Long haul transmission in a dispersion managed optical communication system." U.S. Patent Application No. 09/990,964.

[158] Chandrasekhar, S., and X. Liu. "Impact of channel plan and dispersion map on hybrid DWDM transmission of 42.7-Gb/s DQPSK and 10.7-Gb/s OOK on 50-GHz grid." *IEEE Photonics Technology Letters* 19.22 (2007): 1801-1803.

[159] Hayee, M. I., and A. E. Willner. "NRZ versus RZ in 10-40-Gb/s dispersion-managed WDM transmission systems." *IEEE photonics technology letters* 11.8 (1999): 991-993.

[160] Mu, R-M., et al. "Dynamics of the chirped return-to-zero modulation format." *Journal of Lightwave Technology* 20.1 (2002): 47.

[161] Mu, R-M., and C. R. Menyuk. "Convergence of the chirped return-to-zero and dispersion managed soliton modulation formats in WDM systems." *Journal of lightwave technology* 20.4 (2002): 608.

[162] Kubota, Hirokazu, and Masataka Nakazawa. "Partial soliton communication system." *Optics communications* 87.1-2 (1992): 15-18.

[163] Gnauck, A. H., et al. "25 x 40-Gb/s copolarized DPSK transmission over 12 x 100-km NZDF with 50-GHz channel spacing." *IEEE photonics technology letters* 15.3 (2003): 467-469.

[164] Yan, L. S., et al. "Performance optimization of chirped return-to-zero format in 10-Gb/s terrestrial transmission systems." *Optical Fiber Communication Conference and Exhibit, 2001. OFC 2001*. Vol. 1. IEEE, 2001.

[165] Bakhshi, Bamdad, et al. "Comparison of CRZ, RZ, and NRZ modulation formats in a 64× 12.3 Gb/s WDM transmission experiment over 9000 km." *Optical Fiber Commun. Conf., Anaheim, CA*. 2001.

[166] Hasegawa, Akira, and Frederick Tappert. "Transmission of stationary nonlinear optical pulses in dispersive dielectric fibers. I. Anomalous dispersion." *Applied Physics Letters* 23.3 (1973): 142-144.

[167] Mollenauer, Linn F., Roger H. Stolen, and James P. Gordon. "Experimental observation of picosecond pulse narrowing and solitons in optical fibers." *Physical Review Letters* 45.13 (1980): 1095.

[168] N. J. Smith *et al.*, "Enhanced power solitons in optical fibers with periodic dispersion management", Electronic letter 32,54 (1996)

[169] Mollenauer, L. F., and K. Smith. "Demonstration of soliton transmission over more than 4000 km in fiber with loss periodically compensated by Raman gain." *Optics letters* 13.8 (1988): 675-677.

[170] Hasegawa, Akira, Yuji Kodama, and Shiva Kumar. "Reduction of collision-induced time jitters in dispersion-managed soliton transmission systems." *Optics letters* 21.1 (1996): 39-41.

[171] Nijhof, J. H. B., W. Forysiak, and N. J. Doran. "The averaging method for finding exactly periodic dispersion-managed solitons." *IEEE Journal of Selected Topics in Quantum Electronics* 6.2 (2000): 330-336.

[172] Mollenauer, L. F., et al. "Demonstration of massive wavelength-division multiplexing over transoceanic distances by use of dispersion-managed solitons." *Optics letters* 25.10 (2000): 704-706.

[173] Suzuki, Masatoshi, and Noboru Edagawa. "Dispersion-managed high-capacity ultra-long-haul transmission." *Journal of Lightwave Technology* 21.4 (2003): 916.

[174] Winzer, Peter J., and Renè-Jean Essiambre. "Advanced modulation formats for high-capacity optical transport networks." *Journal of Lightwave Technology* 24.12 (2006): 4711-4728.

[175] Tiwari, Vinita, Debabrata Sikdar, and V. K. Chaubey. "SPM induced limitations for 40Gbps chirped Gaussian pulses in optical channel." *Optik-International Journal for Light and Electron Optics* 123.16 (2012): 1482-1485.

[176] Yonenaga, K., et al. "Optical duobinary transmission system with no receiver sensitivity degradation." *Electronics Letters* 31.4 (1995): 302-304.

[177] Penninckx, D., et al. "The phase-shaped binary transmission (PSBT): A new technique to transmit far beyond the chromatic dispersion limit." *IEEE Photonics Technology Letters* 9.2 (1997): 259-261.

[178] Gu, X., and L. C. Blank. "10Gbit/s unrepeatered three-level optical transmission over 100km of standard fibre." *Electronics letters* 29.25 (1993): 2209-2211.

[179] Lee, Jaehoon, et al. "Chromatic dispersion tolerance of new duobinary transmitters based on two intensity modulators without using electrical low-pass filters." *Journal of lightwave technology* 22.10 (2004): 2264.

[180] Franck, Thorkild, et al. "Duobinary transmitter with low intersymbol interference." *Photonics Technology Letters, IEEE* 10.4 (1998): 597-599.

[181] Lee, Jaehoon, et al. "Chromatic dispersion tolerance of new duobinary transmitters based on two intensity modulators without using electrical low-pass filters." *Journal of lightwave technology* 22.10 (2004): 2264.

[182] Sikdar, Debabrata, Vinita Tiwari, and V. K. Chaubey. "Optimized transmitter module for NRZ-duobinary in long-haul optical transmission link." *Optik-International Journal for Light and Electron Optics* 124.17 (2013): 2597-2601.

[183] Cheng-Chung Chien and Ilya Lyubomirsky, Comparison of RZ versus NRZ Pulse Shapes for Optical Duobinary Transmission, Journal of Lightwave Technology, vol. 25 (2007), 2953-2958.

[184] G. Bosco, A. Carena, V. Curri, R. Gaudino, and P. Poggiolini, Quantum limit of direct-detection receivers using duobinary transmission, IEEE Photon. Technol. Lett., vol. 15 (2003), 102–104.

[185] Sikdar, Debabrata, Vinita Tiwari, and V. K. Chaubey. "Investigation of RZ and NRZ pulse shape for optimum Duobinary transmission at 40Gbps." *Optik-International Journal for Light and Electron Optics* 124.12 (2013): 1148-1151.

[186] Nag, Avishek, Massimo Tornatore, and Biswanath Mukherjee. "Optical network design with mixed line rates and multiple modulation formats." *Lightwave Technology, Journal of* 28.4 (2010): 466-475.

[187] Gnauck, A. H., et al. "10$\,\ times\, $224-Gb/s WDM Transmission of 56-Gbaud PDM-QPSK Signals Over 1890 km of Fiber." *IEEE Photonics Technology Letters* 13.22 (2010): 954-956.

[188] Gnauck, Alan H., et al. "10× 224-Gb/s WDM transmission of 28-Gbaud PDM 16-QAM on a 50-GHz grid over 1,200 km of fiber." *National Fiber Optic Engineers Conference*. Optical Society of America, 2010.

[189] Xie, Chongjin. "Interchannel nonlinearities in coherent polarization-division-multiplexed quadrature-phase-shift-keying systems." *Photonics Technology Letters, IEEE* 21.5 (2009): 274-276.

[190] Tiwari, Vinita, Debabrata Sikdar, and V. K. Chaubey. "Performance optimization of RZ-DQPSK modulation scheme for dispersion compensated optical link." *Optik-International Journal for Light and Electron Optics* 124.17 (2013): 2593-2596.

[191] VS, Rakesh Krishna, Tiwari,Vinita and V.K. Chaubey, “Investigation of Optimum Fiber types for High speed RZ-DQPSK transmission systems” Bangalore, Workshop on Recent Advances in Photonics (WRAP-2015), 16-17 December, 2015, IISc Bangalore, India.

[192] Slavík, Radan, et al. "All-optical phase and amplitude regenerator for next-generation telecommunications systems." *Nature Photonics* 4.10 (2010): 690-695.

[193] Clarke, Chris, Robert Griffin, and Thomas Goodall. "Highly Integrated DQPSK Modules for 40Gb/s Transmission." *National Fiber Optic Engineers Conference*. Optical Society of America, 2009.

[194] Roberts, Kim, et al. "100 G and beyond with digital coherent signal processing." *IEEE Communications Magazine* 48.7 (2010): 62-69.

[195] Yin, Aihan, Li Li, and Xinliang Zhang. "Analysis of modulation format in the 40Gbit/s optical communication system." *Optik-International Journal for Light and Electron Optics* 121.17 (2010): 1550-1557.

[196] Gnauck, Alan H., et al. "High-capacity optical transmission systems." *Journal of Lightwave Technology* 26.9 (2008): 1032-1045.

[197] Renaudier, Jeremie, et al. "Impact of temporal interleaving of polarization tributaries onto 100-Gb/s coherent transmission systems with RZ pulse carving." *IEEE Photonics Technology Letters* 20.24 (2008): 2036-2038.

[198] Lin, Rongping, et al. "Design of WDM networks with multicast traffic grooming." *Journal of Lightwave Technology* 29.16 (2011): 2337-2349.

[199] Liu, Bo, et al. "A WDM-OFDM-PON architecture with centralized lightwave and PolSK-modulated multicast overlay." *Optics express* 18.3 (2010): 2137-2143.

[200] Fatome, Julien, Coraline Fortier, and Stéphane Pitois. "Practical design rules for single-channel ultra high-speed dense dispersion management telecommunication systems." *Optics Communications* 282.7 (2009): 1427-1434.

[201] Burdin, Vladimir A., et al. "Application of dispersion managed soliton regime in radio-over-fiber systems." *Optical Technologies for Telecommunications 2012*. International Society for Optics and Photonics, 2013.

[202] Biondini, Gino, and Sarbarish Chakravarty. "Nonlinear chirp of dispersion-managed return-to-zero pulses." *Optics letters* 26.22 (2001): 1761-1763.

[203] Lakoba, T. I., and G. P. Agrawal. "Optimization of the average-dispersion range for long-haul dispersion-managed soliton systems." *Journal of lightwave technology* 18.11 (2000): 1504-1512.

[204] Berntson, A., et al. "Power dependence of dispersion-managed solitons for anomalous, zero, and normal path-average dispersion." *Optics letters* 23.12 (1998): 900-902.

[205] Turitsyn, Sergei K., et al. "Average dynamics of the optical soliton in communication lines with dispersion management: Analytical results." *Physical Review E* 58.1 (1998): R48.

[206] Nakazawa, M., et al. "Marked increase in the power margin through the use of a dispersion-allocated soliton." *IEEE Photonics Technology Letters* 8.8 (1996): 1088-1090.

[207] Betti, S., M. Giaconi, and M. Nardini. "Effect of four-wave mixing on WDM optical systems: a statistical analysis." *IEEE Photonics Technology Letters* 15.8 (2003): 1079-1081.

[208] Taha, Thiab R., and Mark I. Ablowitz. "Analytical and numerical aspects of certain nonlinear evolution equations. II. Numerical, nonlinear Schrödinger equation." *Journal of Computational Physics* 55.2 (1984): 203-230.

[209] Zharnitsky, Vadim, et al. "Ground states of dispersion-managed nonlinear Schrödinger equation." *Physical Review E* 62.5 (2000): 7358.

[210] "*Split step algorithm code*", reference Matlab code from "mathworks" website, April 2010 http://www.mathworks.com/matlabcentral/fileexchange/14915-split-step-fourier-method

[211] "*Split-Step method*" retrieved from World Wide Web, April 2010 http://en.wikipedia.org/wiki/Split-step_method

[212] Sinkin, Oleg V., et al. "Optimization of the split-step Fourier method in modeling optical-fiber communications systems." *Journal of lightwave technology* 21.1 (2003): 61.

[213] Anderson, Dan, and Mietek Lisak. "Bandwidth limits due to mutual pulse interaction in optical soliton communication systems." *Optics letters* 11.3 (1986): 174-176.

[214] Neill, D. Royston, and Javid Atai. "Collision dynamics of gap solitons in Kerr media." *Physics Letters A* 353.5 (2006): 416-421.

[215] Pinto, Armando Nolasco, Govind P. Agrawal, and J. Ferreira da Rocha. "Effect of soliton interaction on timing jitter in communication systems." *Journal of Lightwave Technology* 16.4 (1998): 515.

LIST OF PUBLICATIONS

Publication in Peer Reviewed Indexed Journals:

1. **V. Tiwari**, D. Sikdar, and V.K. Chaubey, *SPM induced limitation for 40Gbps chirped Gaussian pulses in optical channel,* Optik - International Journal for Light and Electron Optics, 123 (16), 1482-1485 (2012).
2. D. Sikdar, S. Chaubey, **V. Tiwari** and V. K. Chaubey, *Simulation and Performance Analysis of Duobinary 40 Gbps Optical Link,* Journal of Modern Optics, 59 (10), 903-911 (2012).
3. D. Sikdar, **V. Tiwari**, and V. K. Chaubey, *Investigation of RZ and NRZ pulse shape for optimum Duobinary transmission at 40 Gbps,* Optik - International Journal for Light and Electron Optics, 124 (12), 1148-1151 (2013).
4. D. Sikdar, **V. Tiwari,** Y. Saha, and V. K. Chaubey, *Investigation of modulator chirp and extinction ratio in different RZ-and NRZ duobinary transmitter modules for performance optimization,* Optik - International Journal for Light and Electron Optics, 124 (13), 1411-1414 (2013)
5. D. Sikdar, **V. Tiwari,** and V. K. Chaubey, *Optimized transmitter module for NRZ-duobinary in long-haul optical transmission link,* Optik - International Journal for Light and Electron Optics, 124 (17), 2597-2601 (2013).
6. **V. Tiwari**, D. Sikdar, and V. K. Chaubey, *Performance optimization of RZ-DQPSK modulation scheme for dispersion compensated optical link,* Optik - International Journal for Light and Electron Optics, 124 (17), 2593-2596 (2013).
7. **V. Tiwari,** D. Sikdar, M. N. Jyothi, G. Dixit, V.K. Chaubey, *Investigation of optimum pulse shape for 112Gbps DP-DQPSK in DWDM transmission,* Optik - International Journal for Light and Electron Optics, 124 (22), 5567-5572 (2013).
8. D. Sikdar, **V. Tiwari**, and V. K. Chaubey, *Optimum dispersion map profile for a stable DM soliton system,* Journal of Modern Optics 59 (16), 1396-1405 (2012).
9. **V.Tiwari**, V.K.Chaubey, *Modeling of SPM induced jitter for the chirped Gaussian pulse propagation*, Journal of Modern Optics, September 2016, communicated.

Publication in Peer Reviewed Conferences:

1. **V. Tiwari**, D. Sikdar, V. K. Chaubey, *Source Induced Limitations in 40 Gbps post-compensated optical fiber link: A Simulation Study*, Proc. of International Conference on Nanoscience, Engineering & Advanced Computing (ICNEAC-2011), 1, 495-497 (2011).
2. D. Sikdar, **V. Tiwari**, V. K. Chaubey, *Effect of Pulse Width on a 40 Gb/s Lightwave Channel for Chirped Sources Having Different Linewidth and Peak Power*, Proceedings of International Conference on Nanoscience, Engineering & Advanced Computing (ICNEAC-2011), 3, 360-363 (2011).
3. **V. Tiwari**, P Vignan, Rahul Vyas, V. K. Chaubey, "*Investigation of Optimal Duty-Cycle for GVD Undercompensated Optical Link*" presented in ICCS – 2013, BKBIET Pilani and published in IJECET, vol.4, issue 7 pp. 20-27, 2013.
4. T. Ishan, **V. Tiwari**, V.K.Chaubey "Performance Analysis of Different Pulse Shapes for Optical Transmission", IEEE International Conference on Control, Communication and Computing (ICCC), 19-21 November, 2015, Thiruvanathapuram, Kerla, India.
5. V S Rakesh Krishna, **V. Tiwari,** V.K.Chaubey "Investigation of Optimum Fiber types For High speed RZ-DQPSK transmission systems", Workshop on Recent Advances in Photonics (WRAP-2015), 16-17 December, 2015, IISc Bangalore, India.

Brief Biography of Candidate

Vinita Tiwari is a research scholar under faculty development program in the Department of Electrical and Electronics Engineering, Birla Institute of Technology and Science-Pilani, Pilani campus since August 2009. She obtained her B.E degree in Electronic and communication from M.B.M Engineering College, Jodhpur and M.E in Communication Engineering from BITS-Pilani in 2006 and 2009 respectively. Her research interests are High-speed optical communication, Dispersion managed Solitons.

Brief Biography of Supervisor

Dr. V.K.Chaubey is a Professor in Department of Electrical and Electronics Engineering, Birla Institute of Technology and Science-Pilani, Pilani campus. He obtained his M.Sc with specialization in Electronics and Radio physics, and Ph.D in Fiber Optics Communication from Banaras Hindu University, Varanasi in 1985 and 1992 respectively. He was with the department of Applied Physics, Institute of Technology, B.H.U during 1993-1994 as a UGC postdoctoral fellow. He is a senior member of IEEE and has several publications in International, National Journals, and Conferences. His research interests are Optical waveguide and Integrated Optics, Wireless and Optical Communication Networks.